Detection and modelling of soil compaction of arable soils: From field survey to regional risk assessment

Dissertation

zur Erlangung des Doktorgrades
der Mathematisch-Naturwissenschaftlichen-Fakultät
der Christian-Albrechts-Universität zu Kiel

vorgelegt von
Michael Kuhwald

Kiel, 2019

Erster Gutachter: Prof. Dr. Rainer Duttmann

Zweiter Gutachter: PD Dr. habil. Joachim Brunotte

Termin der mündlichen Prüfung: 06.02.2019

Zum Druck genehmigt: 06.02.2019

gez. Prof. Dr. Frank Kempken, Dekan

Danksagung

An dieser Stelle möchte ich all denjenigen danken, die mich im Laufe der letzten Jahre stets unterstützt und so zum Gelingen dieser Doktorarbeit beigetragen haben.

Als erstes möchte ich mich herzlichst bei meinen Doktorvater Rainer Duttmann bedanken. Nicht nur hat er mich bereits als Hiwi "entdeckt" und somit auf einen wissenschaftlichen Weg gebracht, sondern auch die Gelegenheit zum Anfertigen einer Doktorarbeit zu einem spannenden und aktuellen Thema gegeben. Der von Rainer zu jeder Zeit ermöglichte fachliche Austausch bei gleichzeitiger Gewährleistung der freien wissenschaftlichen Entfaltung hat wesentlich zum Gelingen dieser Doktorarbeit beigetragen. Ich denke, dass Verhältnis zwischen Doktorand und Doktorvater lässt sich am besten mit der Tatsache beschreiben, dass ich mich sehr über die Anwesenheit meines Chefs bei meiner Hochzeit gefreut habe.

Mein zweiter Dank geht an meinen Zweitprüfer Joachim Brunotte. Sein umfangreiches Wissen im Bereich der Agrarwirtschaft und den Auswirkungen unterschiedlichster Bearbeitungsvarianten auf die Bodeneigenschaften, welches er mir in zahlreichen Gesprächen und Praxisvorstellungen vermittelt hat, spiegelt sich auch in der vorliegen Doktorarbeit wider. Unzählige Male durften wir auf seinen Flächen unsere Messungen durchführen und den Boden umwühlen. Auch wenn die Flächen danach häufig recht "wild" aussahen, glaube ich doch, dass unsere zahlreichen mittels Penetrologger erzeugten Poren zu einer erheblichen Ertragssteigerung beigetragen haben.

Bedanken möchte ich mich auch bei meinem Drittprüfer Ingmar Unkel und den Prüfungsvorsitzenden Florian Dünckmann. Ohne sie wäre die Disputation und somit das Erlangen des Doktorgrades nicht möglich.

Weiterhin sei all den Hiwis und Studierenden gedankt, die im Laufe der letzten Jahre mit mir in Adenstedt Messungen, Bodenprobenentnahmen und anschließend die Analysen im Labor durchgeführt haben. Besonders hervorheben möchte ich dabei Celina Thomas, die als Hiwi so oft wie kein anderer in Adenstedt war und mir immer zuverlässig geholfen hat.
Ich bedanke mich außerdem bei unseren Laborassistentinnen Antje Berger, Julia Goldmann und Maike Gosse. Ohne sie hätten die zahlreichen Bodenproben nicht analysiert und die Hiwis und Studierenden organisiert werden können.

Bei meinem Dank nicht zu vergessen sei auch die "Kaffeerunde": Katja Augustin, Tim Hartmann, Daniel Knitter, Philipp Saggau und Wolfgang Hamer, sowie die beiden ehemaligen Kollegen Michael Blaschek und Michael Nolde. Mal frustriert, mal genervt aber vor allem belustigt und gut gelaunt, haben wir hier immer über wichtige und belanglose Erkenntnisse diskutiert. Ein besonderer Dank gilt dabei meinem Kollegen und Freund Wolfgang Hamer. Mit seiner friedlichen und freundlichen Art, dem stets offenen Ohr und exzellenten R-Kenntnissen hat er mir bei so manch schwieriger Phase sehr geholfen.

Mein Dank gilt aber nicht nur all jenen, die mittelbar mit dieser Doktorarbeit zu tun haben, sondern auch meinen Eltern und meiner Schwester. Sie haben einem mit allem Wichtigen für das Leben ausgestattet, wodurch diese Arbeit erst ermöglicht wurde.

Mein letzter aber wichtigster Dank geht an meine Frau Katja. Seit mittlerweile über 8 Jahre zusammen und seit 5 Monaten verheiratet, haben wir gemeinsam erst das Studium und nun auch die Doktorandenzeit gemeinsam mit viel Vertrautheit und Verständnis füreinander verbracht.

Summary

Arable soils are exposed to several field traffic activities during the year. Typical activities are primary tillage, sowing, fertiliser application and harvest. Since each of these activities is conducted by heavy machinery, any field traffic may result in (harmful) soil compaction. Soil compaction reduces the water infiltration, air permeability, biological activity, root and plant growth and therefore is one of the main threats to all arable soils.

This thesis focussed on the detection and modelling of soil compaction at different spatial scales. At field scale, fieldwork aimed to analyse and describe the effects of different tillage practices (conventional and reduced tillage) and traffic intensities (inner field and headlands) on the spatial distribution of soil compaction. A one-time inversion tillage was conducted to analyse this measure as a management option to reduce topsoil compaction in conservation tillage. At regional scale, the aim was to develop and apply a new model, which enables a daily assessment of soil compaction risk by considering soil management effects and the dynamic changes of soil properties.

The field scale analyses revealed clear patterns of soil compaction depending on the kind of primary tillage practice and traffic intensity as indicated by penetration resistance measurements. Measurements of soil physical properties (infiltration rate and saturated hydraulic conductivity) showed that soil density itself does not allow a functional assessment of soils; i.e. assessment of soil compaction always necessitates the combination of soil density and functionality (e.g. water infiltration) measurements. The one-time inversion tillage removed the detected dense soil layer in the reduced tilled areas and led to approximately the same soil density as in the continuously conventionally tilled area. The improved soil functionality, which developed during long-term reduced tillage, remained after one-time inversion. Thus, one-time inversion tillage may be a proper measure to overcome the disadvantages of long-term reduced tillage (e.g. soil compaction in the topsoil), while preserving enhanced soil functionality. The SaSCiA-model ("spatially explicit soil compaction risk assessment") was developed to calculate daily soil compaction risk at regional scale by transferring the knowledge of soil management effects from the field surveys and considering additional soil, weather, crop and machinery information. Spatial crop type information was derived from satellite data (Landsat 8, Sentinel-2A) and daily soil moisture was calculated spatially explicit by integrating a soil moisture model. SaSCiA was applied to calculate the soil compaction risk on a daily basis for entire years for the two study areas (region Adenstedt and region Kummerow). By considering the dynamic changes of soil moisture, the developed SaSCiA-model enables a detailed spatio-temporal assessment of soil compaction risk, which exceeds all currently available models.

In summary, this thesis has contributed to a better understanding of the highly dynamic spatio-temporal characteristic of soil compaction and soil compaction risk.

Zusammenfassung

Ackerbaulich genutzte Böden sind im Laufe eines Jahres mehreren Befahrungsaktivitäten ausgesetzt. Beispielsweise wird eine Fläche bei der Bodenbearbeitung, der Aussaat, der Düngerausbringung und der Ernte befahren. Da jede dieser Befahrungen mit schweren Maschinen durchgeführt wird, kann jede Befahrungsaktivität zu (schädlicher) Bodenverdichtung führen. Bodenverdichtung reduziert die Wasserinfiltration, die Luftdurchlässigkeit, die biologische Aktivität, das Wurzel- und Pflanzenwachstum und ist daher eine der Haupursachen für Bodendegradation von ackerbaulich genutzten Böden.

Die vorliegende Dissertation zielte auf die Identifikation und Modellierung der Bodenverdichtung unter Berücksichtigung verschiedener räumlicher Skalen ab. Auf der Feldskala sollten die Auswirkungen verschiedener Grundbodenbearbeitungen (konventionelle und reduzierte Bodenbearbeitung) und Verkehrsintensitäten (Kernfeld und Vorgewende) auf die räumliche Verteilung der Bodenverdichtung analysiert werden. Anschließend wurde eine einmalige wendende Bodenbearbeitung mit dem Pflug durchgeführt, um diese Maßnahme als Managementoption zur Reduzierung der Oberbodenverdichtung in der konservierenden Bodenbearbeitung zu evaluieren. Auf regionaler Skala war die Entwicklung und Anwendung eines Modells zur täglichen Bewertung des Bodenverdichtungsrisikos unter Berücksichtigung der Auswirkungen unterschiedlicher Bodenbewirtschaftung und der dynamischen Änderungen der Bodeneigenschaften das Ziel.

Die Analysen auf der Feldskala zeigten in Abhängigkeit von der Art der primären Bodenbearbeitung und der Verkehrsintensität deutliche Muster der Bodenverdichtung, die durch Messungen des Eindringwiderstandes ermittelt wurden. Ergänzende Messungen der bodenphysikalischen Eigenschaften (Infiltrationsrate und gesättigte hydraulische Leitfähigkeit) zeigten, dass der Eindringwiderstand allein keine funktionale Beurteilung von Böden ermöglicht; d.h. eine Beurteilung der Bodenverdichtung erfordert immer die Kombination von Bodendichte- und Funktionalitätsmessungen (z.B. Wasserinfiltration). Die einmalige wendende Bodenbearbeitung mit dem Pflug entfernte die erkannte dichtere Bodenschicht in den reduziert bearbeiteten Anbauflächen und führte zu einer annähernd gleichen Bodendichte wie in der kontinuierlich konventionell bestellten Fläche. Die verbesserte Bodenfunktionalität, die sich bei der langfristig reduzierten Bodenbearbeitung entwickelt hatte, blieb nach dem einmaligen Pflugeinsatz aber erhalten. Somit zeigten die Ergebnisse, dass die einmalige wendende Bodenbearbeitung eine geeignete Maßnahme sein kann, um die Nachteile einer langfristig angewandten reduzierten Bodenbearbeitung (z.B. Bodenverdichtung im Oberboden) zu verringern und gleichzeitig die verbesserte Bodenfunktionalität zu erhalten.

Das SaSCiA-Modell ("Spatially explicit Soil Compaction risk Assessment") wurde entwickelt, um das tägliche Bodenverdichtungsrisiko auf regionaler Skala zu berechnen. Dazu

wurden die aus den Felduntersuchungen gewonnenen Erkenntnisse über die Auswirkungen der Bodenbewirtschaftung und -befahrungen auf die regionale Skala übertragen und zusätzliche Boden-, Wetter-, Pflanzen- und Maschineninformationen berücksichtigt. Räumliche Informationen über die Fruchtarten wurden aus Satellitendaten abgeleitet (Landsat 8, Sentinel-2A), die tägliche Bodenfeuchte wurde durch die Integration eines Bodenfeuchtemodells räumlich explizit berechnet. Für die beiden Untersuchungsgebiete (Region Adenstedt und Region Kummerow) wurde mit SaSCiA das Bodenverdichtungsrisiko für ganze Jahre in täglicher Auflösung berechnet. Durch die Berücksichtigung der dynamischen Veränderungen der Bodenfeuchte ermöglicht das entwickelte SaSCiA-Modell eine detaillierte räumlich-zeitliche Beurteilung des Bodenverdichtungsrisikos, die über alle derzeit verfügbaren Modelle hinausgeht.

Die Ergebnisse der vorliegenden Arbeit haben damit zu einem besseren Verständnis der hochdynamischen räumlich-zeitlichen Charakteristik der Bodenverdichtung und des Bodenverdichtungsrisikos beigetragen.

Contents

List of figures **V**

List of tables **VII**

1 Introduction **1**
1.1 Motivation and research questions 1
1.2 Outline of the thesis 4

2 State of the Art **7**
2.1 Soil compaction - general remarks 7
2.2 Soil compaction - effects of tillage practices 10
2.3 Soil compaction - modelling approaches 13

3 Study areas, Materials and Methods **19**
3.1 Adenstedt (field scale and regional scale) 19
3.2 Kummerow (regional scale) 21
3.3 Fieldwork and measurements 23
3.4 Laboratory work and measurements 25
3.5 Descriptive statistics and digital soil mapping 25
3.6 Model development (SaSCiA) 26

4 Spatial analysis of long-term effects of different tillages practices based on penetration resistance **29**
4.1 Introduction 30
4.2 Materials and methods 30
4.2.1 Study site and tillage practices 30
4.2.2 Sampling design and methods 32
4.2.3 Laboratory analysis 33
4.2.4 Descriptive and spatial statistics 33
4.3 Results 34
4.3.1 Penetration resistance 34

4.3.2 Spatial patterns of penetration resistance . . . 35
4.3.3 Soil physical properties . . . 37
4.4 Discussion . . . 38
4.4.1 Tillage practice effects . . . 38
4.4.2 Spatial patterns of penetration resistance . . . 39
4.5 Conclusions . . . 40
4.6 Acknowledgements . . . 40

5 Comparing soil physical properties from continuous conventional tillage with long-term reduced tillage affected by one-time inversion 41
5.1 Introduction . . . 42
5.2 Materials and methods . . . 43
5.2.1 Study site . . . 43
5.2.2 Tillage treatments and experimental design . . . 44
5.2.3 Measurement of VSWC, DBD and Ks . . . 46
5.2.4 Measurement of K(h) . . . 46
5.2.5 Statistical analyses . . . 47
5.3 Results . . . 47
5.3.1 Results of VSWC and DBD measurements . . . 47
5.3.2 Results of Ks measurements . . . 47
5.3.3 Results of K(h) measurement . . . 48
5.4 Discussion . . . 49
5.4.1 Effects of one-time inversion tillage in the untrafficked areas . . . 49
5.4.2 Effects of one-time inversion tillage in the trafficked areas . . . 50
5.4.3 One-time inversion tillage as a soil management option . . . 50
5.5 Conclusions . . . 51
5.6 Acknowledgements . . . 51

6 Spatially Explicit Soil Compaction Risk Assessment of Arable Soils at Regional Scale: The SaSCiA-Model 53
6.1 Introduction . . . 54
6.2 The SaSCiA-Model - Material and Methods . . . 56
6.2.1 Input Data and Data Preparation . . . 56
6.2.1.1 Weather Information . . . 56
6.2.1.2 Soil data . . . 57
6.2.1.3 Present crop types . . . 57
6.2.1.4 Crop rotation . . . 58
6.2.1.5 Fertiliser and irrigation information . . . 58
6.2.1.6 Machinery information and field traffic days . . . 58

6.2.2 Soil moisture modelling (MONICA) . . . 59
6.2.3 Soil strength modelling . . . 59
6.2.4 Soil stress modelling . . . 62
6.2.5 Soil compaction risk evaluation . . . 62
6.3 The SaSCiA-model-application . . . 63
6.3.1 Study areas . . . 63
6.3.2 Input data for model application . . . 63
6.3.2.1 Weather information . . . 63
6.3.2.2 Soil information . . . 64
6.3.2.3 Present crop types and crop rotation . . . 64
6.3.2.4 Fertiliser and irrigation information . . . 67
6.3.2.5 Machinery information and field traffic days . . . 67
6.4 Results and Discussion . . . 68
6.4.1 Spatial distribution of soil compaction risk . . . 68
6.4.2 Temporal variation of soil compaction risk . . . 70
6.4.3 Spatio-temporal variation for single crop types . . . 73
6.4.4 Advances and limitations of the SaSCiA-model . . . 74
6.5 Conclusions . . . 78
6.6 Appendix A . . . 79

7 Discussion and conclusions **83**
7.1 Summary of main achievements . . . 83
7.2 Conclusion and further research need . . . 90

References **93**

Erklärung **108**

List of Figures

1.1 Development of combine harvester weight in recent decades. 2
1.2 Workflow of this thesis. 4

2.1 Schematic illustration of stress propagation in the soil I. 8
2.2 Schematic illustration of stress propagation in the soil II. 9
2.3 Schematic illustration of tillage effects on topsoil loosening and inversion. . . 11

3.1 Study areas Adenstedt and Kummerow. 20
3.2 Climate charts of both study areas. 21
3.3 Soil texture distribution of the selected field in Adenstedt. 22
3.4 Field equipment: Penetrologger, mini-disc-infiltrometer and core samples. . . 24

4.1 Study site and sampling points 31
4.2 Box-whisker plots of measured penetration resistance. 33
4.3 Penetration resistance profiles comparing CT, RT1, RT2 and HL, IF. 36
4.4 Spatial distribution of predicted penetration resistance. 37

5.1 Study area and sampling locations. 43
5.2 Example of sampling design for each sampling location. 46

6.1 Graphical Abstract for Sustainability 53
6.2 Schematic structure of the SaSCiA-model. 57
6.3 Classification result of Adenstedt in the year 2016. 66
6.4 Classification result of Kummerow in the year 2015. 67
6.5 Soil compaction risk at Adenstedt on 7 August 2016. 69
6.6 Temporal variation of soil compaction risk at Adenstedt for 2016. 71
6.7 Temporal variation of soil compaction risk for the wet scenario. 72
6.8 Temporal variation of soil compaction risk for cereals at Kummerow. 73
6.9 Soil compaction risk for areas cultivated with cereals at Kummerow for August 2015. 74
6.10 Example of creation of ’rotation-ID’ and ’crop-rotation-ID’. 81

List of Tables

2.1 Frequently used approaches and models in soil compaction research. 15
2.2 Spatial approaches and models in soil compaction research. 18

4.1 Soil profile information. 31
4.2 Statistical characteristics of penetration resistance measurements. 34
4.3 Significance of differences in mean penetration resistance. 35
4.4 Residual variogram characteristics and interpolation accuracy. 36
4.5 Comparison of soil physical properties. 37

5.1 Field activities at the study site. 44
5.2 Technical specifications of the machinery used. 45
5.3 Soil physical properties of the untrafficked and trafficked areas. 48

6.1 Equations to calculate the soil strength at field capacity. 60
6.2 Equations to calculate the soil moisture depended soil strength. 61
6.3 Equations to calculate the effects of gravel on soil strength. 61
6.4 Classification of "Soil Compaction Index" (SCI). 63
6.5 Summary on input data for crop type mapping 65
6.6 Class statistics and accuracy measures of the crop type/land cover classification 65
6.7 Machinery setup used for the SaSCiA-modelling for both study area. 68
6.8 Percentage area of soil compaction risk classes at Adenstedt on 7 August 2016. 69
6.9 Structure and example of input weather information. 79
6.10 Structure and example of input soil data. 79
6.11 Structure and example of input crop unit for MONICA-modelling. 79
6.12 Structure and example of input fertilizer data for MONICA-modelling. 79
6.13 Structure and example of input field traffic data. 80
6.14 Crop type, abbreviations and crop-ID for crop types used in SaSCiA. 80

Chapter 1

Introduction

1.1 Motivation and research questions

Soil compaction is one of the main threats to all arable soils (FAO, 2015). It causes reduced water infiltration, impaired plant/root growth and lower biological activity, whereas surface runoff, soil erosion and nutrient leaching increase. Hence, soil compaction affects soil functionality, agricultural productivity, flood risk and nutrient input to water bodies.

Soil compaction occurs (almost) during each traffic activity, i.e. arable land is exposed to soil compaction risk several times a year and year after year. Recently, Schjønning et al. (2015b) noted that one quarter of all European subsoils are already compacted. Compared to other soil degradation processes such as soil erosion, soil compaction receives low awareness from politics and research. A basic topic search in 'web of science' resulted in three times as many articles in the field of soil erosion (29.749) compared to soil compaction (9.325; 04 December 2018).

The reason for the lower awareness may be associated with a reduced visible recognition of soil compaction compared to soil erosion. For instance, water erosion can result in rills and gullies, wind erosion in dust storms. Soil degradation by compaction is rarely visible. Deep ruts of the tyre may be recognisable at the soil surface, but surface smoothening by tillage and seedbed preparation will remove them. The effects of soil compaction in deeper soil layers are invisible at all. Additionally, soil compaction is an on-site damage, without immediately noticeable effects such as sediment transition to streets (e.g. by water erosion) or dust depositions (e.g. by wind erosion). The fact that soil compaction and soil erosion are mutually dependent is often neglected.

In recent decades, agricultural machinery has become larger and heavier (cf. Figure 1.1), necessitating a growing awareness of soil compaction in politics and research (Morris et al., 2010; Schjønning et al., 2015b). Increasing machine weight expose the soil to increased stress, which results in higher soil compaction risk. Simultaneously, the price of the machinery also increases, which demands for a high time utilization of the machinery.

Thus, the machinery must be used continuously at times of e.g. harvest, impeding field traffic stop during unfavourable soil conditions. Furthermore, contractors perform certain services, for instance harvesting of silage maize, in many cases with the aim of harvesting as much area as possible in a short time. Both, the need for high time utilization and service performance by contractors, increase the soil compaction risk and contribute to a continuous spread of compacted areas. Keller et al. (2017) expect a further expansion of soil compaction due to increasing wheel load, unless a technological innovation or paradigm change will be initiated.

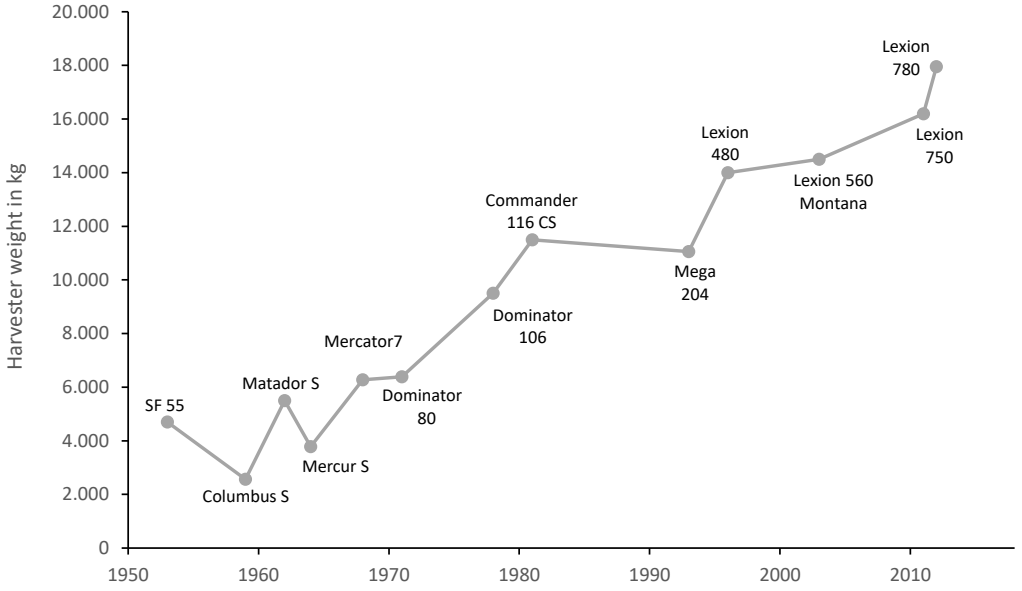

Figure 1.1: Development of combine harvester weight in recent decades using CLAAS as an example. The Figure shows the total machine weight without cutterbar and with empty grain tank. The machine weight alone, however, does not allow the evaluation of contact area and contact area pressure and thus no evaluation of stress propagation in the soil (CLAAS, 1959, 1962, 1964, 1968, 1971, 1978, 1981, 1993, 1996, 2003, 2011).

Soil compaction research tries to generate answers to questions regarding field traffic and its effects on soil properties and functions. Several studies focussed on the description of stress propagation during wheeling (e.g. Koolen et al., 1992; Schjønning et al., 2008), the determination of the effects on soil properties and soil functions (e.g. Gebhardt et al., 2009; Weisskopf et al., 2010; Destain et al., 2016) and the generation of measures to reduce soil compaction (e.g. Alakukku et al., 2003; Chamen et al., 2015). The vast majority of these studies, however, was conducted at point/plot scale and in the laboratory. Only few studies are available which tried to measure the spatial distribution of soil compaction and soil compaction effects at field or larger scales (e.g. Veronesi et al., 2012; Barik et al., 2014). Additionally, only few studies exist which dealt with a spatial evaluation of soil compaction risk (e.g. Jones et al., 2003; van den Akker, 2004; Lamandé et al., 2018). One reason

for the small amount of spatially oriented studies is the lack of spatial data. A regional soil compaction risk assessment, for instance, necessitates spatially high-resolution information about the soil moisture.

As most studies are conducted at point/plot scale or in the lab, there is limited knowledge about the spatial characteristics of soil compaction. To prevent soil compaction, the information about when and where soil compaction may occur is inevitable. Generating this information is challenging: soil compaction depends on dynamic natural processes such as soil moisture variation (e.g. Rücknagel et al., 2012; Gut et al., 2015) and on anthropogenic effects on soil properties by soil management and wheeling activities (e.g. Peth et al., 2006). Furthermore, the effect of field traffic must be assessed at different soil depths. Whereas topsoil compaction may be reversed by tillage practices (usually between 20 and 40 cm), subsoil compaction may persist for long-term (Alakukku, 1996; Berisso et al., 2012). Additionally, the kind of tillage practice influences the soil compaction susceptibility. Conventional tillage with mouldboard plough may loosen former compacted topsoil; simultaneously, it leads to a weak and less structured soil and, therefore, may increase soil compaction risk. Conservation tillage maintains the structure of the soil, but may not be able to remove compacted areas in the topsoil (e.g. Daraghmeh et al., 2009; Afzalinia and Zabihi, 2014).

This thesis aimed to increase the knowledge of spatial distribution and temporal variation of soil compaction in agriculturally used areas at different spatial scales. Considering the mentioned challenges of (i) soil management effects on soil compaction and (ii) the need of spatially high-resolution data for spatial soil compaction risk assessment, this thesis focussed on **three main research questions**:

(1) **Does the type of tillage practice and traffic intensity affect the spatial distribution of soil compaction?**

(2) **Is one-time inversion tillage a suitable measure to lower topsoil compaction in conservation tillage?**

(3) **Is it possible to model the actual soil compaction risk with consideration of spatio-temporal dynamics of soil properties at regional scale?**

To answer research question 1 and 2, comprehensive fieldwork was conducted at one field in Lower Saxony, Germany. The selected field was separated in three plots with different kinds of primary tillage practices (conventional tillage with mouldboard plough, and reduced tillage with chisel plough and reduced tillage with disc harrow). The conducted measurements focussed on the identification of pattern as a result of different tillage practices (conventional and reduced tillage) and traffic intensity (inner field and headlands; cf. Figure 1.2).

In October 2014, the field was completely tilled by mouldboard plough, i.e. a so called "one-time inversion tillage" was performed at the formerly reduced tilled plots. In the following season, measurements were conducted to evaluate the effects of the one-time inversion on soil physical properties in trafficked (tramlines and ruts of fully loaded combine harvester) and untrafficked areas.

The findings of research question 1 and 2 were transferred to answer research question 3. The results of the field scale surveys enabled an evaluation of different types of soil management and field traffic intensities. To asses and model the soil compaction risk at regional scale, this knowledge and additional information on soil, weather, crop and machinery were used for model development. Spatial crop type information was derived from satellite data (Landsat 8, Sentinel-2A), while daily soil moisture was calculated for each raster cell by integrating a soil moisture model. The developed model was applied to calculate the soil compaction risk on a daily basis for entire years for the two study areas (region Adenstedt and region Kummerow).

Figure 1.2 schematically illustrates the workflow of this thesis to answer the research questions.

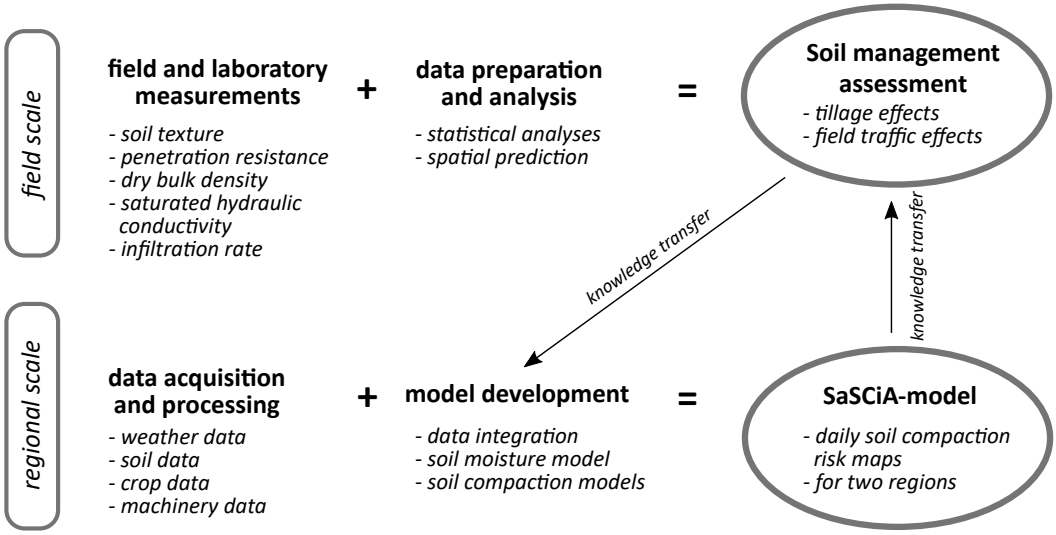

Figure 1.2: Workflow of this thesis.

1.2 Outline of the thesis

Seven chapters structures this thesis. Chapter 1 highlights the motivation for this work and lists the main research questions and objectives. Chapter 2 summarises the state of knowledge in soil compaction research. Chapter 3 provides a description of the study areas and a short overview of the used methods in the field and in the laboratory.

Chapter 4 (first article) addresses research question (1) "Does the type of tillage practice and traffic intensity affect the spatial distribution of soil compaction?". Penetration resistance measurements were conducted on a field with different primary tillage practices and, therefore, with different degree of field traffic intensity and degree of topsoil loosening. The spatial analyses of the measurements illustrated significant differences in penetration resistance depending on primary tillage practices and traffic intensity. This chapter is published as: *Kuhwald, M., Blaschek, M., Minkler, R., Nazemtseva, Y., Schwanebeck, M., Winter, J. & Duttmann, R. (2016): Spatial analysis of long-term effects of different tillage practices based on penetration resistance. Soil Use and Management, 32, 240-249.*

Chapter 5 (second article) focussed on research question (2) "Is one-time inversion tillage a suitable measure to lower topsoil compaction in conservation tillage?". Soil physical measurements were conducted on a field that was tilled by mouldboard plough after long-term reduced tillage, which is called "one-time inversion tillage". The results showed that this measure loosened the formerly more compacted soil, while the improved soil physical properties (saturated hydraulic conductivity, infiltration rate) resulting from the long-term reduced tillage, maintained. This chapter is published as: *Kuhwald, M., Blaschek, M., Brunotte, J. & Duttmann, R. (2017): Comparing soil physical properties from continuous conventional tillage with long-term reduced tillage affected by one-time inversion. Soil Use and Management, 33, 611-619.*

Chapter 6 (third article) concentrates on research question (3) "Is it possible to model the actual soil compaction risk with consideration of spatio-temporal dynamics of soil properties at regional scale?". Using freely available data and software, a model was developed (SaSCiA, Spatially explicit Soil Compaction risk Assessment) to assess the soil compaction risk at region scale on a daily basis. The model applicability was demonstrated for two study areas (Adenstedt and Kummerow). The results showed that soil compaction risk strongly varied in space and time during the year due to dynamic changes in e.g. soil water content. The developed model is the first one that enables a soil compaction risk assessment with these dynamic changes in input data at a spatial scale. This chapter is published as: *Kuhwald, M., Dörnhöfer, D., Oppelt, N. & Duttmann, R. (2018): Spatially explicit soil compaction risk assessment of arable soils at regional scale: The SaSCiA-model. Sustainability, 10, 1618, 1-29.*

Finally, Chapter 7 summarises the findings of this thesis by discussing and answering the main research questions. At the end, an outlook is given on the next possible steps in spatial soil compaction research.

Chapter 2

State of the Art

2.1 Soil compaction - general remarks

Soil compaction is defined as an increase of soil density, while the pore volume decreases within a fixed volume (e.g. Horn et al., 1995). The increase of soil density results in a change of soil properties and functions: compared to an uncompacted soil, a compacted soil is characterised by (in most cases) a lower air capacity, lower field capacity, reduced water infiltration, a reduced air permeability, lower biological activity, reduced water holding capacity, higher dry bulk density and less favourable soil structure (e.g. Horn et al., 1995; Batey, 2009; Gebhardt et al., 2009; Weisskopf et al., 2010; Destain et al., 2016). Compacted soils, therefore, are more susceptible to surface water runoff and soil erosion since infiltration of precipitation and melt water is reduced (Alaoui et al., 2018). Additionally, a compacted soil may hinder plant and root development (e.g. Grzesiak et al., 2013; Szatanik-Kloc et al., 2018), resulting in a lower plant biomass and yield (e.g. Nevens and Reheul, 2003; Botta et al., 2010; Arvidsson and Håkansson, 2014). In certain cases, moderate soil compaction (after loosening) may, however, contribute to a yield increase (Voorhees et al., 1985; Arvidsson et al., 2012; Arvidsson and Håkansson, 2014) e.g. through an enhanced root-soil contact and unsaturated hydraulic conductivity (Kooistra et al., 1992).

Both, natural processes and anthropogenic impacts are responsible for soil compaction. Natural processes, which cause soil compaction, are e.g. soil settlement by gravity, load due to snow, ice, glaciers or sediments, plant weight (from kilogram for sugar beet to several tons for trees), displacement forces during root and plant development and soil development processes (e.g. lessivation). Traffic, livestock farming, material depositions and buildings/constructions of all kinds cause anthropogenic induced soil compaction.

For arable soils, field traffic is the most important cause of soil compaction. Typical field traffic activities are e.g. tillage, seeding/planting, fertilizer and plant protection products application and harvest. Soil compaction occurs when the applied stress from the tyre exceeds the soil strength (e.g. Horn et al., 1995). During the stress application of a tyre,

the soil particles are pressed from top to bottom. After the tyre has left the soil, some soil particles may "rebound" into their old position, which is referred as "elastic deformation". Some soil particles remain in their new position, which is referred as "plastic deformation"; the plastic deformation is the "harmful" soil compaction that causes the above mentioned loss of soil functionality.

The applied stress during field traffic results from wheel load, tyre inflation pressure and contact area of the wheel with the soil surface. The contact area depends on the size and characteristic of the tyre, the tyre inflation pressure and on soil properties (e.g. Söhne, 1953, 1958; Keller and Arvidsson, 2004; Arvidsson and Keller, 2007). A reduction in tyre inflation pressure (for the same tyre and under the same conditions) results in a higher contact area.

The contact area pressure (also referred to as contact area stress or ground contact pressure) can be derived by dividing the wheel load by contact area (Alakukku et al., 2003). An increase in wheel load or a decrease in contact area results in a rising contact area pressure. The contact area pressure is decisive for soil stress propagation and distribution caused by field traffic (e.g. Canillas and Salokhe, 2002; Keller and Arvidsson, 2004; Schjønning et al., 2012): An increase in contact area pressure results in (i) higher total soil stress and (ii) increased vertical soil stress propagation in the subsoil (Figure 2.1).

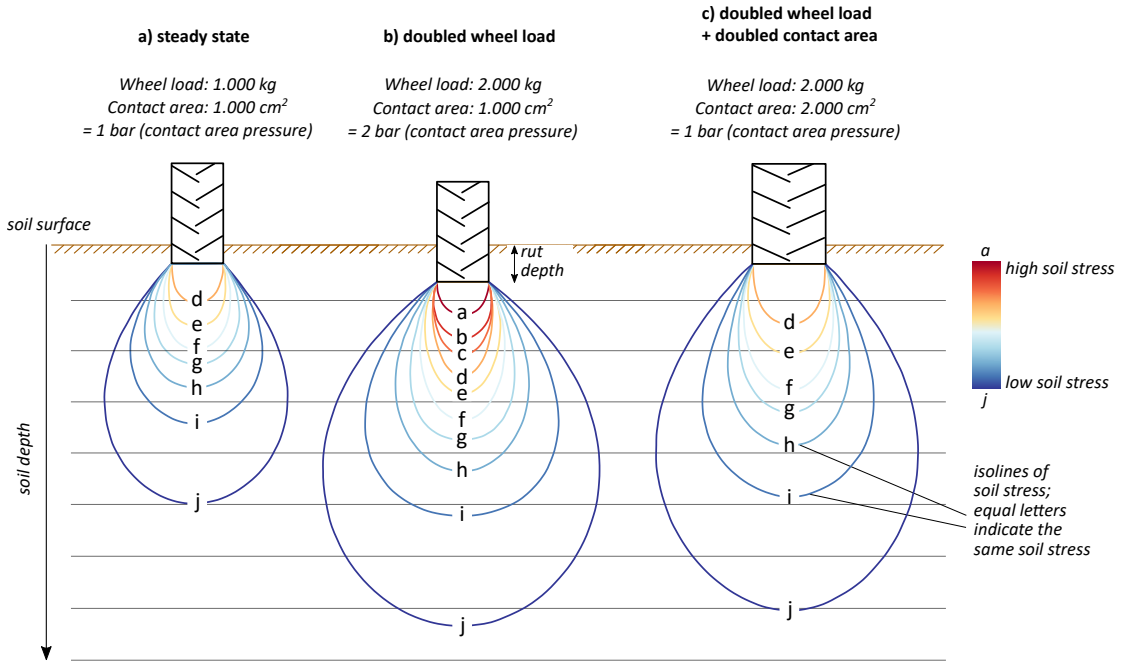

Figure 2.1: Schematic illustration of stress propagation in the soil depending on wheel load, contact area and resulting contact area pressure. Modified according to Bolling and Söhne (1982).

The applied stress leads to soil compaction, when it is higher than the soil strength (e.g. Horn et al., 1995; Horn, 2003). The soil strength depends on soil texture (sand, silt, clay content), carbon content, soil aggregation/structure, dry bulk density and soil moisture

(Lebert and Horn, 1991; Horn and Fleige, 2003). Since soil moisture changes dynamically, e.g. due to precipitation and root water uptake, soil strength also changes continuously (e.g. Rücknagel et al., 2012; Gut et al., 2015). The drier a soil is, the higher is the the soil strength. Accordingly, wet soils have a reduced soil strength and are more susceptible to soil compaction (cf. Figure 2.2).

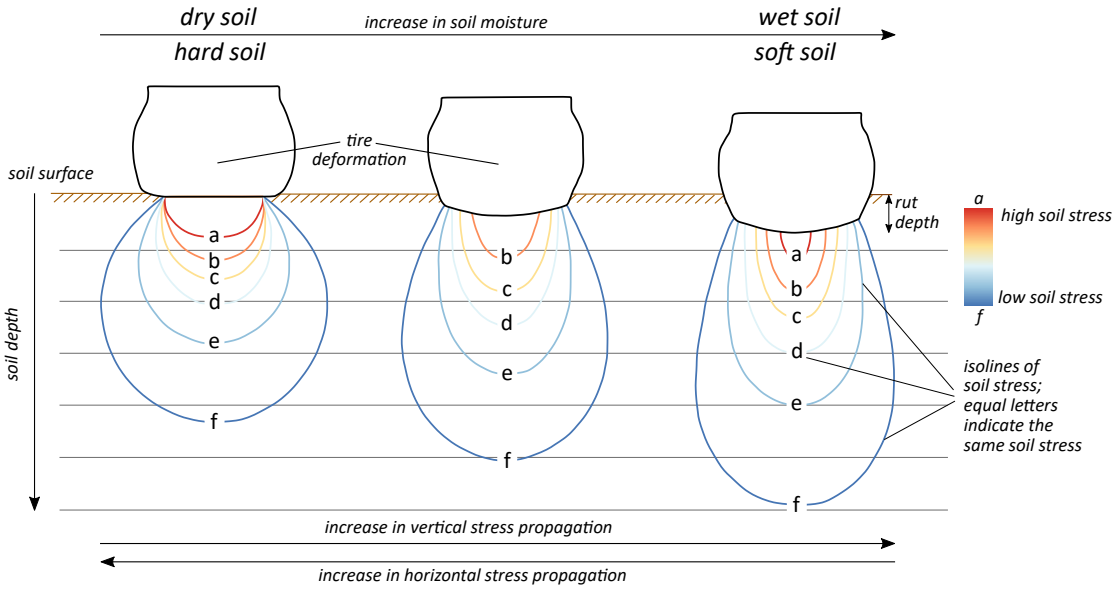

Figure 2.2: Schematic illustration of stress propagation in the soil depending on soil moisture. Modified according to Söhne (1958).

For arable soils, soil compaction can be separated into topsoil (usually between 20 and 40 cm) and subsoil compaction. Topsoil compaction may be reversed by tillage e.g. by using a mouldboard plough; subsoil compaction, however, can persist in the long term (Berisso et al., 2012; Etana et al., 2013). The wheel load mainly determines the soil stress in the subsoil, whereas tyre inflation pressure determines the soil stress in the topsoil (Arvidsson and Keller, 2007).

In addition to the applied soil stress, the amount of wheel passages determines the effect of traffic activity on soil functions. Usually, the first pass of a wheel leads to the highest soil deformation (Canillas and Salokhe, 2002; Nolting et al., 2006; Botta et al., 2009). Further wheel passages lead to depth propagation of soil stress and thus to subsoil compaction (Horn et al., 2003). Furthermore, the shearing effect during wheeling affects the soil functionality. Shearing results from the moving tyre on the rigid soil and is high during wheel slip on e.g. wet soils. The shearing forces may not result in a volume change, but in a deterioration of soil particles and soil structure (Horn et al., 2003), i.e. resulting in decreasing functionality of soil pores (e.g. decrease of infiltration and air permeability due to cutting pore connectivity; Berisso et al., 2013).

Several possibilities exist to measure the effects of soil compaction and tillage practices on soil physical properties. Almost all studies include dry bulk density measurements (Hamza and Anderson, 2005). Measuring penetration resistance is another frequently used method to determine the effect of traffic activity on soil density (e.g. Birkás et al., 2004). However, both measurement techniques have limitations to evaluate changes in soil functionality. Therefore, additional measurements are preferred to describe functional changes induced by field traffic, e.g. hydraulic conductivity (infiltration rate, unsaturated and saturated hydraulic conductivity), air permeability, water retention curve (with associated air and field capacity), aggregate properties (aggregate size, aggregate stability), soil structure and soil strength. Another focus is on the measurement of soil stress, stress distribution and soil displacement in the soil by e.g. load cells, soil stress transducer (SST), displacement transducer system (DTS), Bolling probes (Arvidsson et al., 2001; Horn et al., 2004; Keller and Arvidsson, 2004; Keller, 2005; Nolting et al., 2006; Berisso et al., 2013).

Based on the soil compaction measurements and analyses, several approaches and technical solutions for avoiding soil compaction in arable land were derived. Typical measures are to (i) reduce wheel load, tyre inflation pressure, contact area pressure, amount of wheel passages, (ii) increase contact area, soil organic matter, soil structure and soil aggregation and (iii) traffic at optimal soil moisture. Several review papers give comprehensive descriptions to prevent soil compaction (e.g. Alakukku et al., 2003; Chamen et al., 2003; Hamza and Anderson, 2005; Brunotte et al., 2015; Chamen et al., 2015).

2.2 Soil compaction - effects of tillage practices

The degree of soil compaction of arable soils depends on soil tillage and management practices (e.g. Bogunovic et al., 2018). Typical types of tillage practices are (i) conventional tillage and (ii) conservation tillage. Conventional tillage is used for seedbed preparation with a complete inversion of the topsoil by using e.g. a mouldboard plough. Conservation tillage (also referred to as conservation agriculture), in contrast, aims to reduce soil disturbance, i.e. no complete inversion of the topsoil, and to maintain a high proportion of crop residue on the surface (in minimum 30 % residue coverage; e.g. Holland 2004, Morris et al., 2010). Various further differentiations of conservation tillage/agriculture exist, being separated by e.g. degree and depth of soil disturbance (Townsend et al., 2016). Two important types are reduced tillage (RT) and no-tillage (NT). Reduced tillage is a primary tillage practice without inversion of the topsoil, conducted by e.g. chisel or disc harrow (cf. Figure 2.3). Depending on the working depth, it can be separated into shallow and deep reduced tillage (Townsend et al., 2016). No-tillage (also referred to as zero-tillage) has the lowest soil disturbance among all tillage practices; the seed is sown directly to the soil with only little seedbed

preparation in the seed row. The present thesis focussed on conventional and reduced tillage; the following paragraphs therefore focus on these two tillage practices.

Soil compaction and tillage practices are mutually dependent and influence each other. In conventional tillage, the lifting and inversion of the topsoil for the entire working depth (usually between 20 and 40 cm) results in a loosened soil (cf. Figure 2.3). Former topsoil compaction may be removed, i.e. dry bulk density and penetration resistance are reduced after tillage (e.g. Koch et al., 2008; Afzalinia and Zabihi, 2014). Otherwise, conventional tillage often decreases the soil structure and aggregation (e.g. Tebrügge and Düring, 1999; Vogeler et al., 2006; Daraghmeh et al., 2009). Compared to less disturbed/tilled soils, conventionally tilled soils additionally have a reduced amount of biopores, infiltration rate, saturated hydraulic conductivity and biological activity (e.g. D'Haene et al., 2008; Alvarez and Steinbach, 2009; Capowiez et al., 2009; Jakab et al., 2017). Moreover, the loosened topsoil is unstable, i.e. the load bearing capacity is reduced, resulting in less favourable conditions for field traffic (e.g. Horn, 2004; Zink et al., 2010). Any wheeling activity will again result in soil compaction, even with low wheel loads or high contact area.

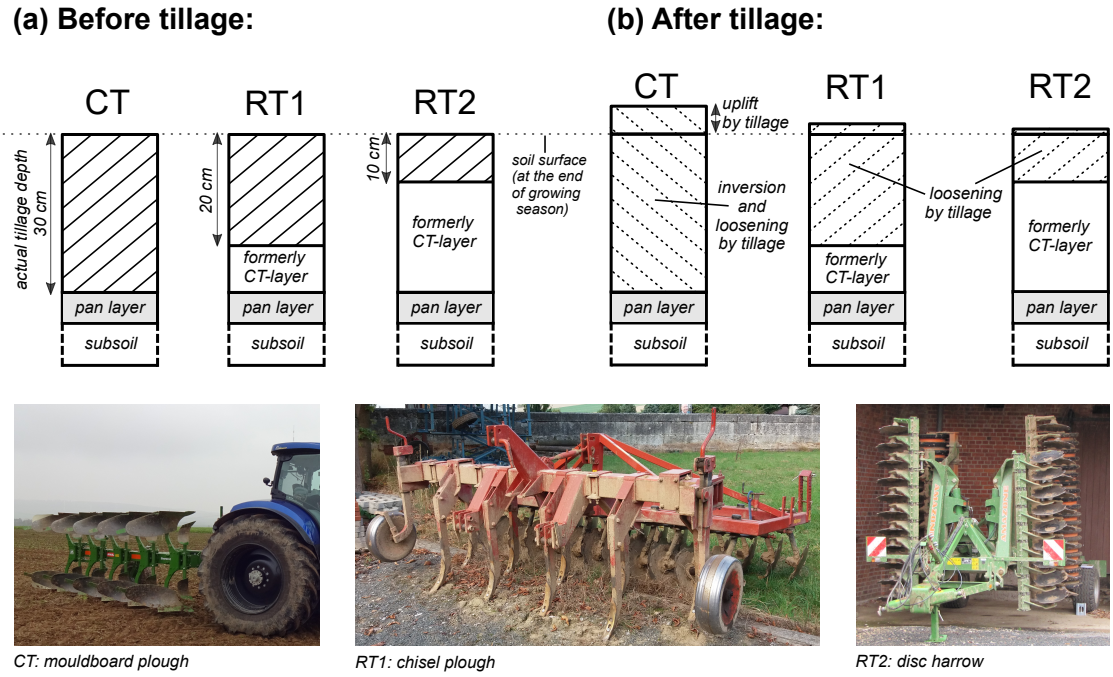

Figure 2.3: Schematic illustration of tillage effects on topsoil loosening and inversion.

The effects of reduced tillage on soil compaction are more complex. They depend on the type of reduced tillage practice, the period since the method was applied (short vs. long term), soil properties (e.g. soil texture, moisture, organic matter) and weather conditions (e.g. Horn, 2004; Bogunovic et al., 2018). Several studies reported that the low loosening effect leads to an improved soil structure and soil aggregation (e.g. Rasmussen,

1999; Alvarez and Steinbach, 2009; Daraghmeh et al., 2009; Capowiez et al., 2012; Lipiec et al., 2015). Reasons are increased biological activity (Tebrügge and Düring, 1999) and remaining existence of aggregates, pores and burrows (D'Haene et al., 2008). The result is an increased infiltration rate, saturated hydraulic conductivity and air permeability compared to conventional tillage (e.g. Horn, 2004; Bhattacharyya et al., 2006; Vogeler et al., 2006; Alvarez and Steinbach, 2009; Gozubuyuk et al., 2014; Parvin et al., 2014). Furthermore, reduced tilled soils exhibit a higher load bearing capacity, i.e. the soil compaction risk through field traffic is lower (e.g. Wiermann et al., 2000; Salem et al., 2015). Additionally, reduced tillage enables the use of smaller machinery with simultaneously increased working width (Holland 2004; Morris et al. 2010), reducing the area affected by field traffic and thus by soil compaction. In addition, the farmer saves fuel and working-time (e.g. Nail et al., 2007; Lahmar, 2010).

Apart from to the positive effects of conservation tillage, more negative properties such as higher dry bulk density and higher penetration resistance compared to conventional tillage are frequently reported (e.g. Koch et al., 2009; Afzalinia and Zabihi, 2014; Gozubuyuk et al., 2014; Schlüter et al., 2018). Due to the low loosening effect of reduced tillage, the compaction effect of natural soil settlement, soil compression by root and plant growth, field traffic etc. cannot be fully removed, resulting in a denser layer compared to conventional tillage. Further negative aspects of long-term reduced tillage may be the stratification of nutrients and soil organic matter (Deubel et al., 2011; Lou et al., 2012) and an increase in weed pressure (Bajwa, 2014; Nichols et al., 2015). The effects of tillage intensity on biomass production and yield are ambiguous (e.g. Verch et al., 2009; Van den Putte et al., 2010; Townsend et al., 2016), depending on e.g. crop rotation, weather conditions and soil moisture.

In tilled soils, a compacted layer directly beneath the tillage depth can develop. This layer is mostly referred to as "pan layer", "hard pan", "plough pan" or "disk-pan" (Alakukku et al., 2003; Birkás et al., 2004; Bogunovic et al., 2018). The pan layer exhibits a high dry bulk density, reduced (vertical) infiltration and often a platy structure (Alakukku et al., 2003; Capowiez et al., 2009; Dörner and Horn, 2009). It develops from the shearing effects of the tillage implements; in case of plough in the furrow, the applied contact area pressure and shearing effects of the wheels in the furrow additionally cause this compacted layer (e.g. Munkholm et al., 2005; Weisskopf et al., 2010). Due to the wheeling in the furrow while applying mouldboard ploughing, the pan layer is usually more pronounced in conventional tillage.

Reducing the tillage depth or a changing from conventional to conservation tillage can lead to a "lost horizon" or "abandoned plough pan" (Brunotte, 2007; Brunotte et al., 2015; Schlüter et al., 2018). The "lost horizon" develops between the former tillage depth of the plough (e.g. 30 cm) and the new, reduced tillage depth (e.g. 20 cm). The unstable hori-

zon cannot withstand the applied stress by e.g. harvest and will be compressed. Since no further loosening will be conducted at this depth, a compacted layer is often formed directly below the new tillage depth (Rasmussen, 1999).

The described tillage practices are conducted in the topsoil. For the subsoil, typical tillage practices are deep tillage and subsoiling (e.g. Schneider et al., 2017). Any kind of deep loosening, however, is expensive (Chamen et al., 2015) and its effect on e.g. yield is controversy discussed (Schneider et al., 2017). Additionally, deep loosening results in unstable soil conditions prohibiting wheeling with heavy machinery after loosening (Raper, 2005; Botta et al., 2006).

2.3 Soil compaction - modelling approaches

Since soil compaction measurements are expensive and time-consuming, various approaches and models have been developed to describe the soil compaction process and its effects. The objectives of soil compaction modelling are to

(i) calculate the tyre-soil surface interactions (e.g. contact area),
(ii) model the stress propagation in the soil,
(iii) model the soil strength/precompression (including the derivation of soil properties required for soil compaction modelling) and
(iv) calculate the natural susceptibility of soils to compaction and the soil compaction risk.

Table 2.1 gives an overview of frequently used approaches and models in soil compaction research. Reviewing the available literature showed that one focus in soil compaction modelling is contact area modelling. Knowledge of the contact area is important as it determines the area affected by wheeling and is necessary to calculate the contact area pressure (cf. chapter 2.1). Calculating contact area is complex as it depends on the tyre properties (e.g. tyre width, tyre inflation pressure), but also on soil properties (e.g. soil texture, soil moisture). The most common approaches for calculating the contact area are those of Keller (2005), Diserens (2002, 2009) and Diserens et al. (2011).

Modelling soil stress and stress distribution is closely linked to the modelling of contact area. It is rather challenging to model soil stress as soils are not homogenous but layered with varying properties such as soil structure, soil moisture and soil density. Early approaches by e.g. Fröhlich (1934) and Söhne (1953, 1958) explained some general rules for stress propagation in the soil. For instance, they introduced the "concentration factor" which enables the description of soil stress propagation depending on soil moisture. De-

fossez and Richard (2002) and Keller et al. (2007) give a detailed overview of early studies regarding contact area and stress propagation in the soil. Based on the early studies, new equations from e.g. Koolen et al. (1992), Keller (2005), Keller et al. (2007) and Schjønning et al. (2008) were developed to enhance the description of stress propagation in the soil.

Another focus is on modelling soil strength (or precompression stress). It is assumed that a given soil has an internal soil strength (in kPa) that is able to withstand the applied stress (in kPa) by field traffic (e.g. Horn et al., 1995). This value is called "precompression" or "soil strength". According to the precompression concept, soil compaction occurs when the applied soil stress exceeds the actual soil strength/precompression. Several pedotransfer functions are available to model the precompression of soils (e.g. Lebert and Horn, 1991; Rücknagel et al., 2012; Schjønning and Lamandé, 2018). Vorderbrügge and Brunotte (2011a) listed further pedotransfer functions to calculate the precompression stress. Although the precompression concept and the measurement of precompression is discussed contrary (e.g. Vorderbrügge and Brunotte, 2011b; Keller et al., 2012; Schjønning et al., 2016), it is the most commonly applied approach for calculating the soil strength.

Modelling the susceptibility to soil compaction and the potential soil compaction risk is another focus in soil compaction research. One frequently used method is the comparison of soil strength/precompression stress with soil stress; if the soil stress is higher than the soil strength, the soil will be compressed and soil functions will decrease (e.g. Horn and Fleige, 2003; Stettler et al., 2014; Rücknagel et al., 2015). Jones et al. (2003) published another approach. They used a classification scheme to calculate first the susceptibility and afterwards the vulnerability to soil compaction. Troldborg et al. (2013) used a Bayesian Belief Network, which includes available data and expert knowledge for soil compaction risk assessment.

Further soil compaction modelling approaches focus on the modelling of crop yield losses due to soil compaction (Arvidsson and Håkansson, 1991), the modelling of traffic-related changes in dry bulk density (O'Sullivan et al., 1999) and cone index (Canillas and Salokhe, 2002), the combined modelling of soil compaction and the least limiting water range concept (Keller et al., 2015), the modelling of traction performance to reduce slippery (Battiato and Diserens, 2017), the development of 3D finite element models (González Cueto et al., 2013) and the modelling of the stress distribution under rubber tracks (Keller and Arvidsson, 2016).

Table 2.1: Frequently used approaches and models in soil compaction research.

Reference	**Aim, focus and remarks**	**Input parameters**
Koolen et al. (1992)	- stress propagation in the soil - soil stress calculation for any soil depth	- wheel load, tyre inflation pressure, concentration factor by Fröhlich 1934 and Söhne 1953, 1958
Lebert and Horn (1991); DVWK 234 (1995)	- calculation of precompression stress - 5 pedotransfer functions	- soil texture, organic matter, dry bulk density, air capacity, available water, non-plant available water, saturated hydraulic conductivity, cohesion, angle of internal friction
DIN V 19688 (2011)	- calculation of precompression stress - 3 pedotransfer functions	- soil texture, organic matter, dry bulk density, air, available water, non-plant available water capacity, cohesion angle of internal friction
Jones et al. (2003)	- calculation of susceptibilty to subsoil compaction - method for vulnerability calculation - classification in low, moderate, high, very high susceptibility	- *for susceptibility*:soil texture, packing density - *for vulnerability*: soil moisture or potential soil moisture deficit
Horn and Fleige (2003)	- calculation of precompression stress (using the 5 pedotransfer functions from Lebert and Horn 1991) - calculation of stress propagation (using Newark) - calculation of changes in air conductivity, available water capacity due to exceeding precompression stress	- soil texture, organic matter, dry bulk density, air, available water, non-plant available water capacity, saturated hydraulic conductivity, cohesion angle of internal friction
van den Akker (2004)	- calculation of soil stress - calculation of maximum allowable wheel load - named 'SOCOMO'	- rut depth, tyre width, tyre inflation pressure, soil texture, dry bulk density, soil moisture
Keller (2005)	- calculation of contact area - calculation of stress distribution - assumed shape of the contact area is a super ellipse (described by Hallonbrog 1996)	- wheel load, tyre width, tyre inflation pressure, recommended tyre inflation pressure, tyre diameter
Keller et al. (2007)	- calculation of soil stress - calculation of soil displacement etc. - named 'SOILFlex' - excel-spreadsheet: user can select different models to calculate e.g. the normal stress (O'Sullivan et al. 1999, Keller 2005) or the stress-strain model (Larson et al. 1980, Bailey and Johnson 1989, O'Sullivan and Robertson 1996)	- varying input parameter, depending on selected models
Schjønning et al. (2008)	- calculation of tyre footprint (contact area) - calculation of stress distribution - named 'FRIDA' - refinement of Keller 2005: footprint by super ellipse, stress distribution by combined exponential and power-law function	- wheel load, tyre width, tyre inflation pressure, recommended tyre inflation pressure, tyre section height, tyre diameter
Diserens (2009)	- calculation of contact area - different equations for cross-ply and radial tyres, but only for trailer tyress	- width of the tyre, wheel load, tyre inflation pressure

Continued on next page

Table 2.1 – *Continued from previous page*

Reference	Aim, focus and remarks	Input parameters
Diserens et al. (2011)	- calculation of contact area - different equations, but only for traction tyres	- tyre size (section width, outer diameter), wheel load, tyre inflation pressure
Rücknagel et al. (2012)	- calculation of precompression stress depended on soil water content	- precompression stress at pF 1.8, soil moisture (in % field capacity), soil texture class
Rücknagel et al. (2013)	- calculating the effect of gravel content on precompression stress	- soil texture class, gravel content
Troldborg et al. (2013)	- calculation of soil compaction risk - developed a Bayesian Belief Network for soil compaction risk assessment - combination of available data and expert knowledge	- *soil and site characteristics*: bulk density, clay content, sand content, texture, packing density, soil structure, soil conductivity, organic matter content, stone content, site drainage, soil depth, inherent susceptibility, compaction vulnerability - *climate and soil wetness*: soil wetness, precipitation, evapotranspiration, temperature, groundwater table, time of the year - *land management*: vegetation type, machinery groups, machinery weight, number of passes per season, tyres, exposure from machinery, animal type, livestock density, livestock or machinery present, exposure from livestock, total exposure
Stettler et al. (2014)	- named 'Terranimo' - calculation of soil strength - calculation of soil stress - soil compaction risk evaluation - web-application with two versions: Terranimo light and Terranimo expert - application of Schjønning et al. 2008 - unpublished pedotransferfunctions to calculate soil strength (from clay content and soil water suction)	- *for Terranimo light*: clay content,soil water suction, wheel load, tyre inflation pressure - *for Terranimo expert additionally*: tyre description (tyre category, manufacturer, tyre name, dimension), soil profile description (horizons, sand, silt, clay content, organic matter content, dry bulk density, water content/matrix potential)
Schjønning et al. (2015a)	- calculation of tyre footprint (contact area) - calculation of stress distribution - developed a stepwise calculation procedure to - enable the contact area and stress distribution calculation as performed by FRIDA, with the FRIDA parameters	- tyre carcass volume (e.g. derived from wheel load and width of the tyre), wheel load, tyre deflection, actual tyre inflation pressure, recommended tyre inflation pressure
Rücknagel et al. (2015)	- calculation of soil strength - calculation of soil stress - soil compaction risk assessment (SCI; soil compaction index) - application of Rücknagel et al. 2012, 2013, Koolen et al. 1992	- soil texture class, gravel content, soil moisture (in % field capacity), precompression stress at pF 1.8, wheel load, tyre inflation pressure
Lorenz et al. (2016)	- calculation of soil compaction risk - expert based model - use of decision matrix	- soil texture, soil moisture (in % field capacity), wheel load, tyre inflation pressure, contact area pressure, amount of wheel passages, percentage of wheeled area
Schjønning and Lamandé (2018)	- developed new pedotransfer functions to calculate of precompression stress	- clay content, dry bulk density, pF-value/matrix potential

Although there are several approaches and models focussing on soil compaction issues, only few of them are applied to a spatial scale. The studies dealing with spatial soil compaction modelling focus on modelling

(i) natural soil strength/soil precompression
(ii) soil stress (for assumed machinery setup)
(iii) soil compaction risk
(iv) wheel load carrying capacity
(v) traffic intensity

Table 2.2 gives an overview of available models and approaches for soil compaction modelling from field to supra-regional scale. Most available spatial studies focus on the calculation of soil strength/precompression, which is contrasted by soil stress (e.g. Horn et al., 2002, 2005; Horn and Fleige, 2009). The value of soil stress is often assumed, e.g. as a constant soil stress of 60 kPa in 40 cm depth (e.g. Horn and Fleige, 2009). The resulting maps show the susceptibility to soil compaction (Jones et al., 2003; Lebert, 2010), changes in air capacity and air conductivity (Horn et al., 2002, 2005) and the potential soil compaction risk (D'Or and Destain, 2014). Furthermore, based on the calculation of the soil strength the maximum allowable soil stress can be calculated. It is referred to as "wheel load carrying capacity" (van den Akker, 2004; Lamandé et al., 2018). Maps of the wheel load carrying capacity are available for the Netherlands (van den Akker, 2004) and for Europe (Schjønning et al., 2015b; Lamandé et al., 2018). The calculated wheel load carrying capacities, however, apply only to one (assumed) soil moisture state and one (assumed) tyre setup (static wheel load, tyre inflation pressure, contact area).

Another important issue in spatial soil compaction modelling is the calculation of traffic intensity (e.g. cumulative wheel load, amount of wheel passage). Kroulík et al. (2009) mapped the wheel track area and wheel passages for an entire cropping season. Using a more advanced approach, Duttmann et al. (2013) modelled the wheel passages, maximum wheel load and maximum mean contact area pressures for maize harvest on different fields. In a next step, Duttmann et al. (2014) modelled the soil strength and stress distribution in 2D and 3D applying the approach from Horn and Fleige (2003). Based on Duttmann et al. (2013, 2014), Augustin et al. (subm) developed a model (FiTraM; Field Traffic Model) which enables the automatic calculation of field traffic intensity for any field traffic (e.g. tillage, sowing, harvest).

Table 2.2: Spatial approaches and models in soil compaction research.

Reference	Aim, focus and product	Used method
Horn et al. (2002)	- maps for Germany: precompression stress, changes in air capacity and air conductivity by applied stress	- application of Horn and Fleige (2003); DVWK (1995)
Jones et al. (2003)	- map of subsoil susceptibility for soil compaction for Europe	- application of Jones et al. (2003)
van den Akker (2004)	- wheel load bearing capacity map of the Netherlands	- used SOCOMO (van den Akker, 2004)
Horn et al. (2005)	- precompression stress, contact area pressure (and their relationship) and change in air conductivity soil maps for Europe, Germany and for a farm /or soil compaction risk (ratio between soil strength and actual soil stress)	- application of Lebert and Horn (1991), DVWK (1995), Horn and Fleige (2003)
Horn and Fleige (2009)	- maps of precompression, change in air capacity, soil stress by 60 and 90 kPa subsoil stress	- application of Lebert and Horn (1991), DVWK (1995), Horn and Fleige (2003)
Kroulík et al. (2009)	- mapping spatial pattern of traffic intensity - wheel track area and wheel passages for entire cropping season	- GPS tracking and tyre measurements (tyre width)
Lebert (2010)	- maps of susceptibility to soil compaction for varying field capacities for entire Germany	- application of Lebert and Horn (1991), DVWK (1995) and DIN V19688 (2002)
van den Akker and Hoogland (2011)	- calculate the soil vulnerability and susceptibility to soil compaction in the Netherlands - calculate the soil strength and the allowable wheel load for the Netherlands	- application of Jones et al. (2003) - application of van den Akker (2004)
Duttmann et al. (2013)	- modelling spatial pattern of traffic intensity - maps of wheel passages, maximum wheel load, maximum mean contact area pressure for maize harvest	- application of Diserens (2002, 2009) - recorded GPS-data and time stamps
Duttmann et al. (2014)	- modelling spatial pattern of traffic intensity - maps of wheel passages, wheel load, mean contact area pressure, soil strength, soil stress(2D and 3D) for maize harvest	- application of Diserens 2002, 2009; Horn and Fleige 2003 - recorded GPS-data and time stamps
D'Or and Destain (2014)	- calculation of precompression stress maps and soil compaction risk maps for Belgium	- application of Horn and Fleige (2003), Keller (2005), Schjønning et al. (2008)
Schjønning et al. (2015b)	- mapping wheel load carrying capacity for Europe	- application of Terranimo algorithm (not further explained, referenced); for a tyre with a diameter of 800 mm, soil depth of 25 cm and traffic at a matric potential of - 300hPa
Lamandé et al. (2018)	- mapping wheel load carrying capacity for Europe (for rubber tracks and wheels)	- application of Frida (Schjønning et al., 2008, 2015) and Schjønning and Lamandé (2018) for soil strength calculation - tyre: 1050/50R32, at a depth of 35 cm, matric potential of -50 hPa
Ledermüller et al. (2018)	- mapping soil compaction risk for a feral state (Lower Saxony) in Germany	- application of Lorenz et al. (2016)
Augustin et al. (subm)	- modelling spatial pattern of traffic intensity - maps of wheel passages, wheel load and contact area pressure	- named FiTraM (Field traffic model) - application of Koolen et al. (1992) - automatically calculate the field traffic intensity on given GPS-coordinates and machinery setup

Chapter 3

Study areas, Materials and Methods

For the regional soil compaction risk modelling, the two regions "Adenstedt" (Lower Saxony) and "Kummerow" (Mecklenburg-Vorpommern) served as study areas. For field scale soil compaction analyses one 5.5 ha field was selected in the Adenstedt-region (Figure 3.1). This field was intensively investigated during each year since 2014.

3.1 Adenstedt (field scale and regional scale)

The study area "Adenstedt" is located in the southern part of Lower Saxony, Germany (Figure 3.1). Mean annual precipitation is 741 mm and mean annual temperature is 9.4°C (weather station Hildesheim, 1978-2008, DWD (2017); cf. Figure 3.2). The study area has a total size of 336 km^2. It is part of the "Innerstebergland", the northern area of the German low mountain range. The geology of the Adenstedt-region is complex and exhibits areas with variegated sandstone and shell limestone (Triassic), limestone (Jurassic and Cretaceous), glacial till (from the Saalian ice age) and loess depositions from the last ice age (Weichselian; Lüttig (1957)). According to the complex geology, the soil parent material is heterogeneous; it ranges from deeply weathered loess along the hill slopes, loamy deposits in the valleys to shallow layers of sandy and clayey weathering residuals at the hilltops. Typical soil types are (stagnic) Luvisols, Cambisol and for the hilltops Leptosol and Regosol. Forests cover the hilly areas and areas with shallow soil development, whereas intensive agriculture predominates the highly productive loess soils. Common crop types are sugar beet (*Beta vulgaris L.*), winter wheat (*Triticum aestivum L.*) and winter barley (*Hordeum vulgare L.*). The introduction of the EEG (Erneuerbare Energien Gesetz; renewable energy law) was accompanied by an increasing number of biogas power stations; a process which was associated with a rising share of silage maize (*Zea mays L.*) cultivation in the study area (Destatis, 2006, 2016).

Within the study area "Adenstedt" one field was selected for further investigation of tillage effects on soil compaction at field scale (Figure 3.1). The width of the field is approx.

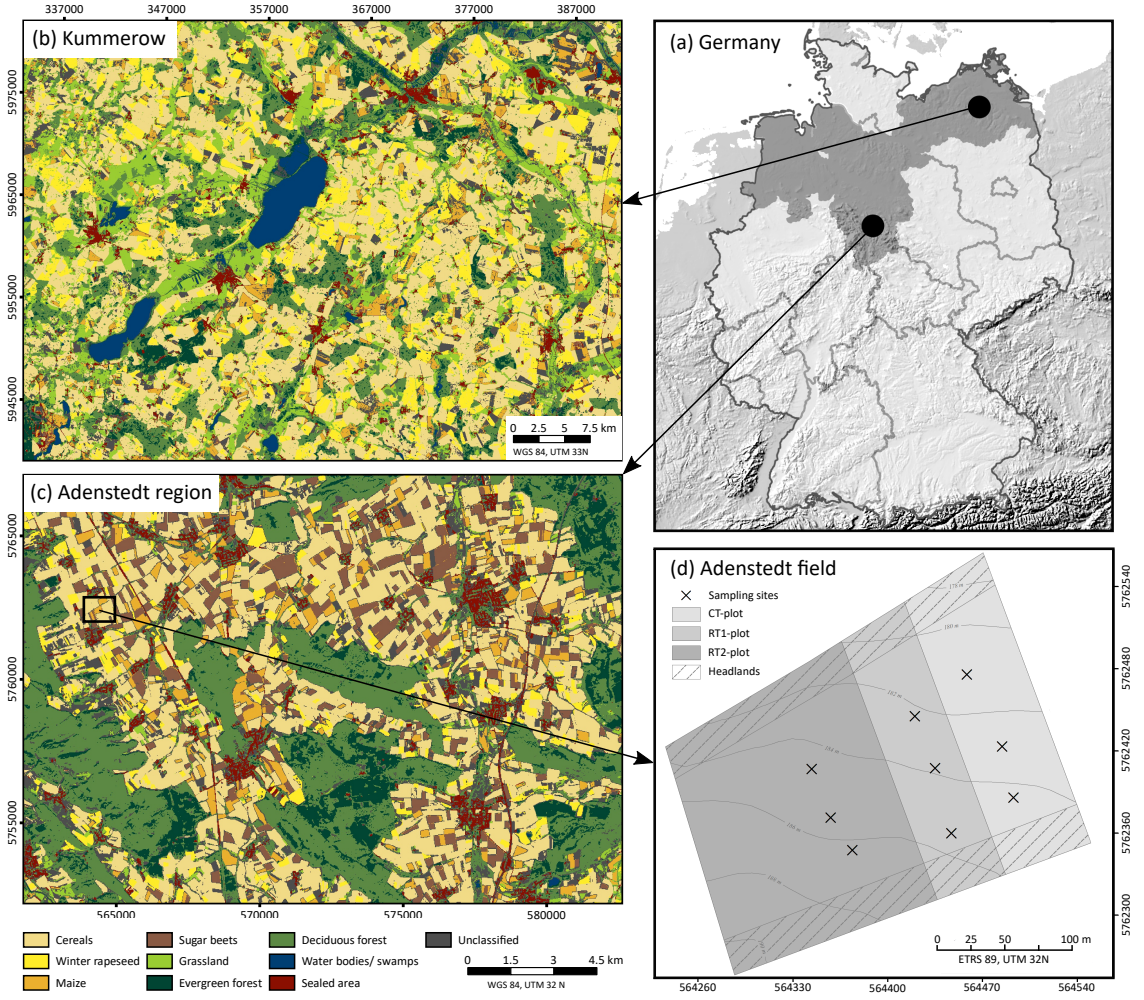

Figure 3.1: Study areas Kummerow (b), Adenstedt (c) and the selected field in Adenstedt (d).

278 m, the length varies between approx. 173 m (west) and 224 m (east). The total area is 5.5 ha. Slope varies between 0.6 and 5.4°, height between 177 and 191 m (AMSL). Soil type is stagnic Luvisol (WRB 2014) developed on deeply weathered loess. Soil texture class is silt loam, whereas silt content predominates ($\sim$ 80 %) and sand content is low ($\sim$ 3 %; Figure 3.3).

Until 1996, the entire field was conventionally tilled with a mouldboard plough to a depth of 30 cm. Since 1996, three different primary tillage practices divided the field into three plots: the eastern part of the field was tilled by conventional tillage (CT-plot) further on, the middle and western plots of the field were cultivated with reduced tillage (RT-plots). The degree and depth of soil treatment differed between the two RT-plots. In RT1 (middle plot) a chisel plough with a working depth of $\sim$20 cm was used; in RT2 a disc harrow with a working depth $\sim$10 cm (Figure 2.3, 3.1). All other field operations (e.g. sowing, spraying, harvesting) were nearly identical for the three plots. The separation of the field was maintained until October 2014. A sugar beet harvest under wet weather and soil conditions and continued

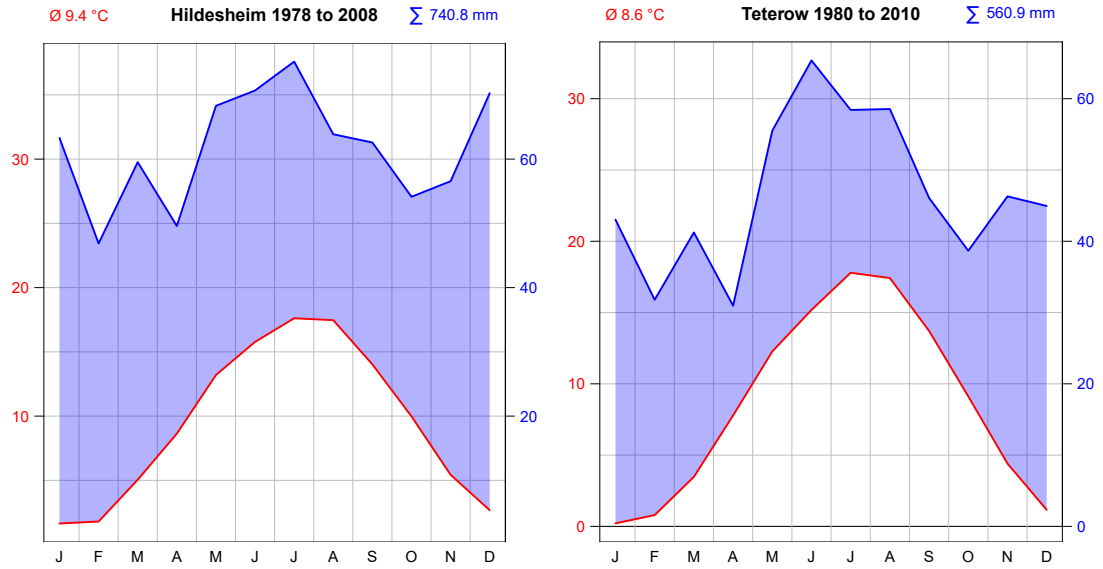

Figure 3.2: Climate charts of both study areas: Hildesheim, Lower Saxony (left) and Teterow, Mecklenburg-Vorpommern (right).

wet weather conditions after harvest impeded the use of reduced primary tillage for seedbed preparation. Thus, the entire field was tilled with a mouldboard plough to a depth of ∼30 cm in October 2014. Tilling fields with a mouldboard plough which were under reduced tillage for several years is referred to as "one-time inversion tillage", "occasional tillage" or "strategic tillage".

In the following years, the threefold division was reintroduced and continued until today. A typical crop rotation for this field was "winter wheat - sugar beet- winter wheat - winter wheat - sugar beet - oat (*Avena sativa L.*)" until 2014. Since October 2014, crop rotation is "winter wheat - maize - winter wheat - sugar beet".

3.2 Kummerow (regional scale)

The second study area "Kummerow" is located in the centre of Mecklenburg-Vorpommern and is part of the Northern German Plain. Mean annual precipitation is 560 mm and mean annual temperature is 8.6 °C (weather station Teterow, 1980-2010, DWD (2017); cf. Figure 3.2). The study area has a total size of 2,500 km^2. Parent material for soil development is glacial till characterised by a heterogeneous distribution of soil substrate with predominating sandy and loamy soil texture classes. The surface is hilly and structured by the typical morphological forms of the glacial series such as kettles and moraines. Numerous small rivers (e.g. Peene, Tollense) and lakes (e.g. Lake Kummerow, Lake Malchin) shape the landscape. Alluvial deposits and bogs typically form along the shorelines of these waters (and the former river courses). Luvisol, Cambisol, Fluvisol, Gleysol and Histosol are typical

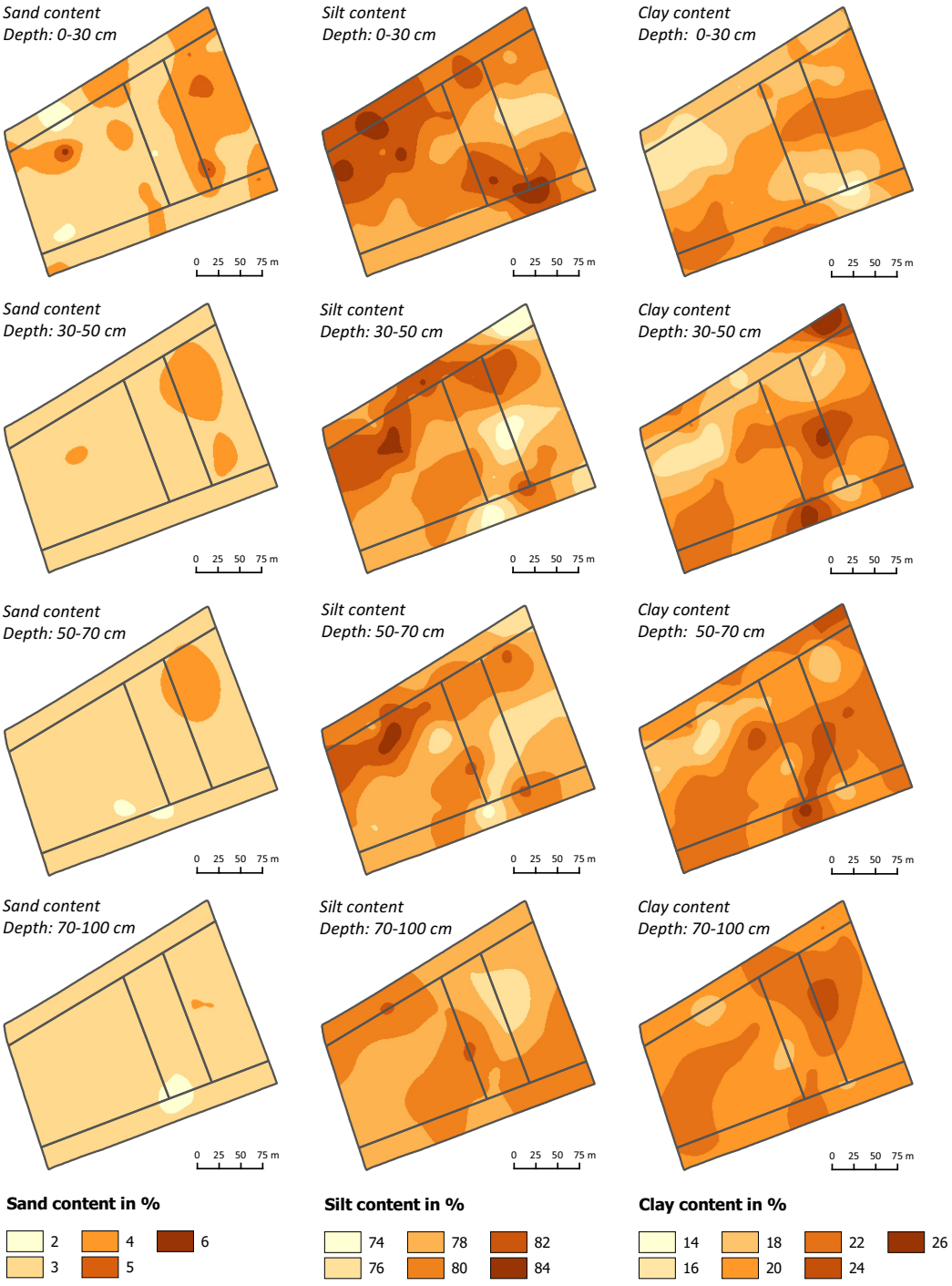

Figure 3.3: Soil texture distribution of the selected field in Adenstedt.

soil types in Kummerow. The soils are intensively used for agriculture; around 50% of the total area are arable land (see Table 6.6). The most common crop types are winter wheat and rapeseed. The study area "Kummerow" was selected to demonstrate the transferability of the developed soil compaction risk model (research question 3).

3.3 Fieldwork and measurements

Since March 2014, several field campaigns have been carried out in Adenstedt to collect soil samples and conduct soil measurements. The focus was on the description of soil physical properties and their spatial distribution at field scale. Various field methods were used for this purpose: collection of disturbed soil samples with a stainless steel auger (Pürckhauer), collection of undisturbed soil samples using rings (100 cm^3 and 250 cm^3), infiltration rate measurements using mini-disc infiltrometer, penetration resistance measurements using a penetrologger, coordinates collection using total station and RTK-GPS. Collecting undisturbed soil samples and measuring infiltration rate aimed to describe functional soil physical properties at selected points. Collecting disturbed soil samples and measuring penetration resistance aimed to describe the spatial variation of soil properties at the entire field. Furthermore, crop type mapping was conducted in the region Adenstedt.

Disturbed soil samples

An auger (Pürckhauer) was used to collect disturbed soil samples to a depth of 1 m for the depth intervals from 0-30 cm, 30-50 cm, 50-70 cm and 70-100 cm. The disturbed soil samples were used to analyse the soil texture (sand, silt, clay content) and soil organic matter. To describe the spatial distribution of both soil properties, 60 points were selected for soil sampling. The points for soil sampling were calculated using the stratified random point calculation scheme by the software environment "Geospatial Modelling Environment" (GME; Beyer (2012)).

Undisturbed soil samples

Undisturbed soil samples were collected to determine the volumetric soil water content, the dry bulk density and the saturated hydraulic conductivity in the laboratory. Core samples with a volume of 100 cm^3 and a diameter of 60 mm were used for measuring volumetric soil water content and dry bulk density. For measuring the saturated hydraulic conductivity core samples with a volume of 250 cm^3 and diameter of 84 mm were selected (cf. Figure 3.4). To collect the core samples, pits of approximately 1 m^2 were excavated to the desired depth. After levelling the pit surface, at least 5 samples were taken for each core size at each point.

Infiltration rate

The infiltration rate was measured in the field using mini-disc infiltrometer with a disc diameter of 4.5 cm (Decagon Devices). Depending on soil moisture, suction rates of 0.5 or 1.0 were applied. The measurements were performed at the same places and depths from which the undisturbed soil samples were taken. The soil surface was carefully prepared and levelled to obtain a close and stable contact between the soil and the mini-disc infiltrometer.

At least 4 measurements with an infiltration time of 6 to 10 minutes per measurement were performed at each point (cf. Figure 3.4).

Penetration resistance

The penetration resistance was measured using a penetrologger (Eijkelkamp, Penetrologger 06.15; cf. Figure 3.4) and a cone with a base area of 1 cm^2 and an angle of 60°. The penetrologger was pressed into the soil by hand to a minimum depth of 40 cm at a mean velocity of 2 cm/s. The penetration resistance was automatically recorded in 1 cm depth intervals. As penetration resistance is highly variable, 5 parallel measurements were conducted at each point. A minimum of 60 points distributed over the entire field was measured. The points to be measured were calculated using the stratified random point method and the software "Geospatial Modelling Environment" (GME).

Figure 3.4: Field equipment: Penetrologger (left), mini-disc infiltrometer (middle) and core samples (right).

Coordinates collection

The coordinates for all points and measuring sites were determined by the use of a total station (in 2014, Leica TCR 407) and RTK-GPS (since 2015, Leica Viva CS 10, GNSS GS08 plus). The exact position (spatial accuracy < 10 cm) was the basis for further spatial statistics.

Crop type mapping

To generate model input parameter for the regional soil compaction risk assessment, crop type mapping was carried out in both study areas. Crop type mapping distinguished between cereals (e.g. winter wheat, rye, and barley), winter rapeseed, maize, sugar beets and grassland. Both study areas were visited by car and actual crop types of several fields were mapped (Adenstedt = 200, Kummerow = 553). The group "Earth Observations and Modelling" (CAU Kiel) kindly provided crop type mapping data for the study area Kummerow.

3.4 Laboratory work and measurements

The collected soil samples (disturbed and undisturbed) were analysed in the laboratory of the Department of Geography at Kiel University. The disturbed soil samples were dried in the oven at 35°C before further analysis. Undisturbed soil samples were stored under cool (4°C) and dark conditions until measurement.

Soil texture

The soil texture was determined by the sieve and pipette method according to Köhn as described in Gee and Bauder (1986) and DIN ISO 11277 (2002). Sieving the oven dried (35°C) soil samples with a 2 mm sieve separated the coarse and fine soil. The fine soil was used for further soil texture analyses. Adding hydrogen peroxide (H_2O_2) destroyed organic matter content; adding sodium pyrophosphate ($Na_4P_2O_7$) led to a full dispersion. Afterwards, sand content (2000-63 µm) was measured by sieving, whereas silt (63-2 µm) and clay (< 2 µm) content were determined by pipetting.

Dry bulk density and volumetric soil water content

The small core samples (100 cm^3) were used to determine the dry bulk density and the volumetric soil water content (Blake and Hartge, 1986; Gardner, 1986). In the laboratory, the samples were weighted, dried at 105°C for 24 hours and weighed again. The dry soil weight in relation to the core sample volume represents the dry bulk density; the weight difference before drying and after drying and the known core volume allow the determination of the volumetric soil water content.

Saturated hydraulic conductivity

The saturated hydraulic conductivity was measured using the 250 cm^3 core samples. After complete saturation, the core samples were placed on a device (Ksat, UMS) that automatically measures and records the saturated hydraulic conductivity. The "falling head" method was selected for measurement (UMS, 2013).

3.5 Descriptive statistics and digital soil mapping

Volumetric soil water content, dry bulk density, saturated hydraulic conductivity

Arithmetic means for volumetric soil water content and dry bulk density were calculated based on the replicate measurements of the individual sampling points.

As saturated hydraulic conductivity and infiltration rate varies highly, both were $\log_{10}$ transformed to obtain a normal distribution. After $\log_{10}$ transformation, the geometric mean of the replicate measurements of the individual sampling points was calculated. Afterwards,

the arithmetic mean and standard deviation were calculated from the geometric mean values of the individual sampling points for each category and date. The two-sample t-test was used to test significant differences in arithmetic mean values using the statistical software environment "R" (R Core Team, 2017).

Penetration resistance and soil texture

Digital soil mapping was performed for penetration resistance and soil texture using the statistical software environment "R" (R Core Team, 2017) with the packages 'gstat' (Pebesma, 2004), 'sp' (Pebesma and Bivand, 2005; Bivand et al., 2013) and 'compositions' (Van den Boogaart et al., 2014).

Kriging with external drift was used to spatially predict the penetration resistance. In a first step, the arithmetic means for each centimetre were calculated based on the five replicate measurements at the individual points. In a second step, the penetration resistance was aggregated to depth intervals (e.g. 16 to 25 cm) by arithmetic mean calculation for each individual point. These aggregated values were used to create experimental variograms. Using a weighted least squares approach and additional manual adjustment by eyes approached the best fit of variograms (Oliver and Webster, 2014). The four different tillage/management zones (the three tillage treatments CT, RT1, RT2 and the headlands) served as categorical predictors for the external drift model. Based on the variogram models, kriging with external drift was computed with a target grid resolution of 1 m^2.

Compositional kriging was used to spatially map the sand, silt and clay content. This interpolation technique considers the restrictions that the sum of sand, silt and clay must not exceed 100 %.

For both, penetration resistance and soil texture, the model accuracy was evaluated by root mean square errors (RMSE) and coefficients of determination (r^2) computed from leave-one-out-cross-validation (LOOCV) errors.

3.6 Model development (SaSCiA)

The developed model for soil compaction risk assessment at regional scale (SaSCiA, chapter 6) was based on freely available software and data. The model was coded in "R" using the packages 'plyr' (Wickham, 2011), 'sp' (Pebesma and Bivand, 2005; Bivand et al., 2013), 'raster' (Hijmans, 2016) and 'rgdal' (Bivand et al., 2016).

Necessary input data are soil data, crop type data, weather information, machinery information and days of field traffic, whereas soil and crop type data must be provided as raster data. The soil map 1:200.00 (BUEK 200, BGR) served as input soil data. Land cover classification using remote sensing data (Landsat 8, Sentinel-2A) and crop type mappings

determined the present crop types for entire regions. The German Weather Service (DWD) provides weather information on a web-based platform (WebWerdis, DWD) on a daily basis. Reviewing the literature (e.g. Achilles et al., 2016; Götze et al., 2016; KTBL, 2017) and collecting manufacturer information (e.g. Grimme, New Holland) helped to define machinery and field traffic information.

SaSCiA contains different formulas to calculate the (moisture depended) soil strength and soil stress (Koolen et al., 1992; Horn and Fleige, 2003; DIN V 19688, 2011; Rücknagel et al., 2012, 2013, 2015). Furthermore, SaSCiA integrated the crop model "MONICA" (Nendel et al., 2011) to calculate daily soil moisture for varying depths. The SaSCiA-model generates daily maps of soil compaction risk for entire regions. The maps were visualised with QGIS (version 2.18.7).

Chapter 4

Spatial analysis of long-term effects of different tillages practices based on penetration resistance

Michael Kuhwald, Michael Blaschek, Robert Minkler, Yaroslav Nazemtseva, Malte Schwanebeck, Jan Winter and Rainer Duttmann
Soil Use and Management (2016), 32, 240-249, doi:10.1111/sum.12254
Received: May 2015, Accepted: December 2015

Abstract

Measuring penetration resistance (PR) is a common technique for evaluating the effects of field management on soils. This study focuses on the effects of long-term tillage on the spatial distribution of PR, comparing reduced and conventional tillage (CT) practices. The study site, located in Lower Saxony (Germany), has been subdivided into three plots, with one plot having been managed conventionally, whereas reduced tillage (RT) practices have been applied to the other two. In total, PR was measured at 63 randomly selected points. The PR data were stepwise interpolated using kriging with external drift. Core samples have been taken at 20 additional sites. The results show significant differences in PR between the different tillage practices. Within the conventionally managed plot, PR ranges to 2.3 MPa less in the topsoil than under RT. However, measured saturated hydraulic conductivity and amount of biopores at the depth of 30-35 cm are significantly greater under RT, indicating improved soil properties under RT. Comparisons between the headlands (HL) and the inner field point out the effects of intense field traffic in the HL, where maximum PR values of about 6 MPa have been measured. The spatial prediction of PR values show that long-term effects of different tillage practices result in clearly structured patterns between CT and RT and the HL. Combining extensive PR measurements and point measurements of additional soil properties supports an adequate interpretation of PR data and can lead to fieldwide derivation of soil functions influenced by field management.

Keywords

Penetration resistance patterns, kriging, conventional tillage, reduced tillage, soil physical properties

4.1 Introduction

The type of tillage practice, in particular the primary tillage method, affects soil properties such as bulk density, saturated and unsaturated hydraulic conductivity, aggregation, pore continuity and soil compaction (Strudley et al., 2008). Penetration resistance (PR) measurement data are widely used as indicators of the influence of tillage practices and traffic intensity on soil functions (Salem et al., 2015). Several studies investigated the effects of repeated wheeling over the same area on penetration resistance, or made a comparison of nontrafficked and trafficked areas (Alakukku, 1998; Carrara et al., 2007; Koch et al., 2008; Usowicz and Lipiec, 2009). It was pointed out that PR increases with increasing traffic intensity. PR values after wheeling is greater than those determined prior to wheeling(Aksakal and Öztas, 2010; Barik et al., 2014; Braunack and Johnston, 2014). Additional studies concerning the effects of different tillage practices on PR have been conducted, usually grouped into conventional tillage (CT), reduced tillage (RT) and zero-tillage practices (Alakukku, 1998; Taser and Metinoglu, 2005; Koch et al., 2009; Celik, 2011; Afzalinia and Zabihi, 2014; Gozubuyuk et al., 2014; Salem et al., 2015). It was found that CT results in smaller PR in the topsoil compared with reduced- and zero-tillage practices. However, the effects on other soil physical properties such as saturated hydraulic conductivity have been controversial. Most of the investigations were based on only a few point measurements; thus, it is difficult to transfer the findings from these measurements to field scale. A few studies have applied interpolation techniques to identify spatial patterns of PR (Kılıç et al., 2004; Aksakal and Öztas, 2010; Veronesi et al., 2012; Barik et al., 2014), but none of these considered different tillage practices. Studies that consider the combined effects of different tillage practices and traffic intensity with their spatial distribution at field scale have not been available until the present study was conducted. Therefore, a field-scale approach was used to detect spatial patterns resulting from the cumulative effects of different long-term tillage practices in the topsoil and subsoil, by comparing CT, RT and the headlands (HL), the areas with highest traffic intensity.

The objectives are as follows: (i) to spatially predict PR for the entire field considering the different tillage practices (CT, RT1, RT2) and traffic intensity (HL), (ii) to identify and compare spatial patterns of PR and (iii) to analyse the long-term effects of different tillage practices and traffic intensity considering PR.

4.2 Materials and methods

4.2.1 Study site and tillage practices

The study site is located in the southern part of Lower Saxony, Germany, close to the city of Hildesheim (52.008° N , 9.938° E). The soil type is Luvisol (FAO, 2014) derived from deeply weathered loess (Table 4.1). Soil texture class is silt loam with approximately homogenous sand, silt and clay content for the entire field.

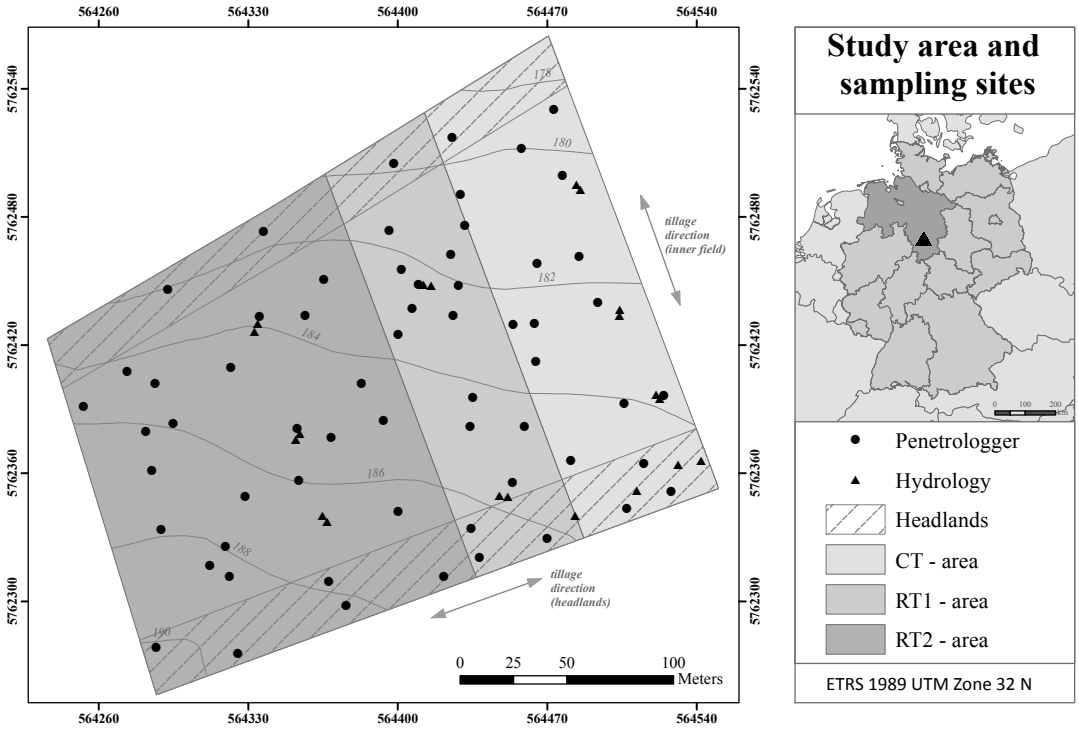

Figure 4.1: Study site and sampling points.

The 5.5-ha field is cultivated with a crop rotation consisting of sugar beet (*Beta vulgaris L.*), winter wheat (*Triticum aestivum L.*), oat (*Avena sativa L.*), winter wheat, sugar beet, winter wheat and winter wheat. Since 1996, the study area has been separated into three plots (Figure 4.1) that have been operated as follows:

Plot A: CT using a mouldboard plough up to 30 cm.
Plot B: RT1 using a chisel up to 20 cm.
Plot C: RT2 using a disc harrow up to 10 cm.

All other field operations during the year like seeding or spraying were the same for all three plots. The field study was conducted from 11 to 13 June 2014. Sugar beet (sowing at 23 March 2014) was the present field crop with a row distance of 60 cm.

Table 4.1: Profile information (location: in the middle of RT1).

Depth [cm]	Horizon [WRB]	Sand [%]	Silt [%]	Clay [%]	Carbon [%]	Bulk density [g/cm^3]
20	Ap1	2.05	79.86	18.09	1.20	1.33
30	Ap2	2.27	79.24	18.49	0.99	1.53
50	E	2.03	77.38	20.59	0.29	1.56
100	Bt	4.51	75.53	19.96	0.11	1.65

4.2.2 Sampling design and methods

For analysing the spatial distribution of penetration resistance, a design-based, stratified random sampling was used to define 63 measurement sites on the whole field.Therefore, the field was divided into nine parts based on the three tillage practices and relief position. Six measuring points were randomly calculated for each of these parts using Geospatial Modeling Environment software (Beyer, 2012) and ArcGIS 10.1 (ESRI). The boundary conditions were defined by a minimum distance of 10 m between each generated point and an additional distance of 10 m to known sampling points from an earlier investigation. The later measured field borders of the three tillage practices disagreed with the assumed borders for calculating the measurement sites, explaining the point distribution shown in Figure 4.1. A handheld GPS (Trimble Juno Sc) was used in the field to find the calculated points. At each site, five penetrologger measurements from the surface down to a depth of 80 cm were performed in an area of 1 m^2. A penetrologger (Eijkelkamp, Penetrologger 06.15) with a cone base area of 1 cm^2 and an angle of 60° was used. The penetrologger recorded the PR (MPa) in 1-cm intervals and was pressed into the soil by hand with a mean velocity of 2 cm/s. A scale bar on the display showed the actual velocity and signalizes when the penetration is too fast or too slow. In this case, the measurement was repeated. The location of the measured points was determined with an absolute accuracy of 20 cm using a total station surveying instrument (Leica TCR 407). Additionally, soil moisture was recorded at each of the 1 m^2 measurement sites with five replicates using a TDR (Trime-Pico 64; IMKO).

To characterize soil hydraulic properties, disturbed and undisturbed soil materials were taken from 20 sampling points distributed across the entire field (Figure 4.1). The selection of the sampling points considered the three different tillage practices, the HL and additional site-specific information from the farmer. In total, six sampling points were located in the CT plot, four in the RT1 plot, six in the RT2 plot and four in the HL. After removing the sugar beet manually, a pit of about 1 m^2 was excavated to a depth of 30 cm at each of the sampling points. Until 1996, the entire field was conventionally tilled with a mouldboard plough, which had a 30-cm tillage depth that resulted in a compacted layer (plough pan) at 30 - 35 cm. In the following years, plot B was tilled with a chisel down to a depth of 20 cm and plot C with a disc harrow down to a depth of 10 cm, while plot A still was conventionally tilled. Due to their smaller working depth, both RT practices were not able to reach the plough pan at 30 - 35 cm impeding a direct tillage influence. Thus, this soil layer can be used as an indicator for comparing the cumulative effects of 20 years of different tillage practices as shown by Horn (2004). He observed an improvement of soil functions in the depth of 30 - 35 cm after 7 years of implementation of RT compared with CT. Therefore, the surfaces of the 30-cm deep pits were prepared carefully for counting biopores and performing soil sampling. At all pits, the number of biopores with a diameter > 1 mm was counted horizontally at a 0.2 x 0.2 m frame, without further differentiation of the diameter. After counting the biopores, three undisturbed samples (100 cm^3) for determining bulk density and volumetric water content, along with five undisturbed samples for measuring saturated hydraulic conductivity (250 cm^3) were taken vertically. In addition, disturbed soil material was collected for soil texture analysis.

4.2.3 Laboratory analysis

Bulk density and volumetric water content were determined by drying the core samples (100 cm^3) for 24 h at 105°C and weighing them prior and after drying (Blake and Hartge, 1986; Gardner, 1986). The saturated hydraulic conductivity was measured with the UMS Ksat system using the falling head method. The disturbed soil samples were air-dried (35 °C), homogenized and sieved (< 2 mm) for further analysis. Particle size distribution was measured by applying the sieve and pipette method in accordance with KOEHN (Gee and Bauder, 1986). Carbon content was determined with a C/N-Analyser (EURO EA HEKAtech).

4.2.4 Descriptive and spatial statistics

For further analysis, arithmetic means were calculated from the replicates of each measuring site (three replicates of bulk density and five replicates of saturated hydraulic conductivity at each of the 20 sampling points). For penetration resistance, the arithmetic means of every measured centimetre were determined based on the five replicate measurements at each of the 63 measuring sites.

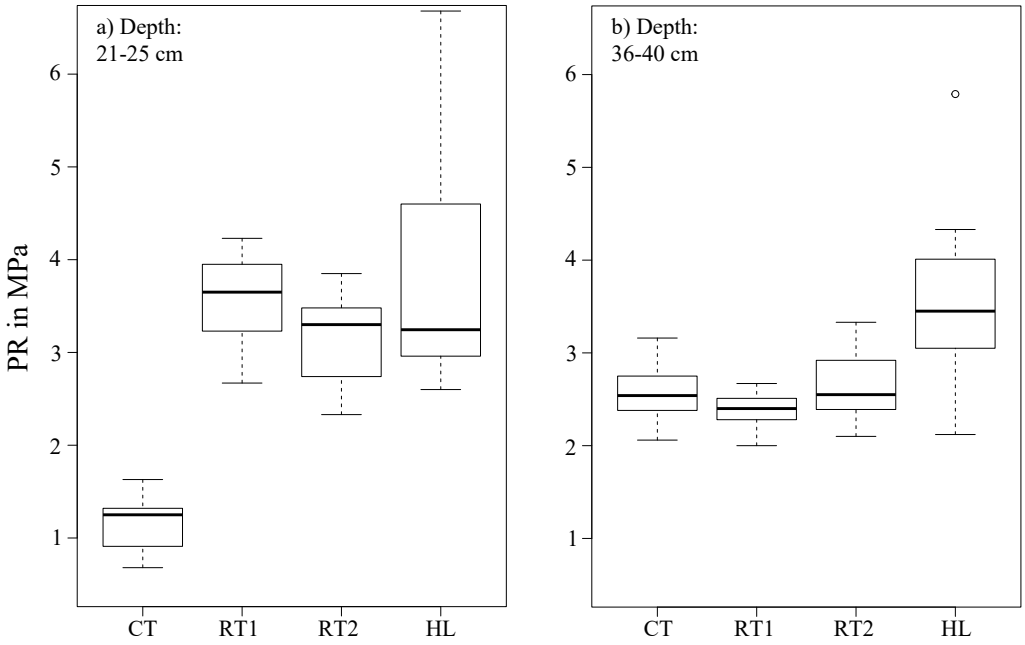

Figure 4.2: Box-whisker plots of measured penetration resistance for 21-25 cm (a) and 36-40 cm (b).

Statistical analysis of results was carried out using the statistical software environment 'R' (R Core Team, 2014) with the packages 'gstat' (Pebesma, 2004) and 'sp' (Pebesma and Bivand, 2005; Bivand et al., 2013). Significant differences in means were tested using Student's t-test. Normal distributions of the single data sets were checked by the Shapiro-Wilk test. To interpolate the penetration resistance, the acknowledged technique of kriging with external drift was used (Oliver and Webster, 2014). Two points had to be excluded from interpolation because of either missing coordinates or missing parallels. For the remaining 61 points, the arithmetic mean values of the five parallel measurements at each point were aggregated to 5-cm intervals. For each interval, the experimental

variogram was computed using spherical models and was then fitted to the empirical variances using weighted least squares and additional adjustment by eyes. Four categories (CT, RT1, RT2 and HL) were used for the external drift, following the point distribution as shown in Figure 4.2. Based on the variogram models, kriging with external drift was computed with a target grid resolution of 1 m^2. As an indicator for the degree of structured spatial dependency, the nugget-to-sill ratio (Cambardella et al., 1994) was calculated. Leave-one-out cross-validation served to assess the quality of the interpolation.

4.3 Results

4.3.1 Penetration resistance

The long-term effects of RT and CT practices on PR are shown in Table 4.2. To separate the effects of intense headland traffic, the comparison of the different tillage types only considers the data collected in the inner of the respective plots.Focusing on the topmost 30 cm, it is obvious that PR calculated for the two RT types significantly differ from CT. While the latter reveals a mean value of about 1.5 MPa, the mean PR under RT1 and RT2 exceeds this value by more than 1 MPa, reaching a maximum at 4.8 and 4.3 MPa. Below 30 cm, the differences in PR disappear.

Table 4.2: Statistical characteristics of penetration resistance (in MPa) measured under conventional and reduced tillage and in the headlands.

	CT [n = 13*]	**RT1** [n = 13*]	**RT2** [n = 21*]	**HL** [n = 15*]	**IF** [n = 47*]
Depth from 0 to 30 cm					
Mean	1.46	2.46	2.44	2.89	2.17
Median	1.40	2.41	2.53	2.72	2.08
Minimum	0.48	0.49	0.43	0.56	0.43
Maximum	3.36	4.81	4.26	6.87	4.81
SD	0.48	0.99	0.90	1.25	0.95
Depth from 31 to 50 cm					
Mean	2.48	2.43	2.70	3.28	2.57
Median	2.44	2.41	2.63	3.07	2.50
Minimum	1.43	1.88	2.01	1.78	1.43
Maximum	4.07	3.36	4.08	5.97	4.08
SD	0.40	0.31	0.42	0.99	0.41
Depth from 51 to 80 cm					
Mean	2.85	2.91	2.94	2.84	2.91
Median	2.60	2.75	2.89	2.57	2.77
Minimum	1.68	1.45	1.79	1.53	1.45
Maximum	4.95	5.20	4.44	5.18	5.20
SD	0.78	0.84	0.51	0.84	0.70

*Five replicates for each site taken in an area of 1 m^2 around a centre point. CT, conventional tillage; RT1, reduced tillage 1; RT2, reduced tillage 2; HL, headlands; IF, inner field

A further comparison revealed differences between inner field (IF) and HL. The IF includes all three tillage practices (CT, RT1, RT2) without HL. The HL are the sections in the front and back of the field, where highest traffic intensity occurs because of turning manoeuvres with the machinery

(Duttmann et al., 2014). The tillage treatment in the HL corresponds to the adjacent plots, as indicated by the different grey levels in Figure 4.1. Table 4.2 shows the effects of traffic intensity in the HL, where the largest values of PR were recorded. Mean PR in HL was calculated at 2.89 MPa for the topsoil. Compared with the arithmetic mean values received from the IF (2.17 MPa), PR in the HL showed an increase of about 33%. The same effect can be identified for the subsoil. At soil depths down to 45 cm, the mean PR values of the HL were still significantly greater ($P < 0.001$) than those calculated for the inner sections of the plots (Table 4.3).

Table 4.3: Significance of differences in mean penetration resistance comparing conventional tillage, reduced tillage practices and the headlands, subdivided into 5-cm depth intervals.

	Depth in cm															
	1-5	6-10	11-15	16-20	21-25	26-30	31-35	36-40	41-45	46-50	51-55	56-60	61-65	66-70	71-75	76-80
CT - RT1	n.s.	n.s.	*	**	**	**	n.s.	n.s.	n.s.	n.s.	n.s.	n.s.	n.s.	n.s.	n.s.	n.s.
CT - RT2	n.s.	n.s.	**	**	**	**	n.s.	n.s.	*	*	n.s.	n.s.	n.s.	n.s.	n.s.	n.s.
RT1 - RT2	n.s.	n.s.	n.s.	n.s.	*	n.s.	n.s.	*	*	*	*	n.s.	n.s.	n.s.	n.s.	n.s.
HL - IF	*	*	*	*	*	**	**	**	**	n.s.	n.s.	n.s.	n.s.	n.s.	n.s.	n.s.

n.s., not significant; *significant at $P < 0.05$; **significant at $P < 0.001$.

Figure 4.3 highlights the vertical changes in mean PR for each centimetre level down to a depth of 80 cm. While the PR profiles showed similar PR values increasing for all three tillage practices up to 1.8 MPa at a depth of 8 cm (Figure 4.3a), significantly greater penetration resistances under RT compared with CT were determined for all depth intervals down to 30 cm, reaching a maximum difference of nearly 1.9 MPa between 21 and 25 cm depth. In contrast to CT, where the PR decreased to 1.13 MPa, the mean PR under RT1 and RT2 increased to 3.6 and 3.2 MPa. Compared with the plough pan located between 31-35 cm, this PR corresponds to an increase by a factor of 1.3. According to the different working depths applied for RT1 and RT2, significant, yet slight differences ($P < 0.05$) in PR were observed. Below a depth of 35 cm, all tillage types showed similar courses of the PR profile lines with a continued increase in penetration resistance.

Figure 4.3b compares the PR in the IF with the HL, showing significant ($P < 0.001$) deviations between both field areas in top- and subsoil. In contrast to IF, where PR varies from about 1.17-2.7 MPa in the topsoil, PR in the HL ranges from about 1.45-3.9 MPa at the same depths. At a depth from 41 to 45 cm, significantly higher PR values could still be observed in the headland, while the PR profiles became equal below.

4.3.2 Spatial patterns of penetration resistance

To predict the spatial patterns of PR for the entire field, kriging with external drift was used for interpolation. Table 4.4 shows the variogram characteristics and the interpolation accuracy. The depth intervals ranging from 1 to 5 cm and from 51 to 80 cm were excluded from the table, because variogram modelling failed for these depths.

Strongly structured spatial dependence occured at a depth between 11 and 15 cm. Except for the depth intervals from 6 to 10 cm and from 36 to 40 cm, which only revealed weakly structured spatial dependences, all other depths exhibited moderate spatial autocorrelation. The evaluation of

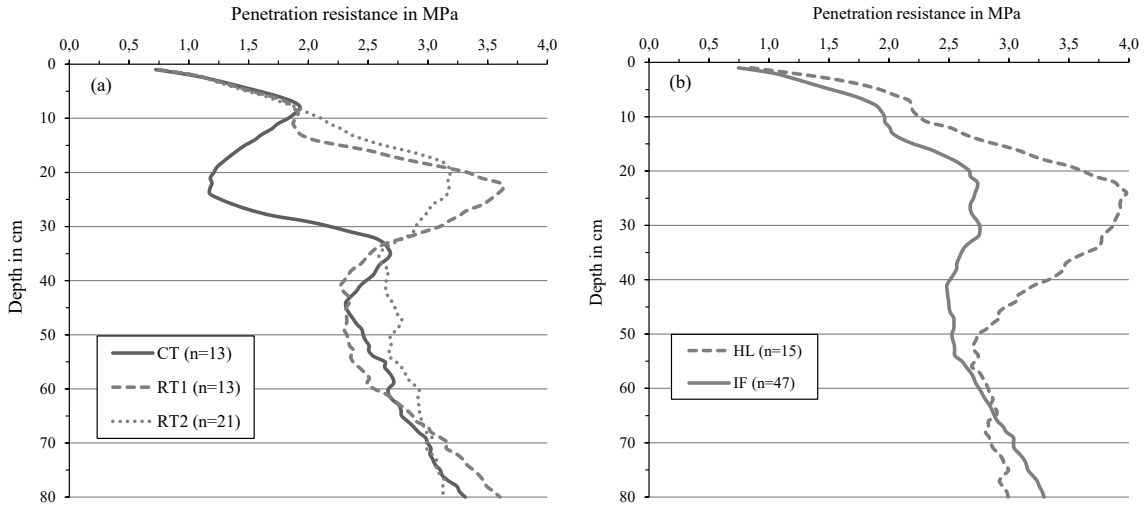

Figure 4.3: Penetration resistance profiles comparing CT, RT1, RT2 (a) and HL, IF (b).

the interpolation using the LOOCV method resulted in r^2 values from 0.27 to 0.64 for the depths between 11 and 40 cm. For soil depths outside of this interval, the predictive performance was limited, as indicated by r^2 values < 0.1.

The interpolation results of PR for the depth intervals 21-25 and 36-40 cm are presented in Figure 4.4. It clearly shows the spatially distributed patterns of PR for the entire field. In the depth zone between 21 and 25 cm, a clear spatial differentiation existed between CT and RT due to extensively higher PR under RT, (Tables 4.2 and 4.3). Moreover, the mapped interpolation results even resulted in slight differences between the two RT types visible. In addition, the spatial distribution of PR inside the HL were clearly separated from the IF. The demarcation lines between HL and IF could be still observed in the depths between 36 and 40 cm, where PR of the HL significantly exceeded the PR values recorded for the IF. In contrast, CT and RT did not exhibit significant differences due to a relative homogenous distribution of PR values at this depth.

Table 4.4: Residual variogram characteristics and interpolation accuracy.

Depth (cm)	Variogram model	Nugget (Co)	Partial sill (Cs)	Total sill (Co + Cs)	Range (m)	Nugget-to-sill ratio	RMSE (MPa)	r^2
6-10	Spherical	0.155	0.035	0.190	75	82*	0.48	0.02
11-15	Spherical	0.056	0.241	0.297	62	19***	0.56	0.27
16-20	Spherical	0.150	0.260	0.410	45	37**	0.68	0.54
21-25	Spherical	0.232	0.282	0.514	148	45**	0.70	0.64
26-30	Spherical	0.120	0.261	0.381	49	32**	0.65	0.52
31-35	Spherical	0.140	0.150	0.290	95	48**	0.60	0.29
36-40	Spherical	0.194	0.046	0.240	71	81*	0.55	0.29
41-45	Spherical	0.164	0.106	0.270	84	61**	0.62	0.09
46-50	Spherical	0.140	0.162	0.302	63	46**	0.62	0.06

Spatial dependence: *weak, **moderate, ***strong (Cambardella et al., 1994); r^2 = coefficient of determination, RMSE = root-mean-squared error computed from LOOCV residuals.

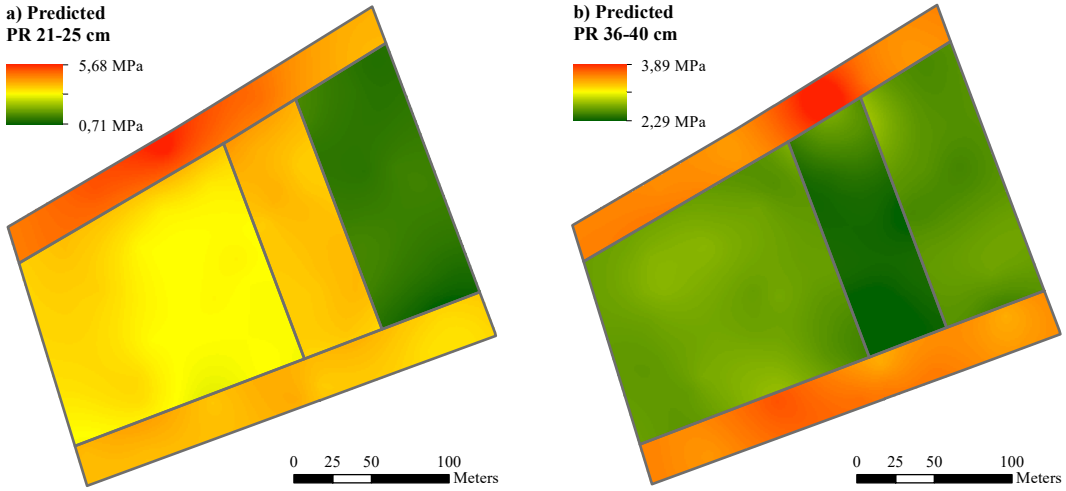

Figure 4.4: Spatial distribution of predicted penetration resistance at a depth between 21 and 25 cm (a) and at a depth between 36 and 40 cm (b).

4.3.3 Soil physical properties

Soil texture varies only slightly over the entire field. For the 20 sampling points, the arithmetic mean for sand is 2.4%, for silt 78.1% and for clay 19.5%, with standard deviations of 1.4, 1.9 and 2.8%, respectively. Table 4.5 summarizes the results of the soil physical parameters measured in the depth zone between 30 and 35 cm. While water content (31.2-32.8 vol.%) and bulk density (1.54-1.6 g/cm^3) do not reveal significant differences between the single tillage types and the HL, noticeable variability was found regarding saturated hydraulic conductivity (ks) and the amount of biopores. Largest ks values were measured under RT2 at a mean value of 722 cm/day, which was 31% greater than under CT (498 cm/day). Similar conditions were observed for the number of biopores. Compared with CT, the amount of biopores under RT significantly increased ($P < 0.05$) with up to 250 biopores per m^2 (RT1). This corresponds to the 1.6- fold (RT2) to 2.2-fold (RT2) more biopores counted in the conventionally managed plot as well as in the HL.

Table 4.5: Comparison of soil physical properties measured in the inner of the field plots and in the headlands at a depth between 30 and 35 cm.

	Water content in vol. %				**Bulk density in g/cm^3**				**Ks in cm/day**				**Biopores/m^2**			
	CT	RT1	RT2	HL	CT	RT1	RT2	HL	CT	RT1	RT2	HL	CT	RT1	RT2	HL
Mean	32.3	32.4	31.2	32.8	1.54	1.60	1.56	1.57	498	453	722	487	63	156	113	63
Median	32.0	32.7	30.1	33.3	1.54	1.62	1.57	1.59	435	426	693	406	63	138	100	63
Minimum	30.7	30.6	30.0	29.5	1.50	1.51	1.44	1.53	349	341	214	307	0	100	25	25
Maximum	35.0	33.7	33.4	35.0	1.59	1.63	1.62	1.59	836	621	1153	829	125	250	250	100
SD	1.6	1.3	1.7	2.5	0.03	0.06	0.07	0.03	186	120	357	234	47	66	88	32

4.4 Discussion

4.4.1 Tillage practice effects

The results of this study confirm a considerable influence of the different tillage practices on PR and its spatial distribution to a depth of 35 cm. Within the first 10 cm, there was no significant difference in PR as well as no spatial dependence due to identical seedbed preparations, seeding processes and natural soil settling for the entire field. Below this depth, the effects of the different tillage practices on PR became clearly visible, especially in the zone between 10 and 35 cm. Down to a depth of 25 cm, the PR under RT was significant greater than for CT as reported by Koch et al. (2008) and Afzalinia and Zabihi (2014). The PR continuously increased to this depth until it reached similar values to those measured under CT at a depth of 35 cm.

One reason for the greater PR under RT is the different intensity of soil loosening during the primary tillage operations. The mouldboard plough applied in the CT plot turned and loosened the soil to a depth of 25-30 cm. Below that depth, a sharp increase in PR demonstrates the existence of a plough pan, which is typical where CT has been practiced over the long term (Batey, 2009). This plough pan may be further affected by heavy machinery during harvest, resulting in a more compacted layer below the depth of tillage. In the RT plots, the soil was just loosened to a depth of 10-20 cm without inversion it; thus, the soil beneath stays intact (Cannell, 1985). Moreover, the shallow loosening under RT was not able to completely remove the compaction effects caused by high ground contact pressure, for example during sugar beet harvest. Thus, the degree of loosening after primary tillage practice was much greater and deeper under CT (Celik, 2011), which resulted in a smaller PR in the topsoil. Before establishing RT practices in 1996, the complete field had been conventionally cultivated down to 30 cm. Following the implementation of RT, the topsoil between 20 and 30 cm was no longer directly affected by primary tillage operations. However, the still unstable depth range was not able to support the high axle load of field traffic, for example sugar beet harvesters, which led to the development of a more compacted layer directly beneath the actual tillage depth (Rasmussen, 1999). The combination of high stresses in the topsoil, the unstable depth range of the former ploughed horizon and the shallow loosening under RT lead to very high PR values under RT, which exceeded the PR of the plough pan at 30 cm. Figure 4.4 clearly shows the spatial dimension of those effects. The complete CT plot had small PR values of around 1.0 MPa, while the RT plots had PR values up to 2.5 MPa.

Below this compacted layer, the PR under RT is still large down to a depth of 35 cm. Similar results have been described by Koch et al. (2008), indicating the existence of an historic (old) plough pan from previous CT. Considering only the measured PR leads to a conclusion that the RT practices causes a compaction layer. However, similar to studies by Tebrügge and Düring (1999) and Gozubuyuk et al. (2014), we detected higher amount of biopores and saturated hydraulic conductivity under RT compared with CT in the depth of 30-35 cm. We assume that the measured soil physical properties indicate a regeneration of the compacted layer. Under CT, aggregates are cracked or destroyed and biopores are disrupted at the bottom of the plough layer. The lower level of soil disturbance under RT conserves a larger proportion of existing aggregates, biopores and earthworms and contributes to the formation of new stable aggregates, for example, through biotic aggregation as described by Rasmussen (1999), Alvarez and Steinbach (2009), Capowiez et al.

(2012) and Lipiec et al. (2015). In addition, plants use the continuous biopores for root development leading to regenerated compaction zones (Tebrügge and Düring, 1999; Ehlers et al., 2000; Alvarez and Steinbach, 2009). The stable biotic aggregation under RT could be one reason for the large PR in the topsoil; however, this was not measured in this study. We interpret the significantly larger values for biopore numbers and saturated hydraulic conductivity under RT at the depth of 30 cm as an overall indicator for improved soil structure formation and stabilization resulting from reduced tillage, as stated by Wiermann et al. (2000) and Horn (2004). To finally evaluate this indicator, however, further sampling of the topsoil over different depths would be required.

As a result, for the assessment of PR, additional soil physical properties always need to be measured. By combining both measurements, it can be stated that the significantly greater PR values under RT do not necessarily indicate the presence of harmful soil compaction.

4.4.2 Spatial patterns of penetration resistance

The interpolation results (Figure 4.4) show a clear spatial differentiation between the different tillage practices investigated. Veronesi et al. (2012) and Barik et al. (2014) demonstrated that techniques like kriging are able to predict the spatial distribution of PR values. The results demonstrate that it is also able to predict PR values related to different tillage practices. However, predictability is limited, when the variations in soil texture and soil water content are spatially different, because of the large dependency of PR on these parameters (Kumar et al., 2012).

Comparing IF and HL, significantly larger PR values are present from surface down to the depth of 45 cm in the HL area. During the year especially during the harvest, the traffic intensity in the HL area is much higher as being the turning zone for field machinery including high axle loads (Duttmann et al., 2013, 2014), leading to high PR values for the whole HL area. Aksakal and Öztas (2010) and Barik et al. (2014) showed that field traffic leads to reduced aggregate stability and aggregate destruction, resulting in significantly higher PR. The clear spatial differentiation of the IF with PR values around 2.3 MPa and the HL with 3.5 MPa indicates a harmful compaction zone under the plough pan. Pardo et al. (2000) and Otto et al. (2011) pointed out that PR values >2.0 MPa, respectively, and 3.0 MPa reduce plant and root development. The area of the HL covers 1.46 ha, meaning that 26.6% of the total field has a PR that restricted root and plant development. However, the larger PR in the HL area does not conform to the measured bulk density, which was expected to be greater in the HL but is similar to that of the whole field. Alakukku (1998) also found no significant differences in bulk density under compacted, compared with noncompacted areas, although PR was significantly higher in the compacted area. One reason could be the small number of measuring points in the HL (4 points) and their unequal distribution within this area, resulting in an unrepresentative description of physical soil properties in the HL. Otherwise the small number of biopores in the HL indicates an impairment of soil function in the HL area. Apart from that, the interpolation technique applied here indicates three areas (CT, RT and HL) with substantial differences in PR and other related soil physical properties.

Thus, the derived patterns of PR may provide information about spatial differences in soil structure resulting from different tillage practices and field traffic intensities. Using the minimal invasive technique of penetrologger measurements enables rapid acquisition of data at many points with low soil disturbance. The combination of extensive PR measurements and point measurements of ad-

ditional soil physical properties at areas with significantly differing PR values supports an evaluation of the PR and can lead to a fieldwide derivation of soil functions influenced by field management.

This study presented a feasible method for predicting PR for entire fields and deriving spatial information under in situ field conditions and real field management. Although the measured soil properties showed significant differences depending on type of tillage practice and traffic intensity, an assessment of soil functions can only be performed after determining additional soil properties at further depths. Finally, it should be noted that our results are based on the status of a soil at a single time within 1 year. Further analyses have begun to consider soil dynamics and temporal changes within the year.

4.5 Conclusions

This study showed clearly that there is a significant spatial difference in PR caused by the two tillage practices, CT and RT, in the depth from 10 to 35 cm. In addition, the difference between HL and IF, with significantly larger PR down to 45 cm in the HL area, compared with IF was identified. Using kriging with external drift, the spatial pattern of PR caused by the different tillage practices and traffic intensities could be illustrated. For a proper assessment of soil penetration resistance, further physical properties like bulk density, saturated hydraulic conductivity, amount of biopores and aggregate stability must be determined. Combining the areawide measurements of PR as a minimally invasive technique with additional point-measured soil properties enables an extensive assessment of soil functions for entire fields.

4.6 Acknowledgements

The authors thank the anonymous reviewers for improving the article with very helpful comments. We are very thankful to Prof. Dr. J. F. Petersen (Institute of Geography, Texas State University, San Marcos, USA) for linguistic editing. Our gratitude also goes to Dr. habil. J. Brunotte (Institute of Agricultural Technology, Thünen Institute, Braunschweig, Germany) who is the owner of the study site and an expert in agricultural tillage practices. We thank our geodesist R. Gabler-Mieck for accurate surveying and A. Berger and J. Becker for assistance in the lab analyses. The Federal Ministry of Education and Research (BMBF) supported this study within the framework of the BonaRes-initiative (grant no.: 031A563C).

Chapter 5

Comparing soil physical properties from continuous conventional tillage with long-term reduced tillage affected by one-time inversion

Michael Kuhwald, Michael Blaschek, Joachim Brunotte and Rainer Duttmann
Soil Use and Management (2017), 33, 611-619, doi:10.1111/sum.12372
Received: February 2017, Accepted: August 2017

Abstract

In addition to various positive aspects, long-term reduced tillage may cause disadvantages such as increased weed pressure and soil compaction. Thus, single inversion tillage is customarily used for overcoming these drawbacks; however, the effects on the enhanced soil functions are unknown. The main objective of this study was therefore to assess whether improved soil physical properties following long-term reduced tillage remain after one-time inversion tillage by mouldboard plough. The study was undertaken on a silt loam field in Lower Saxony, Germany. Since 1996, this field has been subdivided into three treatments; one was managed conventionally using a mouldboard plough (CT), while on the others a chisel plough (RT1) and a disc harrow (RT2) were employed. In October 2014, the entire field was mouldboard ploughed. The following year, four field campaigns were conducted to compare the soil physical properties of the continuously conventional tilled plot with those affected by one-time inversion tillage (RT1 and RT2). Dry bulk density (DBD), saturated hydraulic conductivity (Ks) and infiltration rate [K(h)] were analysed in untrafficked and trafficked areas in each plot. There were clear differences between CT and RT. At all sampling dates, both RT plots had higher Ks and K(h) compared with CT. These differences also occurred to some extent on the trafficked areas. This suggests that improved soil hydraulic properties remained after one-time inversion tillage of a long-term reduced tilled field. Thus, one-time inversion tillage may offer a suitable measure for overcoming some of the main disadvantages associated with long-term reduced tillage, while preserving the positive effects on soil physical properties.

Keywords

Soil management, primary tillage practice, occasional tillage, strategic tillage

5.1 Introduction

Reduced tillage is a common method of conservation tillage used as an approach for combining ecological, economic and social requirements in agricultural landscapes. Several studies have shown that long-term conservation tillage may lead to improved soil physical characteristics compared with conventional tillage. Increased saturated hydraulic conductivity and infiltration rates in reduced tillage have been measured by Horn (2004), Bhattacharyya et al. (2006), Vogeler et al. (2006), Alvarez and Steinbach (2009), Gozubuyuk et al. (2014) and Parvin et al. (2014). The small loosening effect of reduced tillage can lead to enhanced biological activity and contribute to the resilience of earthworm channels (D'Haene et al., 2008). Additionally, stable aggregates can develop over time as shown by Tebrügge and Düring (1999), Vogeler et al. (2006), D'Haene et al. (2008), Alvarez and Steinbach (2009) and Daraghmeh et al. (2009). The dry bulk density (DBD) of the topsoil, however, is often increased in reduced tilled systems as a consequence of soil settlement and reduced loosing (Capowiez et al., 2009; Afzalinia and Zabihi, 2014). As stated by Capowiez et al. (2009), the greater number of macropores and pore continuity in reduced tillage offset the negative aspects of higher DBD. Subsequently, reduced tillage reduces the susceptibility to soil erosion, decreases runoff, supports an increased soil strength and leads to a higher load-bearing capacity (Wiermann et al., 2000; Salem et al., 2015). In addition, farmers may save costs for machinery, fuel and labour-time (Nail et al., 2007; Lahmar, 2010). Despite all these advantages, conservation tillage may cause negative effects, in particular under long-term use. Possible problems include soil compaction (Salem et al., 2015; Destain et al., 2016), stratification of nutrients and soil organic matter (Deubel et al., 2011; Lou et al., 2012), and increased weed pressure (Bajwa, 2014; Nichols et al., 2015).

One-time inversion tillage (also referred to as occasional tillage or strategic tillage) by mouldboard plough provides an opportunity to reduce the negative effects of conservation tillage. Prior research has mainly addressed the effects of one-time inversion tillage on soil organic matter (VandenBygaart and Kay, 2004; Koch and Stockfisch, 2006), nutrient distribution (Garcia et al., 2007), weed control (Renton and Flower, 2015), crop growth and yield (Kettler et al., 2000; Crawford et al., 2015), and soil erosion (Smith et al., 2007; DeLaune and Sij, 2012). Only a few studies refer to the effects of one-time inversion tillage on the physical properties of soil (Quincke et al., 2007; Baan et al., 2009; Stavi et al., 2011). Summarizing the results of the various studies, one-time inversion tillage can reduce weed pressure as well as herbicide resistance and can lead to a redistribution of nutrients and organic matter. The effects on crop growth, crop yield, the loss of organic matter, and soil erosion have been inconsistent. However, most authors have investigated the effects of one- time inversion tillage on no-tillage areas. No-tillage is the conservation tillage practice with least soil disturbance; the transferability of these findings to reduced tilled fields, therefore, is limited.

It is unclear whether and to what extent one-time mouldboard ploughing affects soil physical properties such as saturated hydraulic conductivity after long-term reduced tillage. Information about the effects of one-time inversion tillage on soil physical properties is, however, important for soil management. Dang et al. (2015a) stated that farmers often continue conservation tillage although one-time inversion tillage would be necessary to reduce, for example, weed pressure. This measure is rarely used, as it is not known what will happen to the improved soil structure and the related soil functions that may have developed following long-term reduced tillage.

This study contributes to a better understanding of the effects of one-time inversion tillage on soil physical properties after long-term reduced tillage. The objectives were as follows: (i) to analyse and compare soil physical properties of the one-time mouldboard ploughed areas with the continuously conventional tilled area of the field during the following growing season, and (ii) to evaluate the use of one-time inversion tillage as a management option for long-term reduced tillage.

5.2 Materials and methods

5.2.1 Study site

The experiment was conducted on a 5.5-ha field in the southern part of Lower Saxony, Germany (Figure 5.1). The soil type is Luvisol (FAO, 2014) developed from deeply weathered loess. The soil texture class is silt loam. Soil texture variation in the topsoil (0-30 cm) of the entire field is low, and the sand content is 2.9% ($\pm$ 0.8), silt content 79.1% ($\pm$ 2.2) and clay content 18.0% ($\pm$ 2.1). The climate is humid with a mean annual precipitation of 735 mm and mean annual temperature of 9.5 °C (1970-2000, DWD).

A 6-yr crop rotation [winter wheat (*Triticum aestivum L.*),sugar beet (*Beta vulgaris L.*), winter wheat, winter wheat, sugar beet and oats (*Avena sativa L.*)] was followed, and the crop was winter wheat in 2015. This crop rotation is quite common for this region, although a 3-yr crop rotation ofsugar beet, winter wheat and winter wheat is the most frequent.

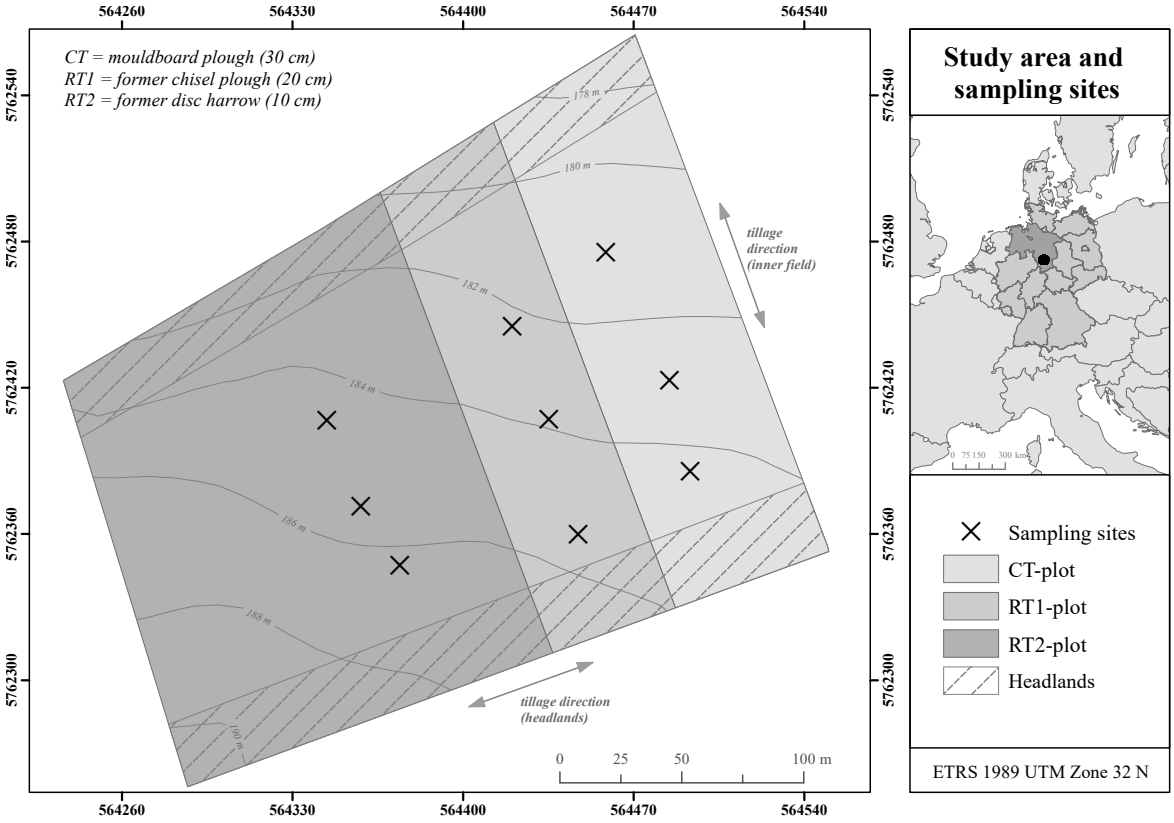

Figure 5.1: Study area and sampling locations (according to Kuhwald et al., 2016).

5.2.2 Tillage treatments and experimental design

Until 1996, the field was conventionally tilled with a mouldboard plough having a tillage depth of 30 cm. Since 1996, the field has been separated into three plots (Figure 5.1). One plot was further tilled conventionally (CT), while reduced tillage was implemented at the other two plots (RT1 and RT2). The primary tillage practice (also referred to as main tillage) at RT1 was performed by a chisel plough with a working depth of 20 cm. RT2 was primary tilled with a disc harrow to the depth of 10 cm. According to Townsend et al. (2016), RT1 can be classified as deep reduced tillage and RT2 as shallow reduced tillage. All other field operations such as sowing, manuring, spraying or harvesting were identical for the three plots since 1996 (Table 5.1). The separation was maintained until October 2014. After the sugar beet harvest in October 2014, the entire field was ploughed with a mouldboard plough to a uniform depth of 30 cm.

Table 5.1: Field activities at the study site.

Date	CT	RT1	RT2
20 to 21 April 2014	Primary tillage by mouldboard plough (since 1996)	Primary tillage by chisel plough (since 1996)	Primary tillage by disc harrow (since 1996)
23 April 2014	Sowing of sugar beet		
08 to 16 October 2014	Harvest of sugar beet		
18 October 2014	Primary tillage by mouldboard plough (one-time inversion tillage of RT1 and RT2)		
18 October 2014	Sowing of winter wheat		
28 October 2014	Application of plant protection agents		
9 March 2015	Application of fertilizer		
24 March 2015	Application of plant protection agents		
23 to 27 March 2015	First field campaign		
	Three points (ut)	Three points (ut)	Three points (ut)
7 April 2015	Application of plant protection agents		
17 April 2015	Application of fertilizer		
29 April 2015	Application of plant protection agents		
17 May 2015	Application of fertilizer		
22 May 2015	Application of plant protection agents		
26 to 29 May 2015	Second field campaign		
	Three points (ut)	Three points (ut)	Three points (ut)
	Three points (tl)	Three points (tl)	Three points (tl)
10 June 2015	Application of fertilizer		
16 June 2015	Application of plant protection agents		
10 to 11 August 2015	Third field campaign		
	Three points (ut)	Three points (ut)	Three points (ut)
13 August 2015	Harvest of winter wheat		
19 to 21 August 2015	Fourth field campaign		
	Three points (ut)	Three points (ut)	Three points (ut)
	Three points (hw)	Three points (hw)	Three points (hw)

CT, continuous conventional tillage plot; RT1, former reduced tillage (chisel plough) plot; RT2, former reduced tillage (disc harrow) plot; ut, untrafficked; tl, tramlines; hw, wheel tracks of fully loaded combine harvester.

In the following growing season, all three plots were sampled four times. The sampling aimed to compare the soil physical properties of the continuously conventional tilled plot with those affected by one-time inversion tillage after long-term reduced tillage. The investigations focussed on volu-

metric soil water content (VSWC), dry bulk density (DBD), saturated hydraulic conductivity (Ks) and infiltration rate [K(h)]. The first set of field measurements took place from March 23 to 27, the second from May 26 to 29, the third from August 10 to 11 (before harvest) and the fourth from August 19 to 21 (after harvest). On all plots, three locations for soil sampling were selected along a tramline. The tramlines were not planted and were used as driveways for application of fertilizer and plant protection agents. During each field campaign, these locations were revisited and sampled; the sampling position was shifted some metres with every field campaign to avoid sampling of a former disturbed position.

To find out whether the soil physical characteristics persisted against the stresses applied by field traffic, the trafficked areas were measured in May and August (after harvest). The trafficked areas were located in close proximity to the untrafficked areas, as shown in Figure 5.2. In May, three sampling points in each plot were located inside the tramlines to consider the effects of repeated field traffic. Up to this date, the tramlines had been trafficked eight times, five times for spraying and three times for fertilizer application (Table 5.1). Table 5.2 lists the machinery used and the machinery set-up. During fertilizer application, two wheels (front and rear) with mean contact stresses ranging from 48 to 96 kPa passed the tramlines each time. Crop protection operations resulted in three wheel passages (front, rear and trailer) for each application. Mean contact stresses applied by the machinery varied between 29 and 92 kPa.

Table 5.2: Technical specifications of the machinery used.

	Tyre description		**Tyre inflation pressure (kPa)**		**Wheel load (Mg)**		**Soil stress (kPa)[a]**	
Machinery	Front	Rear	Front	Rear	Front	Rear	Front	Rear
Primary tillage								
New Holland T 7.270 + FG 500 + Lemken Opal 140	Michelin 600/70R30 MachXbib	Michelin 710/70R42 MachXbib	90	100	2.3	2.5	88	87
Sowing								
New Holland M160 + FPW 860 + Amazone KG302/AD302	Michelin 540/65R28 MultiBib	Michelin 650/65R38 MultiBib	100	100	1.0	1.8	46	70
Fertilizer								
Fiatagri 85-90 Turbo DT + Amazone ZAM 1200	Mitas 380/70R24	Mitas 420/85R34	120	100	0.9	2.3	48	96
Crop protection								
Lamborghini R6.150 + Amazone UG 2200[b]	Continental 540/65R28 AC65	Continental 520/85R38 AC 85	250	180	0.6	1.1	29	46
	Continental 16.9-34 AS Farmer	-	150	-	2.2	-	92	-
Harvest								
New Holland TX 63	Goodyear 800/65 R32 DT822	Alliance 500/60-22.5 Flotation 328	100	100	7.1	2.1	119	92

[a]Calculated using Terranimo (Stettler et al., 2014), [b]The trailed sprayer had just one axle.

To consider the highest mean contact stresses (119 kPa) during the cropping season, three additional points were sampled in each treatment at locations which were trafficked by a fully loaded combine harvester (referred to as wheel tracks of the combine harvester; Figure 5.2). For this

purpose, the loaded harvester was directed along a field section that had not been trafficked before. Altogether, 54 points were sampled during the year, 36 located in untrafficked and 18 located in trafficked areas.

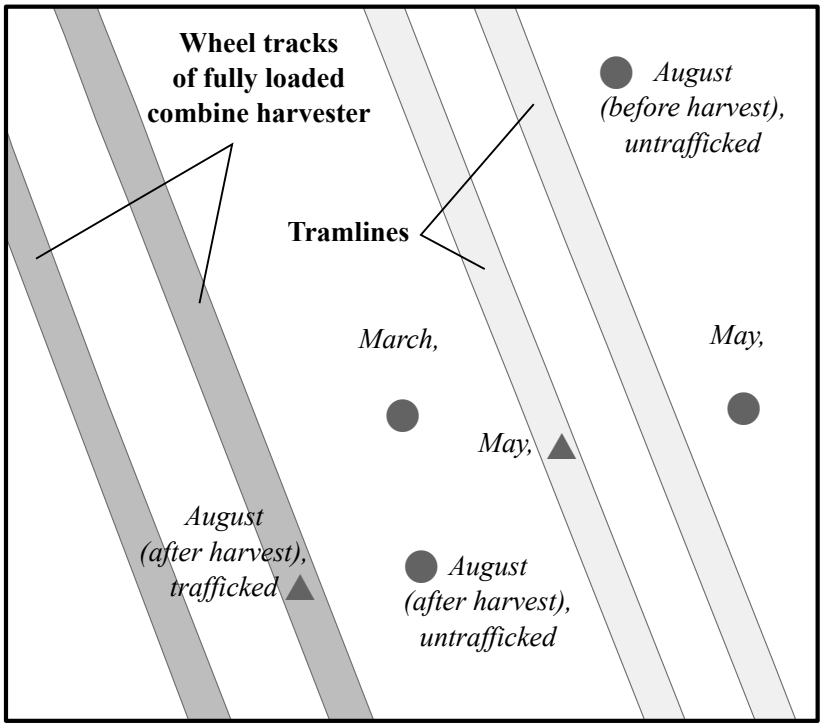

Figure 5.2: Example of sampling design for each sampling location.

5.2.3 Measurement of VSWC, DBD and Ks

At each of the 54 sampling points, crops were removed and pits of approximately 1 m^2 were excavated to a depth of 18 cm. Five undisturbed soil samples with 100 cm^2 (diameter 60 mm) and seven undisturbed samples with 250 cm^2 (diameter 84 mm) were taken from each sampling point at a depth of 18-23 cm.

In the laboratory, the 100 cm^2 samples were weighed, oven dried at 105°C for 24 h and weighed again to determine DBD and VSWC. The 250 cm^2 samples were stored under cool, dark conditions before measurement. After complete saturation, the samples were placed on a Ksat-system, applying the falling head method to determine Ks (UMS, 2013). In August (before harvest), the comparison lacks DBD and VSWC data as no small core samples were taken.

5.2.4 Measurement of K(h)

In May and August (after harvest), infiltration rate measurements were performed using a mini-disc infiltrometer. The infiltrometer had a total length of 32.7 cm and disc diameter of 4.5 cm. The infiltration rate was measured four times in each pit and at the same depth from which the undisturbed soil samples were taken. Before measurement, the surface was carefully levelled to obtain a close and stable contact between soil and infiltrometer. A suction rate of 1.0 cm (May) and 0.5 cm

(August) was applied. Infiltration calculations were performed using the spreadsheet given by the producer, which is linked to the Van Genuchten equations (Decagon Devices, 2016).

5.2.5 Statistical analyses

Statistical analyses were performed using the statistical software environment 'R' (R Core Team, 2016). For VSWC and DBD, arithmetic means were calculated from the replicate measurements for each sample point. Measurements of Ks and K(h) were $\log_{10}$ transformed to obtain a normal distribution. After $\log_{10}$ transformation, the geometric mean of the replicates of each sampling point was calculated. Subsequently, the arithmetic means and standard deviations were determined from the mean values of the single sampling points for each plot and date. Significant differences in mean values ($P < 0.05$) were tested using the two-sample t-test.

5.3 Results

5.3.1 Results of VSWC and DBD measurements

In March, VSWC varied between 35 and 39 vol.%, but decreased to 25 vol.% at the end of May (Table 5.3). After harvest, soil moisture increased to 34 and 36 vol.%. CT had significantly higher soil moisture than either of the RT plots in the untrafficked areas in March and August and in the tramlines in May, but there were no significant differences in the untrafficked area in May and in the wheel tracks of the fully loaded combine harvester in August. Dry bulk density measurements showed an opposite trend. The lowest values throughout the growing season were in March, ranging from 1.38 g/cm (RT2) to 1.43 g/cm (CT). In May, all plots had the same DBD of 1.55 g/cm, decreasing to 1.44-1.46 g/cm in August. Considering the changes between March and August, the increase in DBD was larger in both RT plots (3.4%, 5.8%) compared with CT (0.7%). There were no significant differences in DBD between untrafficked and trafficked areas in May. However, effects of wheeling were observed in August. DBD in the wheel tracks of the fully loaded combine harvester was significantly higher than the untrafficked areas in CT and RT2.

5.3.2 Results of Ks measurements

Ks in the untrafficked areas was higher in both RT plots compared with CT for all four sampling dates (Table 5.3). Comparing CT with RT2, significant differences occurred in March and August (after harvest). Except for May, $\log_{10}$ Ks in RT1 was lower than RT2. Comparison between CT and RT1 showed no significant differences. Apart from differences caused by tillage treatment, wide variations occurred during the year. While $\log_{10}$ Ks reached its highest values in March, it was significantly lower in May for all three plots and increased again until harvest, reaching approximately the same order of magnitude as in March.

Measurements in the trafficked areas showed a large decrease in $\log_{10}$ Ks compared to the untrafficked areas for all three plots in May and August. In the tramlines, the decrease in $\log_{10}$ Ks was significant in CT and RT2, while reduction in RT1 was not significant. For the wheel tracks of the

combine harvester, Ks was approximately the same for the three plots (log_{10} Ks 2.31-2.51 mm/day). During the growing season, smallest log_{10} Ks were measured in the tramlines in May, and CT had the smallest values.

5.3.3 Results of K(h) measurement

Similar findings to Ks were observed for K(h) (Table 5.3). In the untrafficked areas, log_{10} K(h) was at 1.51 (CT), 1.82 (RT1) and 2.02 (RT2) mm/day in May and 1.63 (CT), 1.86 (RT1) and 2.00 (RT2) mm/day in August. However, the treatments were not significantly different.

There was a reduction of log_{10} K(h) in the trafficked areas compared to the untrafficked areas independent of former tillage practice. In May, log_{10} K(h) values in the tramlines were reduced by 20% in CT, 11% in RT1 and 12% in RT2 compared with the untrafficked areas. In August, measurements in the wheel tracks of the fully loaded combine harvester showed a relative reduction in log_{10} K(h) of 10% (RT1), 40% (CT) and 28% (RT2) when comparing untrafficked and trafficked areas.

Independent of traffic intensity (tramline or wheel tracks of fully loaded combine harvester), however, both RT plots had higher log_{10} K(h) than CT, although the differences were only significant in May.

Table 5.3: Soil physical properties of the untrafficked and trafficked areas.

Date	Tillage plot	VSWC %	DBD g/cm^3	log_{10} Ks mm/day	log_{10} K(h) mm/day
Untrafficked					
March 2015	CT	38.5 ($\pm$ 0.8)^{a}	1.43 ($\pm$ 0.03)^{a}	2.88 ($\pm$ 0.39)^{a}	-
	RT1	35.8 ($\pm$ 2.2)^{ab}	1.40 ($\pm$ 0.04)^{a}	3.41 ($\pm$ 0.60)^{ab}	-
	RT2	34.6 ($\pm$ 1.9)^{bc}	1.38 ($\pm$ 0.06)^{a}	3.80 ($\pm$ 0.22)^{bc}	-
May 2015	CT	25.2 ($\pm$ 0.3)^{a}	1.55 ($\pm$ 0.03)^{a}	1.82 ($\pm$ 0.33)^{a}	1.51 ($\pm$ 0.25)^{a}
	RT1	24.9 ($\pm$ 2.0)^{a}	1.55 ($\pm$ 0.05)^{a}	2.34 ($\pm$ 0.50)^{a}	1.82 ($\pm$ 0.07)^{a}
	RT2	24.5 ($\pm$ 4.1)^{a}	1.54 ($\pm$ 0.09)^{a}	2.76 ($\pm$ 0.57)^{a}	2.02 ($\pm$ 0.55)^{a}
August 2015	CT	-	-	2.82 ($\pm$ 0.65)^{a}	-
(before harvest)	RT1	-	-	3.41 ($\pm$ 0.22)^{a}	-
	RT2	-	-	3.39 ($\pm$ 0.19)^{a}	-
August 2015	CT	36.0 ($\pm$ 0.6)^{a}	1.44 ($\pm$ 0.01)^{a}	2.91 ($\pm$ 0.30)^{a}	1.63 ($\pm$ 0.25)^{a}
(after harvest)	RT1	34.9 ($\pm$ 0.4)^{b}	1.45 ($\pm$ 0.03)^{a}	3.10 ($\pm$ 0.48)^{ab}	1.86 ($\pm$ 0.06)^{a}
	RT2	33.8 ($\pm$ 1.2)^{b}	1.46 ($\pm$ 0.02)^{a}	3.55 ($\pm$ 0.30)^{bc}	2.00 ($\pm$ 0.39)^{a}
Trafficked					
May 2015*	CT	30.2 ($\pm$ 1.3)^{a}	1.55 ($\pm$ 0.04)^{a}	1.15 ($\pm$ 0.10)^{a}	1.21 ($\pm$ 0.17)^{a}
	RT1	24.1 ($\pm$ 1.5)^{b}	1.54 ($\pm$ 0.03)^{a}	1.97 ($\pm$ 0.64)^{a}	1.62 ($\pm$ 0.16)^{b}
	RT2	26.9 ($\pm$ 1.3)^{b}	1.56 ($\pm$ 0.06)^{a}	1.43 ($\pm$ 0.49)^{a}	1.79 ($\pm$ 0.23)^{b}
August 2015	CT	36.0 ($\pm$ 0.5)^{a}	1.47 ($\pm$ 0.01)^{a}	2.47 ($\pm$ 0.15)^{a}	0.97 ($\pm$ 0.54)^{a}
(after harvest)**	RT1	37.0 ($\pm$ 0.8)^{a}	1.48 ($\pm$ 0.03)^{ab}	2.51 ($\pm$ 0.48)^{a}	1.68 ($\pm$ 0.10)^{a}
	RT2	35.4 ($\pm$ 1.0)^{a}	1.51 ($\pm$ 0.01)^{bc}	2.31 ($\pm$ 0.25)^{a}	1.43 ($\pm$ 0.25)^{a}

VSWC, volumetric soil water content; DBD, dry bulk density; log_{10} Ks, Saturated hydraulic conductivity; log_{10} K(h), Infiltration rate; ($\pm$), standard deviation; CT, continuous conventional tillage plot; RT1, former reduced tillage (chisel plough) plot; RT2, former reduced tillage (disc harrow) plot. *Measurements in the tramlines. **Measurements in the wheel tracks of fully loaded combine harvester; same letters indicate no significant differences at $P < 0.05$ (two-sample t-test) within the three tillage plots for the single dates.

5.4 Discussion

5.4.1 Effects of one-time inversion tillage in the untrafficked areas

Clear differences in soil physical properties between the three plots for all investigated dates were found, especially between the RT plots and the CT plot. This indicates the maintenance of the beneficial soil hydraulic properties as previously developed under long-term reduced tillage after a single mouldboard ploughing.

Before one-time inversion tillage in October 2014, DBD, Ks and the amount of biopores at a depth of 30-35 cm were higher in RT compared with CT, as previously reported by (Kuhwald et al., 2016). This observation corresponds with several studies (e.g. Gozubuyuk et al., 2014) focussing on effects of long-term reduced tillage. Due to the lack of inversion of the topsoil, DBD increased under long-term reduced tillage as a result of soil settlement and wheeling activities (Wiermann et al., 2000; Horn, 2004; Alvarez and Steinbach, 2009). Simultaneously, soil aggregation processes and biological activity increased, contributing to the formation of stable aggregates. The lower level of soil disturbance in RT conserved existing aggregates, biopores and earthworms (D'Haene et al., 2008), resulting in a higher aggregate stability and an enhanced intra- and interaggregate pore system. The improved soil structure may result in an increased hydraulic conductivity due to a higher porosity, connectivity and continuity of pores, as shown by Horn (2004), Capowiez et al. (2009), Vogeler et al. (2009), Gozubuyuk et al. (2014) and Parvin et al. (2014). In contrast, conventional tillage destroys soil structure and decreases structure stability because of intense soil loosening every year, resulting in less favourable hydraulic properties (Wiermann et al., 2000; D'Haene et al., 2008).

The results of this study showed that Ks and K(h) in both RT plots were higher compared with CT at all sampling dates. All other field operations (e.g. sowing, fertilizer application, harvesting) were the same for the three plots and soil texture is approximately homogenous for the entire field, discounting these factors as an explanation for the differences. Therefore, the reason for higher hydraulic conductivity in RT plots is an enhancement of soil structure and soil aggregation developed in long-term reduced tillage. Although size of aggregates and aggregate stability was not measured, improved soil structure under long-term reduced tillage is well documented. Ks and K(h) were higher in both RT plots after one-time inversion tillage; some of the soil structure improvements, therefore, must have been retained in the RT plots even after one-time inversion tillage. To confirm this assumption, further studies should focus on a more detailed analyses of the behaviour of soil structure affected by one-time inversion tillage, for example by means of computer tomography (Gao et al., 2017).

In addition, the degree of former reduced tillage is observable in the data. Except for August (before harvest), RT2 had higher Ks and K(h) for all measuring dates than RT1. In RT2, shallow reduced tillage (10 cm) by disc harrow was conducted, while RT1 was treated by deep reduced tillage (20 cm) by chisel plough. Thus, disturbance by tillage was lower in RT2. Consequently, soil structure may have developed more strongly in RT2, resulting in higher hydraulic conductivity even after one-time inversion tillage.

Furthermore, enhanced soil structure and structural stability is probably the reason for the differences in DBD. In March, after one-time inversion tillage in October, DBD was lower in the RT plots compared with CT. Lesser soil stability in CT led to faster settlement of the soil after tillage by rain-

drops along with an increased DBD (Alletto and Coquet, 2009; Jirků et al., 2013). Soil settlement in the RT plots was lower, probably because the more stable aggregates withstood the inïňĆuence of rain. Thus, in March, DBD was lower in the RT plots compared with CT. During the season, the values converged for all three plots due to seasonal effects.

5.4.2 Effects of one-time inversion tillage in the trafficked areas

In May and August, Ks and K(h) were lower in the trafficked areas compared with untrafficked ones for all plots. Stresses applied by wheeling caused the reduced hydraulic conductivity, an effect which has been well documented (e.g. Horn, 2003). However, Ks and K(h) were higher in the tramlines (May) of both RT plots compared with CT. This indicates a higher load-bearing capacity in the RT plots, which was able to withstand the pressure by wheeling to a higher degree than CT. Long-term reduced tillage led to a more structured and stable soil. Thus, the load-bearing capacity would increase as well (Wiermann et al., 2000; Horn, 2004; Vogeler et al., 2006). Ks and K(h) were still higher in the RT plots after wheeling compared with CT. Therefore, the positive effects of long-term reduced tillage have remained after one-time inversion tillage.

In all three plots, Ks was similar in the wheel tracks of the fully loaded combine harvester. K(h), however, was higher in both RT plots compared with CT. The combine harvester caused the highest soil stress of all wheeling activities during the season (Table 5.2). Soil moisture in the topsoil was high (35-35 vol.%), resulting in an increased susceptibility to soil compaction. We assume that the contact area pressures of the combine harvester exceeded the enhanced structure stability of the RT plots (Barik et al., 2014)). Thus, the pore system was compressed, which particularly affects soil macropores and results in lower Ks regardless of the former tillage practice. In contrast, the higher K(h) in both RT plots indicated an improved hydraulic conductivity even after wheeling. To characterize the pore structure affected by wheeling in more detail, however, more measurements and analyses of pore size distribution are necessary.

5.4.3 One-time inversion tillage as a soil management option

This study indicates that the enhanced Ks and K(h) developed over a long period of reduced tillage remained even after one-time inversion. Additionally, one-time inversion tillage may reduce the negative effects of reduced tillage. The mouldboard plough led to lower DBD in March and approximately the same DBD on both RT plots and the CT plot during the rest of the year. Hence, a new soil management option may be open to farmers. For instance, if a field is impaired by high weed pressure or high soil compaction after long-term reduced tillage, farmers can now overcome these disadvantages by one-time inversion tillage, without losing the positive effects of reduced tillage. Therefore, a combination of long-term reduced tillage with one-time inversion tillage when necessary may combine the positive aspects of both tillage treatments.

However, the frequency with which inversion tillage can be applied without losing the improved soil properties is unknown. In this study, one-time inversion tillage was applied after nearly 20 years of reduced tillage. Whether or not a shorter frequency, such as every 5 or 10 years, will retain the improved soil physical functions, still needs to be investigated.

Further attention should be also given to the analyses of possible improvements of those soil

properties that are damaged by long-term reduced tillage such as increased DBD (Capowiez et al., 2009; Afzalinia and Zabihi, 2014). In this study, data availability before one-time inversion tillage was limited and only available for a depth of 30-35 cm. Hence, an assessment on the effects of one-time inversion tillage on former compacted areas was not feasible. Additionally, soil characteristics and environmental conditions as well as agricultural aspects have to be considered (Crawford et al., 2015; Renton and Flower, 2015). In this study, the soil type was Luvisol and the texture was silt loam. It will be necessary to expand the analyses conducted here to additional soil types and soil texture classes to evaluate the wider applicability of this study's results. In addition, potential negative aspects, such as loss of soil organic matter (Koch and Stockfisch, 2006) and higher susceptibility to soil erosion by burying the surface residue cover (Kettler et al., 2000), must be considered to decide whether one-time inversion tillage is useful. However, the combination of reduced tillage and single events of inversion tillage to avoid disadvantages could result in a greater acceptance of conservation tillage.

5.5 Conclusions

This study showed that improved soil physical properties developed by long-term reduced tillage remain after one-time inversion tillage. Independent of seasonal variations, Ks and K(h) were higher at the former reduced tilled plots compared with continuously conventional tilled plot. Additionally, even after wheeling K(h) was higher in both RT plots.

Thus, one-time inversion tillage can be a suitable management option for farmers to alleviate the disadvantages of long-term reduced tillage. The findings may encourage a greater acceptance and usage of reduced tillage. Further studies should evaluate the transferability of one-time inversion tillage to other soils or landscapes and investigate the maximal frequency of inversion tillage.

5.6 Acknowledgements

The authors thank the anonymous reviewers, the associate editor and the editor for improving the manuscript with very helpful comments. Our special gratitude goes to J. F. Petersen and K. Etter for linguistic editing. We are grateful to A. Berger, J. Becker and M. Gosse and to our student assistants C. Thomas and I. Nofz for assistance with field and laboratory work. Funding of the project by the FederalMinistry of Education and Research (BMBF) within the BonaRes research initiative under grant no. 031A563C is greatly acknowledged.

Chapter 6

Spatially Explicit Soil Compaction Risk Assessment of Arable Soils at Regional Scale: The SaSCiA-Model

Michael Kuhwald, Katja Dörnhöfer, Natascha Oppelt and Rainer Duttmann
Sustainability (2018), 10, 1618, 1-29, doi:10.3390/su10051618
Received: 18 April 2018, Accepted: 15 May 2018

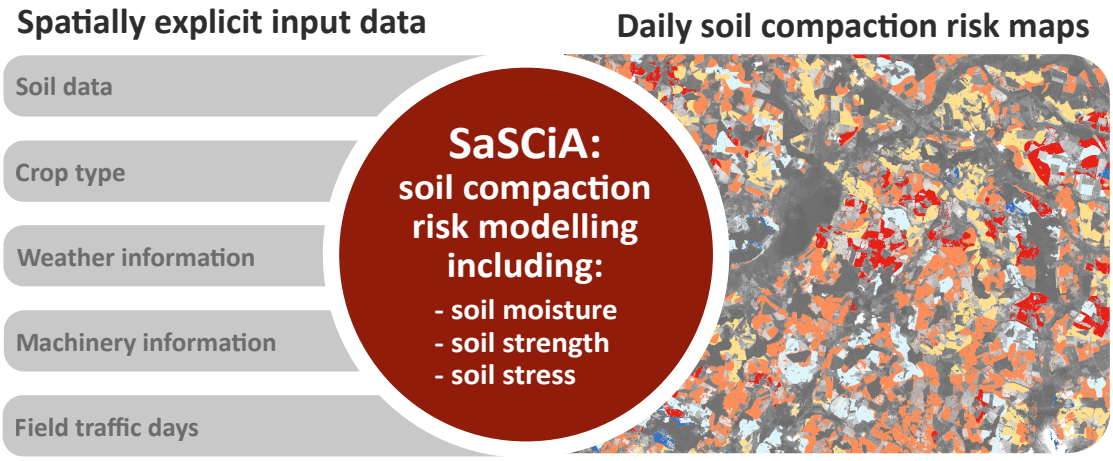

Figure 6.1: Graphical Abstract for Sustainability.

Abstract

Soil compaction caused by field traffic is one of the main threats to agricultural landscapes. Compacted soils have a reduced hydraulic conductivity, lower plant growth and increased surface runoff resulting in numerous environmental issues such as increased nutrient leaching and flood risk. Mitigating soil compaction, therefore, is a major goal for a sustainable agriculture and environmental protection. To prevent undesirable effects of field traffic, it is essential to know where and when soil compaction may occur. This study developed a model for soil compaction risk assessment of arable soils at regional scale. A combination of (i) soil, weather, crop type and machinery information; (ii) a soil moisture model and (iii) soil compaction models forms the SaSCiA-model (Spatially explicit Soil

Compaction risk Assessment). The SaSCiA-model computes daily maps of soil compaction risk and associated area statistics for varying depths at actual field conditions and for entire regions. Applications with open access data in two different study areas in northern Germany demonstrated the model's applicability. Soil compaction risks strongly varied in space and time throughout the year. SaSCiA allows a detailed spatio-temporal analysis of soil compaction risk at the regional scale, which exceed those of currently available models. Applying SaSCiA may support farmers, stakeholders and consultants in making decision for a more sustainable agriculture.

Keywords
Land degradation; environmental management; decision support system; open source software; legacy data

6.1 Introduction

Soil compaction represents one of the main threats to soils worldwide (FAO, 2015); it causes increased surface runoff, soil erosion and nutrient leaching, while infiltration rate, plant growth, root growth and biological activity decrease (Horn et al., 1995; Batey, 2009; Gebhardt et al., 2009). Hence, soil compaction affects soil functionality, agricultural productivity, food security, flood risk and nutrient input to water bodies (Weisskopf et al., 2010; Nawaz et al., 2013; Alaoui et al., 2018).

Soil compaction occurs when the exposure to field traffic exceeds soil strength (Horn et al., 1995). It is commonly separated into topsoil and subsoil compaction. While primary tillage may reverse topsoil compaction, subsoil compaction persists in the long term (Berisso et al., 2012; Gut et al., 2015). Restoring compacted subsoil by e.g., deep loosening is cost and time-consuming; resulting unstable soil conditions prohibit wheeling with heavy machinery after loosening (Botta et al., 2006). Preventing soil compaction, in particular subsoil compaction, is therefore the best way to preserve soil functionality.

A first step to prevent soil compaction is the knowledge about where and when soil compaction may occur. A spatial evaluation of soil compaction risk of arable soils is challenging. Highly dynamic natural processes such as the variation in soil moisture strongly influence soil compaction risk (Rücknagel et al., 2012; Gut et al., 2015; Edwards et al., 2016). Moreover, anthropogenic influence by soil management and wheeling activities continuously changes soil properties (Peth et al., 2006). Over the last decades, masses and sizes of agricultural machinery increased noticeably resulting in higher loads and stresses imposed on the soils (Schjønning et al., 2015b). To minimize undesirable effects of heavy-load field traffic, a reliable estimation of soil compaction risk gains increasing importance. Here, risk means the risk of soil damage (soil compaction) through a certain event such as wheeling activity. The risk is high when the susceptibility to soil compaction of soil (soil properties, wetness) is high and wheeling activities occur (e.g., sowing, fertilizing, harvesting period). The risk is low when wheeling activities are unlikely even if the susceptibility is high (e.g. Rücknagel et al., 2012; Schjønning et al., 2015b).

Despite its importance, only few approaches exist to estimate soil compaction risk. Most studies focus on the interaction between tyre and soil surface, and stress propagation in the soil under single wheels (e.g. Horn and Fleige, 2003; Diserens, 2009; Keller et al., 2014; Schjønning et al., 2015a).

Models developed from these studies such as SOILFlex (Keller et al., 2007) and Terranimo (Stettler et al., 2014) enable the evaluation of soil compaction risk at single points for individual machines. These models are well suited to support farmers to estimate the potential trafficability of a single point/field.

Studies dealing with soil compaction risk at field, regional or higher scale are rare (Jones et al., 2003; van den Akker, 2004; Horn et al., 2005). Jones et al. (2003) developed a generalized approach to calculate the subsoil compaction risk for Europe. The authors suggested the use of data with higher spatial resolution in combination with pedotransfer functions to improve the prediction of soil compaction risk. Pedotransfer functions calculate soil properties (e.g. field capacity, hydraulic conductivity) based on available soil data (e.g. soil texture, carbon content). SOCOMO, a model developed by van den Akker (2004), derives maps of calculated maximum allowable wheel loads. Assuming static soil moisture conditions and static machinery setup, however, limits this approach. van den Akker and Hoogland (2011) applied the approaches from Jones et al. (2003) and van den Akker (2004) to the Netherlands. Although both models identified the same risk areas, the validation with measured laboratory data was low (van den Akker and Hoogland, 2011).

Horn and Fleige (2003) published a frequently used method to calculate soil compaction risk at different spatial scales. This method is based on the precompression-stress-concept as described in detail by DVWK 234 (1995) and Horn and Fleige (2003). It uses pedotransfer functions to calculate the soil compaction risk for two different soil moistures (suction rate of -6 kPa and -30 kPa, respectively, pF 1.8 and 2.5). Horn et al. (2005) and Horn and Fleige (2009) applied this approach from the farm scale to the supra-regional scales. To estimate the soil compaction risk at the spatial scale, they used constant stress scenarios (e.g., 60 kPa for low and 200 kPa for high stress) for the entire regions. Fritton (2008) applied the Horn and Fleige (2003) approach for Pennsylvania (USA), D'Or and Destain (2014) for Wallonia (Belgium). Following the same approach, Duttmann et al. (2014) presented a 3D-model to assess the soil compaction risk caused by silage maize harvest. Although the approach of Horn and Fleige (2003) is often used for spatial soil compaction risk assessment, it is controversially discussed (e.g. Vorderbrügge and Brunotte, 2011a; Keller et al., 2012). One criticism addresses the fact that the prediction of soil compaction risk only accounts for two states of soil moistures (pF 1.8 and pF 2.5). Trafficability depends on the current soil water content (Gut et al., 2015; Edwards et al., 2016); the Horn and Fleige (2003) approach, however, is limited to assess the potential soil compaction risk. It further neglects temporal changes and spatial heterogeneity in soil moisture. Moreover, the aforementioned studies assumed constant soil stresses for the investigated regions, but disregard the real conditions in terms of crop types, soil tillage and machinery setups.

Rücknagel et al. (2015) therefore developed a new approach, which enables a soil compaction risk assessment for any soil moisture condition. Using this model, Götze et al. (2016) demonstrated the variation of soil compaction risk during the growing season at the farm scale. Their results clearly showed the dynamic changes of load bearing capacity of the soil and, hence, the risk of soil compaction. Hitherto, this approach is limited to single fields where measured soil moisture is available.

The aim of this study was (1) to develop and (2) to apply a soil compaction model for an assessment of soil compaction risk at the regional scale for dynamic field conditions. To this end, we developed the SaSCiA-model (Spatially explicit Soil Compaction risk Assessment) operating upon readily and freely available data and software. The SaSCiA-model incorporates (i) soil, weather, crop and machinery information; (ii) a soil moisture model (MONICA, Nendel et. al, 2011) and (iii) soil

compaction models (Horn and Fleige, 2003; DIN V 19688, 2011; Rücknagel et al., 2015). Considering the dynamic changes of soil properties depending on the present crop types and growing stage, we hypothesize that the SaSCiA-model supports a more realistic estimation of soil compaction risk at regional scale compared to currently available models. The term "regional scale" as it is used in the presented study means a spatial extent of landscape between tens to thousands of square kilometres. To demonstrate the applicability of the model, SaSCiA was applied at two study areas with different soil and weather conditions in northern Germany.

Applying the SaSCiA-model enables the production of daily maps of soil compaction risk, identification of areas exposed to soil compaction and estimation of optimal field traffic days. These regional maps are essential to understand where and to what extent soil compaction may occur. Furthermore, these maps may help to prevent soil compaction by e.g., showing the effects of adapted management strategies.

6.2 The SaSCiA-Model - Material and Methods

Figure 6.2 provides a schematic overview of the SaSCiA-model. Input data include weather information, soil data, crop information, machinery setups and field traffic days. Using this input data, the SaSCiA-model generates daily maps of soil compaction risk estimates for entire regions by coupling various models. In detail, it involves spatially explicit

- modelling of soil water content at daily intervals using the MONICA-model (Nendel et al., 2011),
- calculation of actual soil strength (Horn and Fleige, 2003; DIN V 19688, 2011; Rücknagel et al., 2012, 2013),
- estimation of soil stress (Koolen et al., 1992; Rücknagel et al., 2015).

The model is implemented in "R" (version 3.3.1, R Core Team (2017)). Data and models employed are freely available to enable widespread application by interested users. The script including a test dataset is available on request from corresponding author. In case of adaptations or modifications, users can easily replace individual modules or data sets.

6.2.1 Input Data and Data Preparation

The required input data for the model are weather data, soil data, present crop type, crop information (fertilizer applications; irrigation; dates of sowing, harvest and primary tillage), machinery information and days of field traffic. Soil data and present crop types must be provided as spatially explicit (raster) data. All other input data have to be stored as tables (CSV).

6.2.1.1 Weather Information

The weather information is necessary to calculate the actual soil moisture with the MONICA-model. The model requires daily values of temperature (average, minimum and maximum), wind speed, precipitation, relative humidity and sun duration (Table A1, Appendix A).

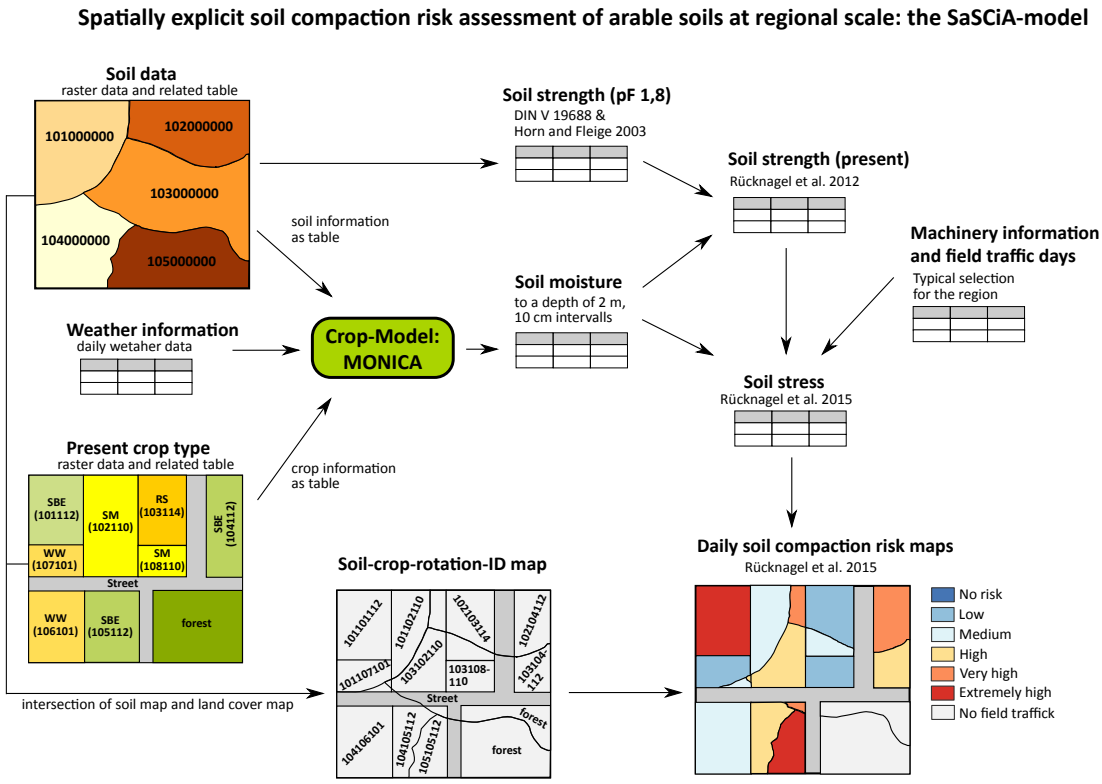

Figure 6.2: Schematic structure of the SaSCiA-model (Spatially explicit Soil Compaction risk Assessment).

6.2.1.2 Soil data

The soil data are used to calculate soil moisture and soil strength. A minimum set of soil parameters includes soil texture class, dry bulk density, gravel content, organic carbon content, soil aggregate structure, air capacity, field capacity, available field capacity and horizon depths. The soil data is required as soil profiles (soil data from soil surface to a depth of 2 m). Additionally, each soil profile must be identifiable by a unique soil identifier ("soil-ID"). The soil profile information has to be stored in a table (Table A2, Appendix A). Moreover, the spatial distribution of all soil profile/soil identifier must be provided as raster data.

6.2.1.3 Present crop types

Knowing the present crop types for the year of soil compaction risk assessment is essential. The cultivated crop type affects the soil moisture of a certain soil and determines the field traffic activities (e.g., times of sowing, fertilizing, spraying, harvesting, used machinery). The crop type information must also be provided as raster data. A reclassification of the crop types by unique crop identifiers ("crop-ID") converts the raster into a structure readable for the SaSCiA-model. Table A6 (Appendix A) lists the assigned crop-IDs.

6.2.1.4 Crop rotation

To consider the effects of previously cultivated crop types on the water balance of the soil, a three-year crop rotation is assumed. The present crop type and the crop types of the preceding two years compose the crop rotation. Intersecting the spatial distribution of crop types from the three consecutive years results in a raster with all possible combinations of crop rotations; a unique identifier ("rotation-ID") clearly distinguishes all combinations. Figure A1 (appendix A) demonstrates this principle exemplarily. Joining the "rotation-ID" and "crop-ID"-raster results in a "crop-rotation-ID"-raster, which is used to spatially allocate the crop-information in the SaSCiA-Model.

If the crop type of a previous year is unknown, a representative crop rotation has to be assumed, e.g., winter wheat, winter barley and sugar beet.

In addition to the spatial allocation of the individual crop-rotations, further crop information such as tillage, sowing and harvest dates and tillage depth needs to be added (Table A3, Appendix A).

6.2.1.5 Fertiliser and irrigation information

Information about nitrogen application and irrigation can be included to stimulate plant growth. This information must be stored in individual tables (Table A4, Appendix A). Input parameters include the "crop-rotation-ID", amount of nitrogen, kind of fertilizer, the application date and incorporation for fertilizer application. For irrigation, the "crop-rotation-ID", amount of irrigation water and date of irrigation are necessary. Fertilizer and irrigation information is assigned to the crop types based on the "crop-rotation-ID".

6.2.1.6 Machinery information and field traffic days

The machinery used and machinery characteristic are crucial to calculate the mechanical stress imposed on the soil. Therefore, wheel load, tyre inflation pressure and field traffic days need to be parameterized for each field. Due to a huge variety of agricultural machinery, the spatial allocation of machinery used on the different fields of a region is mostly unknown.

To enable both, a spatially and a crop type dependent differentiation, the user has to define typical machinery setups used in the study area for each crop type, based on e.g., literature review and manufacturer's information. In general, the same machinery setup will be applied for each crop type (e.g., maize, sugar beet) within the entire study area.

A similar assumption is required for field traffic activities. The time of field traffic is highly variable at regional scale. To achieve a region-specific approximation, reasonable periods of field traffic activities for each crop type have to be predetermined (if the real dates are unknown). Typical field operations, e.g., primary tillage, sowing and harvest form categories of periods. Each category contains a date for the beginning and ending of potential field traffic activity. The wheel loads and tyre inflation pressures are related to each period and crop type. One value for wheel load and tyre inflation pressure can be considered per period and crop type. Table A5 (Appendix A) shows an example of the table structure for the machinery and field traffic days.

6.2.2 Soil moisture modelling (MONICA)

Soil compaction risk mainly depends on the soil moisture. Wet soils have a low load bearing capacity and a high susceptibility to soil compaction (Lamandé and Schjønning, 2011; Destain et al., 2016). Increasing desiccation reduces the susceptibility to soil compaction. The actual soil moisture therefore is essential to evaluate field traffic activities on soil functionality. Soil moisture varies strongly, temporally, spatially and with depth. Thus, a continuous update of soil moisture in space and time is necessary to increase the reliability of soil compaction risk assessment.

At the regional scale, soil moisture models may overcome the limited field measurements to provide such an update. A variety of models exist to determine soil moisture; they often are included in crop-growth models (e.g., HYDRUS, DAISY). For the SaSCiA-model, the crop-model MONICA (version 2.0; Nendel et al., 2011) was selected. MONICA computes daily soil moisture content at 10 cm depth intervals from top to a depth of 2 m. Several studies demonstrated the usability of the model (e.g. Nendel et al., 2013; Specka et al., 2016). MONICA is applicable to freely available data and transferable to regional scale (Nendel et al., 2013). Nendel et al. (2011) and Nendel and Specka (2014) give a detailed description of MONICA.

Soil data, crop type and rotation data, fertilizer data and weather information form the input tables for soil moisture modelling with MONICA in the SaSCiA-model. Matching soil and crop tables results in all possible combinations between soil profiles and crop types. Each combination receives a unique identifier ("soil-crop-rotation-ID") and guarantees a spatial allocation at the end of calculation. The SaSCiA-model automatically converts all input-tables into the MONICA-specific table format. Afterwards, the MONICA model is applied to each "soil-crop-rotation-ID". The resulting tables include the calculated soil moisture for each soil and crop combination, forming the basis for subsequent soil strength calculation.

6.2.3 Soil strength modelling

Soil strength describes the resistance of a soil against an applied pressure (Horn et al., 1995). Soil strength depends on several soil properties, e.g., soil texture, organic carbon content and soil structure. Wet soils have a reduced soil strength compared to dry soils; therefore, the soil strength changes continuously depending on soil moisture. Calculating soil strength in the SaSCiA-model follows an approach published by Rücknagel et al. (2015), which considers varying soil moisture and therefore enables a soil compaction risk assessment for dynamic field conditions. Furthermore, the approach is transferable to the regional scale by combining spatially explicit soil and crop type data and soil moisture modelling.

To calculate the soil moisture dependent soil strength, the soil strength at field capacity (water content at a suction rate of -6 kPa or pF 1.8) is necessary. Soil strength at field capacity may be measured directly, calculated from measured dry bulk density and aggregate density (Rücknagel et al., 2007) or may be derived by pedotransfer functions(Horn and Fleige, 2003).

At regional scale, measured values of soil strength and aggregate density are usually unavailable, necessitating the use of pedotransfer functions. Horn and Fleige (2003) provide common pedotransfer functions (see introduction) to derive soil strength at field capacity. The structure of the pedotransfer functions enables an application with freely available soil data and the transfer to the regional scale. Lebert (2010) and D'Or and Destain (2014) however, demonstrated that the pedo-

transfer functions provided by Horn and Fleige (2003) tend to overestimate soil strength of certain texture classes (e.g., loam).

Lebert (2010) recommended the use of pedotransfer functions by Horn and Fleige (2003) for sandy soils and DIN V 19688 (2011) for loamy, silty and clay soils. The pedotransfer functions of DIN V 19688 (2011) are based on the same data and assumptions as the approach by Horn and Fleige (2003), but calculate more reliable values (Lebert, 2010). The used pedotransfer functions disregard organic soils. These soils are therefore excluded from further analyses, i.e., SaSCiA calculates the soil compaction risk only for mineral soils, not for organic soils. Table 6.1 lists the equations (Equations (1)-(4)) for calculating the soil strength at field capacity for various soil texture classes as implemented in the SaSCiA-model.

Table 6.1: Equations to calculate the soil strength at field capacity (pF 1.8) for varying soil texture class (Horn and Fleige, 2003; DIN V 19688, 2011).

Formula	Soil texture class*
(1) $\sigma_{(1.8)}$ = 438.1 $\times$ DBD - 0.0008 $\times$ Phi^3 - 3.14 $\times$ WP - 0.11 $\times$ AFC^2 - 465.6	Sand (Ss); slightly silty sand (Su2); slightly loamy sand (Sl2); slightly clayey sand (St2)
(2) $\sigma_{(1.8)}$ = 69.5 $\times$ DBD - 13.3 $\times$ Corg - 23.3 $\times$ $\sqrt{AC}$ + 1.45 $\times$ Coh + 0.085 $\times$ Phi^2 - 56.6	medium/highly silty sand (Su3, 4); medium loamy sand (Sl3); silty loamy sand (Slu); silt (Uu); sandy silt (Us); sandy loamy silt (Uls); slightly/medium clayey silt (Ut2, 3)
(3) $\sigma_{(1.8)}$ = 119 $\times$ DBD - 10.1 $\times$ Corg - 12.6 $\times$ $\sqrt{WP}$ + 11.1 $\times\sqrt{Coh}$ - 78.9	highly loamy sand (Sl4); highly clayey silt (Ut4); slightly/medium/highly sandy loam (Ls2, 3, 4); silty loam (Lu); highly silty clay (Tu4)
(4) $\sigma_{(1.8)}$ = -42.7 $\times$ DBD - 20.7 $\times$ $\sqrt{Corg}$ - 14.2 $\times$ $\sqrt{AFC}$- 20.8 $\times$ $\sqrt{AC}$ + 5.17 $\times$ $\sqrt{Phi}$ + 1.23 $\times$ $\sqrt{Coh}$ + 23	medium clayey sand (St3); slightly/medium clayey loam (Lt2, 3); sandy clayey loam (Lts); slightly/medium/highly sandy clay (Ts2, 3, 4); slightly/medium silty clay (Tu2, 3); loamy clay (Tl); clay (Tt)

*German soil texture classification (Ad-Hoc-AG Boden, 2005); $\sigma_{(1.8)}$ = soil strength at field capacity (kPa), DBD = dry bulk density (g/cm^3), AC = air capacity (vol. %), AFC = available field capacity (vol.%), WP = non-plant available water (vol.%), Corg = soil organic matter (%), Coh = cohesion (kPa), Phi = angle of internal friction (°).

The cohesion (Coh) and angle of internal friction (Phi) are derived from the given soil texture class and the soil structure according to Horn and Fleige (2003) and Lebert (2010). The calculated values represent the soil strength at field capacity ($\sigma_{1.8}$) for each depth of the individual soil types in the study area.

Subsequently, soil strength at field capacity is joined with the actual soil moisture values calculated by the MONICA-model. Afterwards, SaSCiA-computes the moisture-dependent soil strength at daily intervals, using the pedotransfer functions provided by Rücknagel et al. (2012) (Table 6.2, Equations (5)-(9)).

Table 6.2: Equations to calculate the soil moisture depended soil strength for varying soil texture class (Rücknagel et al., 2012).

Formula	Soil texture class*
(5) log σ_{Moist} = 2.8335 + -0.9271 $\times$ log$\sigma_{1.8}$ + -0.0279 $\times$ %FC + 1.67 $\times$ 10^{-7} $\times$ %FC^2 + 0.00906 $\times$ log$\sigma_{1.8}$ $\times$ %FC	Sandy Clay, Sandy Clay Loam
(6) log σ_{Moist} = 2.7833 + -1.0 $\times$ log$\sigma_{1.8}$ + -0.0289 $\times$ %FC + 116 $\times$ 10^{-15} $\times$ %FC^2 + 0.01 $\times$ log$\sigma_{1.8}$ $\times$ %FC	Loam, Sandy Loam
(7) log σ_{Moist} = 4.3056 + -1.4444 $\times$ log$\sigma_{1.8}$ + -0.0431 $\times$ %FC + 537 $\times$ 10^{-16} $\times$ %FC^2 + 0.0144 $\times$ log$\sigma_{1.8}$ $\times$ %FC	Clay, Clay Loam
(8) log σ_{Moist} = 2.5333 + -0.6667 $\times$ log$\sigma_{1.8}$ + -0.0253 $\times$ %FC + 21 $\times$ 10^{-14} $\times$ %FC^2 + 0.00667 $\times$ log$\sigma_{1.8}$ $\times$ %FC	Silty Clay Loam, Silty Clay
(9) log σ_{Moist} = 1.7611 + -0.5556 $\times$ log$\sigma_{1.8}$ + -0.0176 $\times$ %FC + 4.11 $\times$ 10^{-14} $\times$ %FC^2 + 0.00556 $\times$ log$\sigma_{1.8}$ $\times$ %FC	Sand, Silt Loam, Silt, Loamy Sand

* USDA soil texture classification (FAO, 2014); σ_{Moist} = soil strength at actual soil moisture (kPa), $\sigma_{1.8}$ = soil strength at field capacity (kPa), %FC = actual soil moisture in percent of field capacity (%).

In addition to soil moisture, the gravel content in the soil influences soil strength, whereby higher gravel content increases soil strength (Horn and Fleige, 2003; Rücknagel et al., 2013). The SaSCiA-model considers these effects using the pedotransfer functions (Table 6.3, Equations (10)-(12)) as introduced by Rücknagel et al. (2013).

Table 6.3: Equations to calculate the effects of gravel on soil strength for varying soil texture class (Rücknagel et al., 2013).

Formula	Soil texture class*
(10) log σ_{Gravel} = 0.0434 $\times$ e$^{0.0777 \text{ x Gravel}}$	Clay
(11) log σ_{Gravel} = 0.031 $\times$ e$^{0.083 \text{ x Gravel}}$	Silt Loam
(12) log σ_{Gravel} = 0.0772 $\times$ e$^{0.0631 \text{ x Gravel}}$	Sandy Loam

* USDA soil texture classification (FAO, 2014); σ_{Gravel} = Gravel effect on soil strength (kPa), Gravel = gravel content (%), e = Euler's number.

Finally, the total soil strength (σ_{Total}; in kPa) for the actual soil moisture results from soil strength at field capacity ($\sigma_{1.8}$), effects of gravel content (σ_{Gravel}) and influence of actual soil moisture (σ_{Moist}) (Equation (13), (Rücknagel et al., 2015)):

(13) logσ_{Total} = log $\sigma_{1.8}$ + log σ_{Gravel} + log σ_{Moist}

The SaSCiA-model calculates the total soil strength for all "soil-crop-rotation"-combinations in the study area and all defined periods/days of field traffic. The results are daily information of actual soil strength depending on actual soil moisture calculated. The actual soil moisture is calculated by the MONICA-model using the crop information (crop type and crop rotation), the soil data and weather information.

6.2.4 Soil stress modelling

Soil stress is applied by field traffic and depends, among other factors, on wheel load and tyre inflation pressure. Several approaches exist to calculate the soil stress and stress distribution in the soil (e.g. Keller, 2005; Duttmann et al., 2013; Schjønning et al., 2015a). These approaches, however, often need various input parameters (e.g., exact tyre descriptions), which are unavailable at regional scale. Koolen et al. (1992) published a generalized method, which only requires wheel load (WL; in kg), tyre inflation pressure (TIP; in bar), concentration factor (ν) and the depth (Depth; in cm) to calculate the soil stress at a certain depth (σ_{Depth}; in kPa) (Equation (14)):

(14) σ_{Depth} = 2 $\times$ TIP $\times$ (1 - $\cos{}^{\nu}$ $\times$ ($\arctan$ ((1/Depth) $\times$ ((WL/ π)/(2 $\times$ TIP/100))0.5))).

This approach is transferable to the regional scale and therefore was integrated in the SaSCiA-model. Rücknagel et al. (2015) developed an equation to calculate the concentration factor (ν) based on soil strength at field capacity and actual soil moisture in percent of field capacity (%FC) (Equation (15)):

(15) ν = -2/log $\sigma_{1.8}$ + 0.03 $\times$ %FC + 3.2

The concentration factor determines the stress distribution in the soil. Söhne (1958) developed this approach and classified the concentration factor into 4 (for dry soils), 5 (for moist soils) and 6 (for wet soils). Equation (15) determines the concentration factor for any soil moisture.

The SaSCiA-model contains both soil stress equations (Equations (14) and (15)). The daily soil moisture calculated by the MONICA-model and the calculated soil strength at field capacity (pF 1.8) is used to determine the concentration factor. The present crop type, provided field traffic days and the date of calculation define the wheel load and tyre inflation pressure used for soil stress calculation. When the present crop type is sugar beet, for instance, a wheel load of 11.200 kg and tyre inflation pressure of 2.2 bar is used for stress calculation at harvest time (e.g., 30 September 2016). At the same time, but with crop type maize, a wheel load of 5.100 kg and tyre inflation pressure of 2.2 bar are selected. Thus, SaSCiA conducts the calculation of soil stress for each single field in the study area for each day; on days without traffic activity, no stress is applied to the soil.

6.2.5 Soil compaction risk evaluation

Field traffic affects various soil functions negatively when the applied soil stress exceeds the soil strength. Subtracting the applied soil stress from soil strength (Equation (16)) results in the so called "Soil Compaction Index" (SCI;(Rücknagel et al., 2015)), which is used in the SaSCiA-model:

(16) SCI = log σ_{Depth} - log σ_{Total}

SCI values (in log(kPa)) smaller than or equal to 0 indicate that expected field traffic will not affect soil functionality (no soil compaction risk). Values greater than 0 point to an increasing soil compaction risk due to plastic soil deformation, going along with degrading soil functionality (Rücknagel et al., 2015; Götze et al., 2016). Table 6.4 lists the classification of the SCI; each SCI-class

represents a soil compaction risk class, ranging from "no risk" to "extremely high" (Rücknagel et al., 2015; Götze et al., 2016).

As the final result, SaSCiA computes the "Soil Compaction Index" (Equation (16)) ranked into different classes of compaction risk (Table 6.4) for each soil-crop combination on a daily basis. The model outcomes are spatially explicit daily maps of the soil compaction risk and associated tables summarizing the area statistics throughout the entire region.

Table 6.4: Classification of "Soil Compaction Index" (SCI, in log(kPa)) (Rücknagel et al., 2015; Götze et al., 2016).

SCI	Soil Compaction Risk
≤ 0	No risk
0-0.1	Low
0.1-0.2	Medium
0.2-0.3	High
0.3-0.4	Very high
>0.4	Extremely high

6.3 The SaSCiA-model-application

6.3.1 Study areas

The SaSCiA-model was applied to two study areas in northern Germany. The first one, named "Adenstedt" with a total area of 336 km^2, is located in the southern part of Lower Saxony, the Lower Saxon Loess Hill Country. The soil parent material ranges from shallow layers of clayey and sandy weathering residuals at the hilltops, deeply weathered loess along the hill slopes and loamy deposits in the valleys, forming a wide variety of soil types. Predominating soil types under arable use are Luvisols and stagnic Luvisols, which are highly susceptible to soil compaction. Typical crop rotations in this region include sugar beet, (*Beta vulgaris L.*), winter wheat (*Triticum aestivum L.*) and winter barley (*Hordeum vulgare L.*) with an increasing share of silage maize (*Zea mays L.*) in the last decades.

The second study area, named "Kummerow" with a total area of 2500 km^2, is located in the center of Mecklenburg-Vorpommern. Kummerow is part of the Northern German Plain. The parent material is glacial till, pervaded by numerous rivers and lakes. Typical soil types are Luvisol, Cambisol, Fluvisol, Gleysol and Histosol. Most common crop types are winter wheat and rapeseed (*Brassica napus L.*).

6.3.2 Input data for model application

6.3.2.1 Weather information

In Germany, the German Weather Service (DWD) provides weather data on a web-based platform (WebWerdis, DWD (2017)). All necessary input data (minimum, maximum and average temperature, wind speed, precipitation, relative humidity, sun duration) are available free of charge.

The data are updated daily, allowing the calculation of soil moisture and consequently the soil compaction risk at almost real-time field conditions. The weather stations Teterow and Sukow-Levitzow were chosen for the Kummerow area, weather station Alfeld for the Adenstedt area.

6.3.2.2 Soil information

A soil map at a scale of 1:200,000 (BUEK 200, BGR (2017)) was used for both study areas. The Federal Institute for Geosciences and Natural Resources (BGR) provides the map free of charge. Soil maps with higher resolution are only available on payment. The BUEK 200 consists of a shape file including the geometries of the individual soil types and related tables with the elementary soil attributes (e.g., soil texture). Based on the soil texture class, the dry bulk density and content of organic matter the more complex physical soil properties such as air capacity, field capacity, available field capacity and the wilting point were derived using the pedotransfer functions provided by Wessolek et al. (2009). They provide classified tables (34 soil texture classes, five dry bulk density classes, four organic matter classes), which enable the derivation of the target values. An additional script was created to automatically calculate the necessary soil properties.

6.3.2.3 Present crop types and crop rotation

Freely available data of present and spatially explicit data on cultivated crop types are rare. Remote sensing data are a valuable source of present and former land use/land cover and therefore on cropland and crop types mapping (e.g. Ozdogan et al., 2010; Calvao and Pessoa, 2015; Khatami et al., 2016). The 'Semi-Automated Classification' plug-in (Congedo, 2016) for QGIS (QGIS, 2017) provides a freely available implementation of classical supervised image classification approaches. These approaches are able to learn the spectral signatures of target classes from user-defined training pixels and categorize image pixels according to statistical similarities in their reflectance behaviour (Campbell and Wynne, 2011). To this end, a certain amount of field mapping data on crop types is required (Foody, 2002). Crop type mappings in the field were conducted in Kummerow (2015) and in Adenstedt (2016) during the summer months from July to September. Field mapping data covered the following target classes: cereals (e.g., winter wheat, rye, barley), maize, winter rapeseed, sugar beets, and grassland. Google Earth imagery supported the identification of less dynamic land cover classes such as water bodies, evergreen/deciduous forest and sealed areas. The field mapping data were divided randomly into a validation and training data set. Recent studies demonstrated the suitability of multispectral Landsat 8 and Sentinel-2 datasets for crop type mapping with a spatial resolution between 10 and 30 m (e.g. Immitzer et al., 2016; Kussul et al., 2016; Sonobe et al., 2017). The United States Geological Survey (USGS) and the European Space Agency (ESA) provide free of charge Landsat 8 (Roy et al., 2014) and Sentinel-2 (Drusch et al., 2012) data on a regular basis (every 5-16 days).

For Kummerow, four Landsat 8 scenes were available during the vegetation period in 2015. Atmospherically corrected Landsat 8 Surface Reflectance products provided by USGS (Vermote et al., 2016) were delivered geo-referenced on Transverse Mercator UTM Zone 33N (WGS84). The data showed a highly accurate co-registration (RMSE < 8 m).

For Adenstedt, Sentinel-2A data form the database for the vegetation period 2016; due to cloud coverage, however, three images are available (processing baseline: 02.04). Sentinel-2A products

of processing baseline 02.04 showed highly accurate co-registration (RMSE < 11 m, Transverse Mercator UTM 32 N WGS 84, (ESA, 2017)). Atmospheric correction was conducted using Sen2Cor (version 2.1.2; Müller-Wilm (2016)), which is implemented in the SNAP toolbox (version 5.0; ESA (2014)). Table 6.5 lists the acquisition dates for both study areas.

Table 6.5: Summary on input data for crop type mapping (date system: dd/mm/yyyy)

	Adenstedt	**Kummerow**
Field mapping year	2016	2015
Satellite data	Sentinel-2A	Landsat 8
Atmospheric correction	Sen2Cor	USGS Surface reflectance product
Spectral bands	490, 560, 665, 705, 740,	440, 480, 560, 655,
(center wavelengths [nm])	783, 842, 865, 1610, 2190	865, 1610, 2200
Spatial resolution [m]	20	30
Acquisition dates	2 May 2016, 30 August 2016,	10 April 2015, 3 May 2015,
	12 September2016	13 June 2015, 23 August 2015

Using the field mappings and satellite data, a supervised classification (minimum distance; distance threshold: 0.2) was conducted for each study area with the plug-in 'Semi-Automated Classification' (Congedo, 2016) developed for the open source software QGIS (version 2.18.7; QGIS (2017)). To this end, atmospherically corrected satellite data from the different dates were merged into one dataset and then classified. Thus, class separability benefited from phenological characteristics (multi-temporal classification). Figure Figure 6.3 shows the classification for Adenstedt, Figure Figure 6.4 for Kummerow.

Table 6.6: Class statistics and accuracy measures of the crop type/land cover classification

	Adenstedt			**Kummerow**		
Class	**Share[%]**	**PA[%]**	**UA[%]**	**Share[%]**	**PA[%]**	**UA[%]**
Unclassified	15.0	-	-	7.8	-	-
Arable land	44.9	49.8				
- Cereals	29.7	97.9	94.3	34.7	87.8	86.5
- Winter rapeseed	4.3	94.2	100	10.3	80.6	86.2
- Maize	4.7	84.4	97.3	4.5	65.3	65.7
- Sugar beets	6.3	98.6	93.7	0.3	NA*	NA*
Non-arable land	40.1			42.3		
- Grassland	2.1	56.6	82.8	16.1	93.8	81.9
- Water bodies/swamps	0.1	100.0	100	2.6	100.0	100
- Evergreen forest	7.7	100.0	97.1	4.3	98.7	97.5
- Deciduous forest	26.5	98.1	89.6	15.6	98.8	97.5
- Sealed area	3.7	69.8	100.0	3.7	93.1	98.5
Overall accuracy [%]		91.5			89.2	
Cohen's kappa		0.8992			0.8741	

PA = producer's accuracy is the share of all correctly classified pixels and the sum of all validation pixels of a class; UA = user's accuracy is the share of all correctly classified pixels and the sum of all classified pixels of a class; overall accuracy is the share of all correctly classified pixels and the sum of all validation pixels; the kappa coefficient additionally includes erroneously classified pixels and considers agreement by chance; * due to rare cultivation in Kummerow area all mapped sugar beet fields were used for classifier training impeding an independent validation.

Accuracy assessment followed the suggestions by Foody (2002) using the independent field mapping data for validation. Table 6.6 lists the percentage share of each class and calculated accuracy measures separately for each study area. Both classifications exceeded a widely reported orientation value of overall accuracy, i.e., 85% (Foody, 2002) indicating sufficient classification accuracy of the entire data set. In particular, the classes cereals, winter rapeseed, maize (Kummerow) and sugar beets (except Kummerow), which were relevant for the SaSCiA-model, performed well with class accuracies >80%. The spectral similarity of winter wheat, rye and barley hampered their differentiation; they therefore were aggregated as cereals.
Both study areas showed a high share of arable land, i.e., 49.8% at Kummerow and 44.9% at Adenstedt. Cereals predominated in both study areas. In Kummerow, winter rapeseed had the second highest share, while sugar beets were second in Adenstedt. In both study areas, unclassified pixels appeared as entire fields, which probably resulted from spectral signatures (crop types) uncovered by the field mappings.

Both study areas lack information on crop types mapping in the preceding two years impeding a remote sensing based derivation of crop rotations (e.g. Kandziora et al., 2014). Assuming common crop rotations based on crop types in 2015 (Kummerow) and 2016 (Adenstedt) allowed considering effects of preceding crop types on soil moisture calculation. For instance, when the present crop type was sugar beet, the crop types for former years were winter wheat, resulting in a crop rotation winter wheat, winter wheat and sugar beet.

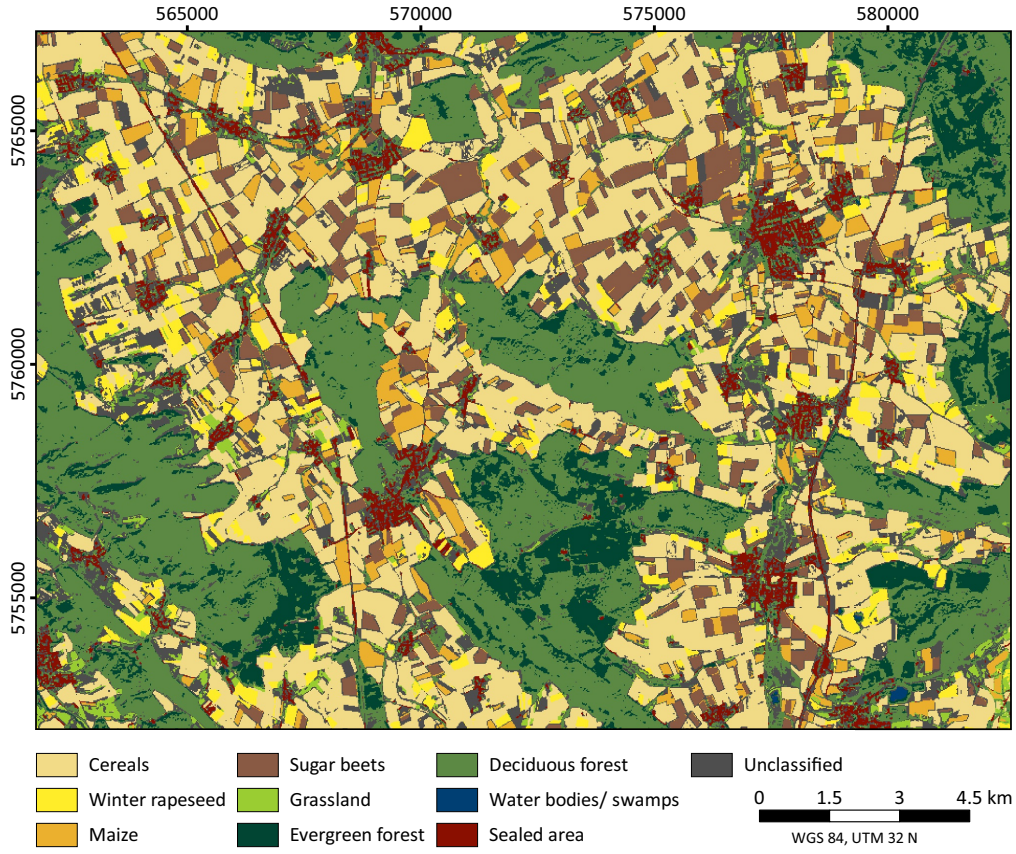

Figure 6.3: Classification result of Adenstedt based on Sentinel-2A data in the year 2016.

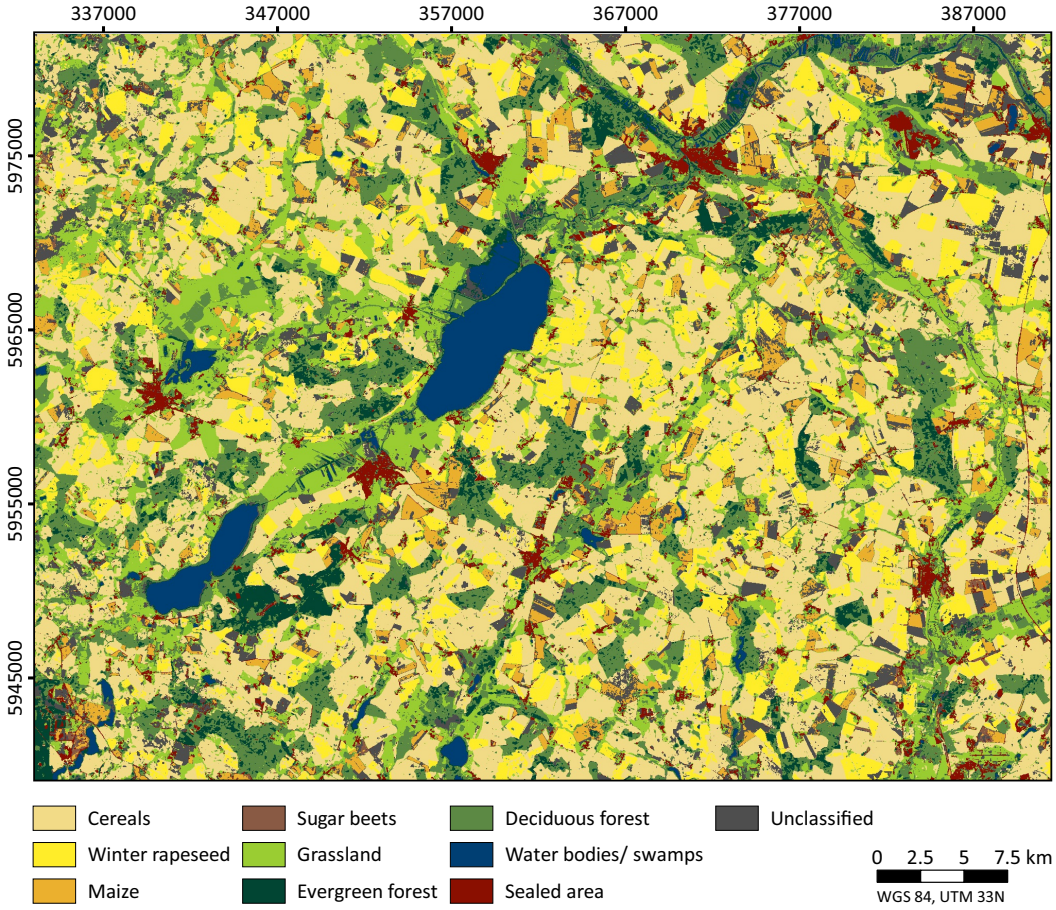

Figure 6.4: Classification result of Kummerow based on Landsat 8 data in the year 2015.

6.3.2.4 Fertiliser and irrigation information

At a regional scale, fertilizer types and applied amount differ; therefore, the most common fertilizers and averages of applied amounts for the regions were chosen based on the information provided by Achilles et al. (2016) and KTBL (2017).

As no information about irrigation was available, the irrigation was set to zero for both study areas.

6.3.2.5 Machinery information and field traffic days

Table 6.7 shows machinery setup used in this study, in particular wheel load and tyre inflation pressure. The machinery selection is based on literature review (e.g. Götze et al., 2016) and manufacturer information (e.g., Grimme for sugar beet harvester). The maximum possible wheel load was assumed for soil compaction risk assessment. For instance, the wheel load of fully loaded combine harvester was used and not the empty or half-filled weight.

Since explicit field traffic days were unavailable, general information provided by Achilles et al. (2016) and KTBL (2017) were used to define reasonable mean periods for field traffic activity (Table A5, Appendix A).

Table 6.7: Machinery setup used for the SaSCiA-modelling for both study area.

Field Traffic	Machinery	Tractor/Trailor	
		max. WL* (in kg)	TIP (in Bar)*
Primary tillage	Tractor (120 kW) + chisel	2500	0.8
Secondary tillage			
- Maize	Tractor (83 kW) + rotary harrow	2200	1.0
- Sugar beet	Tractor (83 kW) + rotary harrow	2200	1.0
Sowing			
- Cereals, Rapeseed	Tractor (120 kW) + seed drill combination	1700	1.0
- Maize	Tractor (67 kW) + precision seeder	1800	1.0
- Sugar beet	Tractor (67 kW) + precision seeder	1800	1.0
Fertilizer			
- All other	Tractor (83 kW) + mounted spreader (1200 L)	2400	1.6
- Maize	Tractor (120 kW) + slurry tank (14m ^{3})	4600	2.1
Crop protection	Tractor (67 kW) + trailed sprayer (2500 L)	1100	1.8
Harvest			
- Cereals, Rapeseed	Combine harvester (220 kW, 8300 L) 8	200	2.0
- Maize	Self-propelled harvester + tractor + trailer (42 m^3)	5100	2.2
- Sugar beet	Self-propelled harvester (390 kW, 22 Mg)	11,200	2.2
Stubble machining	Tractor (120 kW) + disc harrow	2500	0.8

*WL = wheel load, TIP = tyre inflation pressure.

6.4 Results and Discussion

The SaSCiA-model as presented in the Material and Methods section was applied to the data sets listed in the section 3 ("The SaSCiA-model application"). The following section contains selected results of both study areas, which are discussed to demonstrate the spatio-temporal advantages and limitations of the developed model.

6.4.1 Spatial distribution of soil compaction risk

Figure 6.5 illustrates the spatial distribution of soil compaction risk in three different depths at Adenstedt on 7 August 2016 as modelled with SaSCiA. Table 6.8 summarizes the area percentage for each compaction risk class and each of the four crop types. The selected depths are 20 cm (topsoil), 35 cm (soil directly beneath the maximum tillage depth) and 50 cm (subsoil). On 7 August 2016, field traffic potentially affected 80.13% (Table 6.8) of the total arable area at Adenstedt. The areas covered by maize (10.36%) and rapeseed (9.51%) were not endangered through soil compaction since no field traffic activity took place at this time. In 20 cm depth, 73.52% showed "high" to "extremely high" risk. Only 3.99% were classified as "no risk" during field traffic activity. The prevailing red colours in Figure 6.5a clearly demonstrate the high share of areas classified as "high" to "extremely high". Bluish areas ("no risk" to "medium" risk) were distributed over the entire study area without showing any spatial pattern. In 35 cm depth, the area proportions changed; only 2.30% of the total area, which related entirely to "cereals", was classified as "high" or "extremely high". The percentage area classified as "no risk" during field traffic increased up to 21.12%. Figure 6.5b highlights the shift with predominating bluish tones, especially light blue. Two regions with higher soil compaction risk are prominent, i.e., a region with "very high" soil compaction risk in the southwestern part and an area with "high" soil compaction risk along a north-to-south corridor in the East.

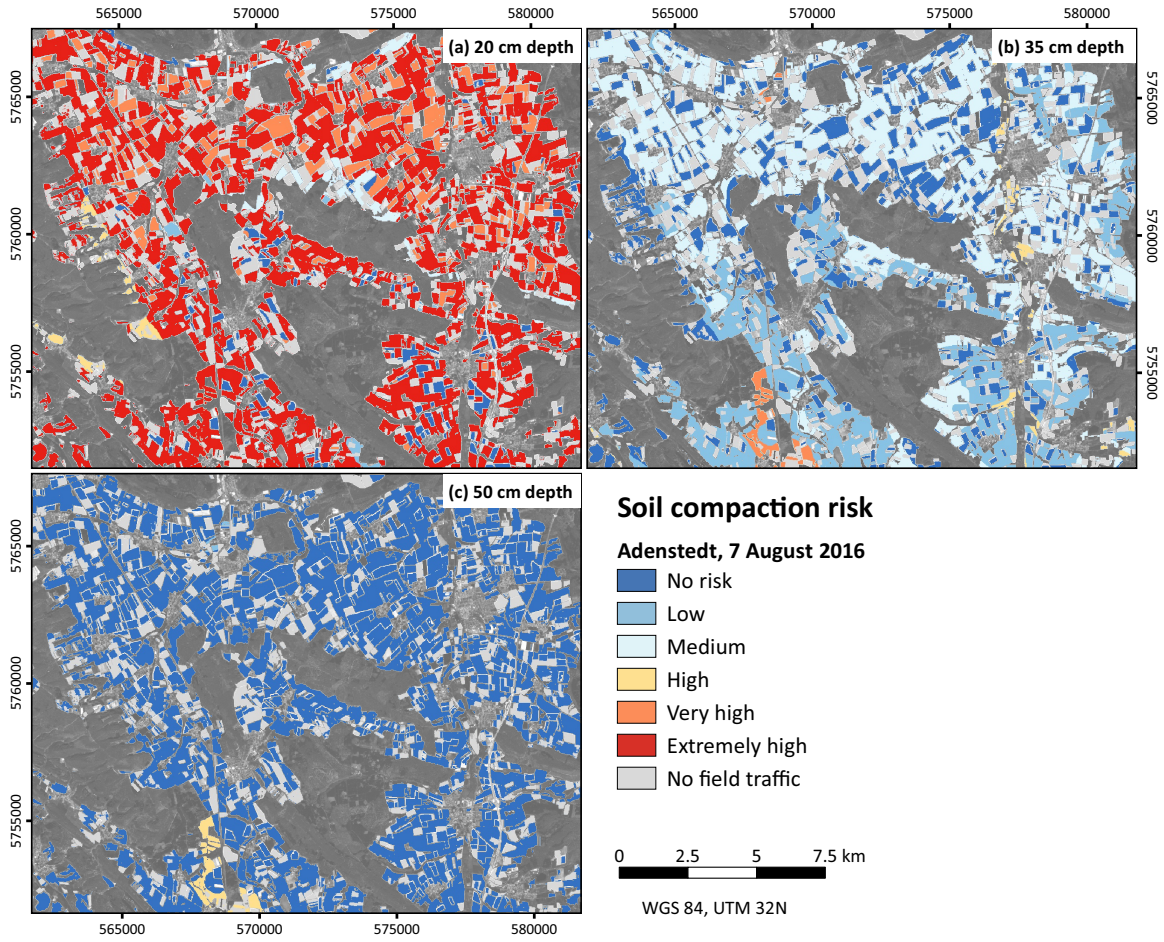

Figure 6.5: Soil compaction risk in (a) 20 cm; (b) 35 cm and (c) 50 cm depth at Adenstedt on 7 August 2016.

Table 6.8: Percentage area of soil compaction risk classes at Adenstedt on 7 August 2016.

Crop	No field traffic	No Risk	Low	Medium	High	Very high	Extremely high	Total
Depth 20 cm								
Cereals	0.00	0.19	0.23	2.06	0.96	0.02	62.63	66.07
Maize	10.36	0.00	0.00	0.00	0.00	0.00	0.00	10.36
Sugar beet	0.00	3.80	0.32	0.04	0.00	9.91	0.00	14.06
Rapeseed	9.51	0.00	0.00	0.00	0.00	0.00	0.00	9.51
Depth 35 cm								
Cereals	0.00	7.06	20.42	36.29	1.07	1.23	0.00	66.07
Maize	10.36	0.00	0.00	0.00	0.00	0.00	0.00	10.36
Sugar beet	0.00	14.06	0.00	0.00	0.00	0.00	0.00	14.06
Rapeseed	9.51	0.00	0.00	0.00	0.00	0.00	0.00	9.51
Depth 50 cm								
Cereals	0.00	64.84	0.10	0.00	1.12	0.00	0.00	66.07
Maize	10.36	0.00	0.00	0.00	0.00	0.00	0.00	10.36
Sugar beet	0.00	14.06	0.00	0.00	0.00	0.00	0.00	14.06
Rapeseed	9.51	0.00	0.00	0.00	0.00	0.00	0.00	9.51

In 50 cm depth, most of the arable area (78.90%) showed "no risk"; only 1.12% was classified as "high". Dark blue colors therefore predominate in Figure 3c except in a region in the southwest with "high" and some fields in the northwest with "low" soil compaction risk.

The spatial detail of the soil compaction risk maps depends on the spatial resolution of the soil and crop type data used for soil moisture modelling. The spatial resolution of crop type mapping was 20 m (Adenstedt) and 30 m (Kummerow). As field sizes are often several hectares, the spatial resolution of the crop type information was sufficient for the soil compaction risk assessment. The soil map used in the study area, however, was only available at a scale of 1:200,000. Hence, the spatial distribution of soil properties is highly aggregated and small-scale variations in soil properties remain disregarded. Using a more detailed soil map within SaSCiA-model may enable a more differentiated soil compaction risk assessment.

6.4.2 Temporal variation of soil compaction risk

The spatial distribution of soil compaction risk for individual days enables the analysis of the temporal variation for an entire year. Temporal changes of soil compaction risk depend on weather conditions, related crop growth and varying wheel loads. Figure 6.6 illustrates an example for different depths (20, 35 and 50 cm) at Adenstedt. The area percentage of the individual soil compaction risk classes (ordinate) is highlighted for each day in 2016 (abscissa).

The percentage area affected by field traffic varied between 0% and 100% for arable land throughout the year. No field traffic occurred during winter (January, second half of November and December), in the first half of March and from mid-June to mid-July leading to 0% affected area. During the second half of September and second half of October, field traffic affected the entire arable area, i.e., 100%. During the remaining months, the percentage varied between 9.8% and 85%.

Figure 6.6 depicts strong leaps of the percentage of soil compaction risk area between certain dates, e.g., 9.5% on 31 July 2016 and 80% on 1 August 2016. These sharp transitions marked the edges of field traffic periods defined in SaSCiA prior to the model run and depend on the particular crop type. This explains, why the area percentage of soil compaction risk at a given date remained the same for all depths (Figure 6.6a-c), while the share of the soil compaction risk classes varied at the different depths.

For the topsoil (20 cm), the SaSCiA-model revealed the highest soil compaction risk with a high proportion of "high" and "extremely high" risk classes throughout the year. During spring, almost each field traffic activity resulted in an "extremely high" soil compaction risk. In November, each field traffic activity resulted in "high" and "very high" soil compaction risk. In spring and autumn, the high percentage of "high" risk area resulted from high soil moisture. In northern Germany, most precipitation occurs from November to March, while plant transpiration is very low. The wet soil therefore has a low soil strength and is unable to withstand the applied stresses, even of low wheel loads. In summer, the amount of precipitation is low, while plant transpiration rate is high. Soil strength increases with decreasing soil moisture, resulting in a reduced soil compaction risk. Accordingly, the percentage of soil compaction risk classes "low" and "no risk" increased at the beginning of August. Nevertheless, Figure 6.2 shows that a high percentage of fields remained highly exposed to soil compaction in summer and early autumn. At this time, the harvest activities led to highest wheel loads (5,000-10,000 kg), causing soil pressures that exceeded the soil strength even of dry soils.

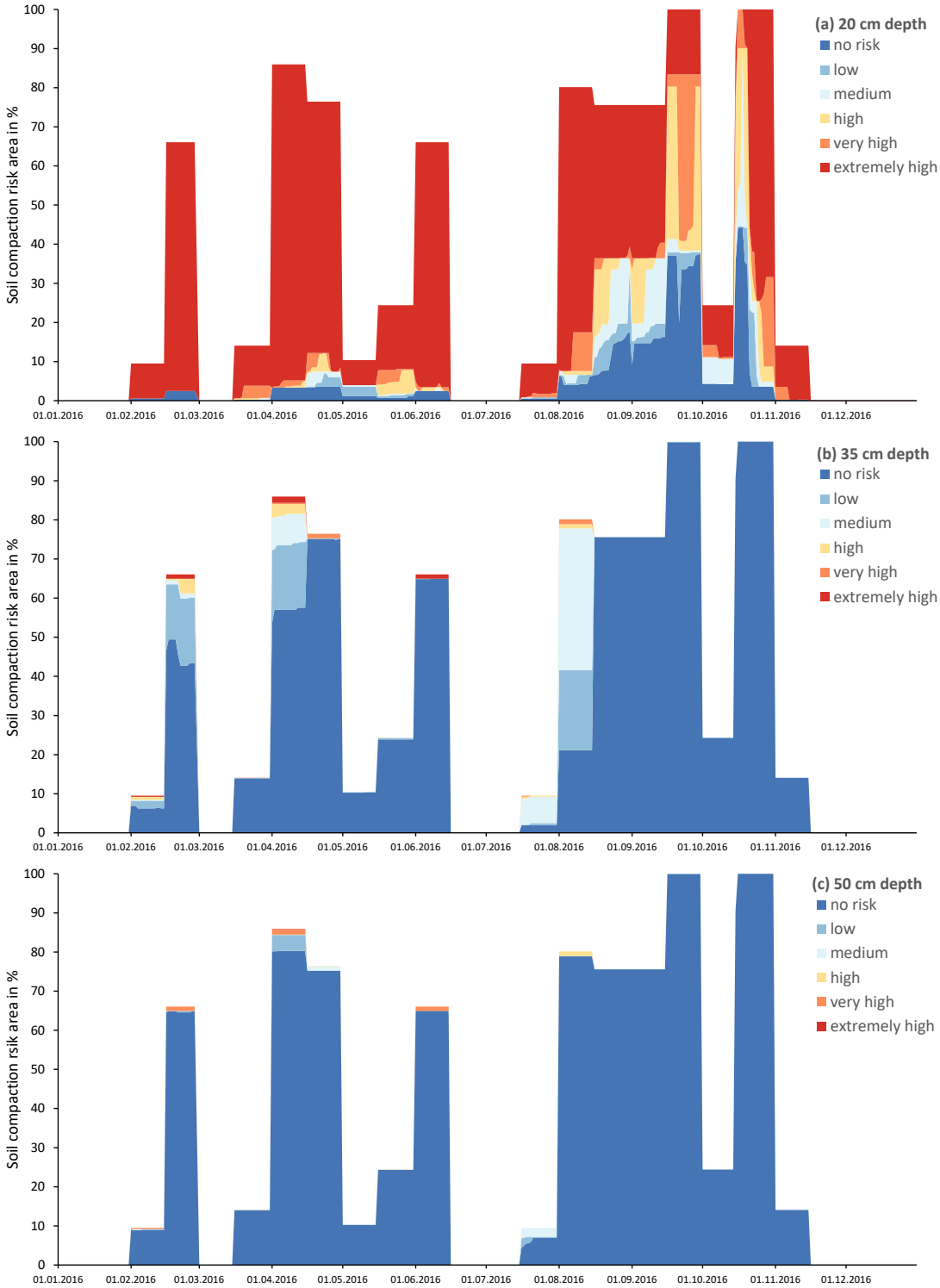

Figure 6.6: Temporal variation of soil compaction risk for (a) 20 cm; (b) 35 cm and (c) 50 cm depth at Adenstedt for 2016. The unit is percentage of the total arable used area. The gap up to 100% represents the percentage area where no field traffic activity occurred on this date (date system: dd/mm/yyyy).

Below the tillage depth (35 cm) and in the subsoil (50 cm), the soil compaction risk was low for the entire cropping season. At a depth of 35 cm, "no risk" areas predominated. From February to the end of June, SaSCiA revealed a "high" or "extremely high" soil compaction risk only for 3% of the arable land. "Low" to "medium" classes shared 23%. The majority of the trafficked area, however, showed "no risk". During the first half of August, only 3% were classified as "high" and "very high", 55% were classified as "low" to "medium". From the second half of August until the end of the year, all field traffic activities resulted in "no risk" of soil compaction. At a depth of 50 cm, the soil compaction risk decreased continuously compared to the depths at 35 cm. The class "extremely high" never occurred; classes "high" and "very high" had a maximum of 2%. Soil compaction risk classes "low" and "medium" resulted in a maximum of 7%. The majority of field traffic activities were classified as "no risk". The low soil compaction risk in autumn contradicts the expectation that maize and sugar beet harvest cause the highest soil compaction as reported by e.g., Nevens and Reheul (2003), Peth et al. (2006) and Destain et al. (2016). In 2016, precipitation sum from July to September was 50% lower (93.2 mm) compared to long-term measurements (184.7 mm) (DWD, 2017). The low precipitation led to dry soils especially in the subsoil. The dry soil compensated most of the applied soil pressure in the topsoil, resulting in a less affected subsoil.

To demonstrate the influence of weather conditions, the soil compaction risk assessment for Adenstedt was repeated with the weather data from 2014. In 2014, precipitation sum was 240.6 mm (DWD, 2017) from July to September representing a year with wet soil conditions during harvest. All other input data remained the same for this scenario. Figure 6.7 shows the results of the wet scenario at a depth of 35 cm: a clear increase in soil compaction risk for harvest times (16 July to 15 August 2016 and 16 September to 15 October 2016) emphasizes the effects of high wheel loads during wet soil conditions compared with dry soil conditions in Figure 6.6. The results of the wet weather scenario are in agreement with the findings of the former mentioned studies (Nevens and Reheul, 2003; Peth et al., 2006; Destain et al., 2016): high wheel loads during maize and sugar beet harvest increase soil compaction risk.

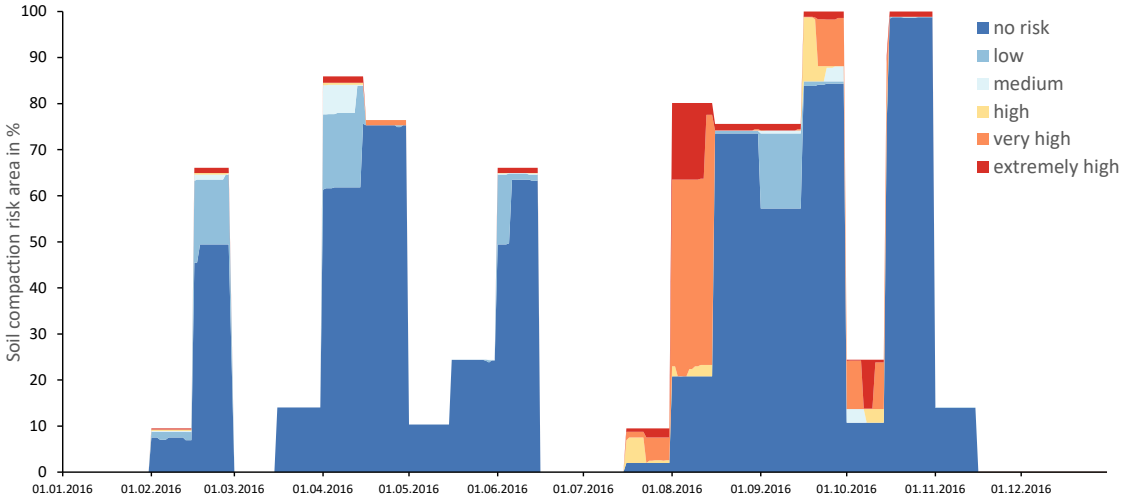

Figure 6.7: Temporal variation of soil compaction risk at a depth of 35 cm in Adenstedt for the wet scenario (using weather condition of 2014) (date system: dd/mm/yyyy).

6.4.3 Spatio-temporal variation for single crop types

The SaSCiA-model enables analyses of varying soil compaction risk for single crop types. Selecting only one crop type (e.g., sugar beet) enables the analysis of varying soil properties on soil compaction risk. Figure 6.8 shows an example of the temporal dynamics in soil compaction risk at a depth of 20 cm for areas cultivated with cereals at Kummerow in 2015.

Since cereals was the focused crop type and SaSCiA considers similar field traffic for one crop type, the area affected by field traffic activity was either 0% (no field traffic) or 100% (field traffic on all cereal cultivated areas). Six periods had no field traffic activity. During the year, however, all soil compaction risk classes occurred, whereas spring and autumn showed the highest soil compaction risk. Changes in soil compaction risk classes became apparent within a traffic period. As an example, Figure 6.9 shows the changes in soil compaction risk during the cereal-harvest period (1 August 2015-15 August 2015) in the Kummerow area.

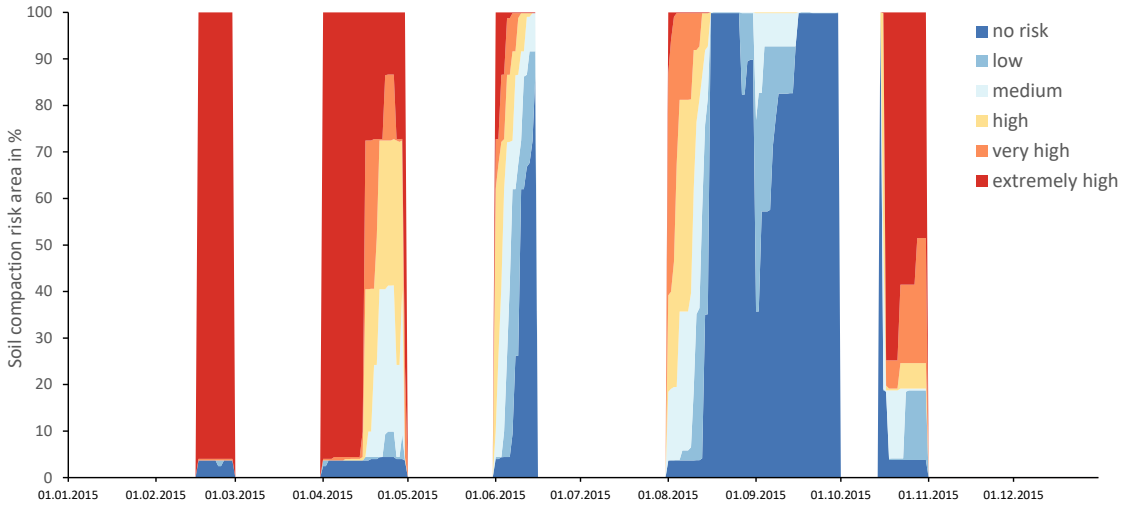

Figure 6.8: Temporal variation of soil compaction risk for cereals at a depth of 20 cm at Kummerow (date system: dd/mm/yyyy).

At the beginning of the harvest period (Figure 7a; 1 August 2015), soil compaction risk was heterogeneously distributed, whereas classes "high" to "extremely high" (81.52%) predominated. Only 3.67% of the area showed "no risk" and 14.81% "low" to "medium" soil compaction risk. Rainy days in July (precipitation sum of 72.4 mm; DWD) caused an increased soil moisture with decreased soil strength. In the following days, however, the desiccating soil led to a decreasing soil compaction risk in the entire region.

On 7 August 2015 (Figure 7b), "low" to "medium" soil compaction classes increased to 32.02%, while "high" to "extremely high" decreased to 64.27%. On 15 August 2015 (Figure 7c), the majority of the trafficked area (57.58%) was classified as "no risk". Only 7.30% remained with "high" to "extremely high" soil compaction risk class.

The analysis of the cereal-harvest in the Kummerow area (Figure 6.9) demonstrated how weather conditions may influence the spatial distribution of soil compaction risk on short term. Furthermore, the different soil compaction risk classes for a particular day highlighted the influence of varying soil

properties; as crop type, weather information and machinery setup were the same for the entire region, the spatio-temporal variations in soil compaction risk result from different soil conditions.

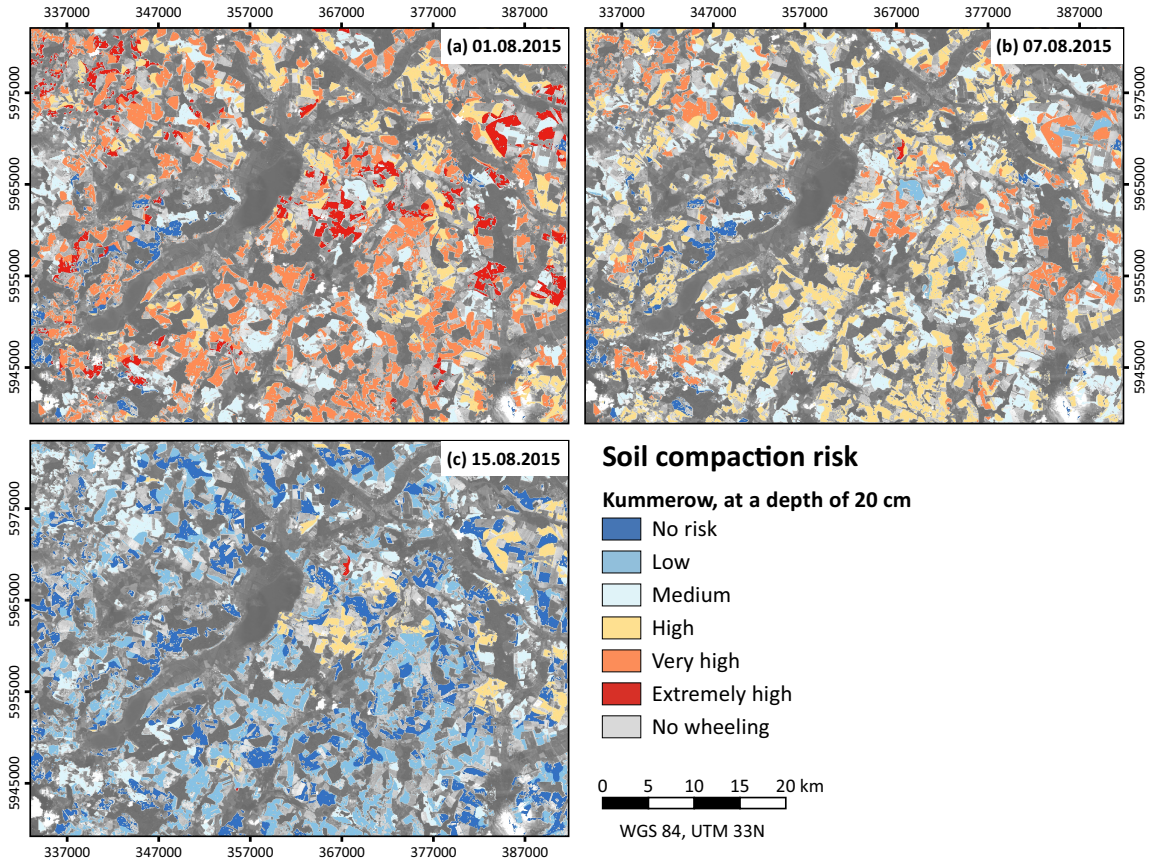

Figure 6.9: Soil compaction risk for areas cultivated with cereals at a depth of 20 cm at Kummerow for (a) 1 August 2015; (b) 7 August 2015 and (c) 15 August 2015 (date system: dd/mm/yyyy).

6.4.4 Advances and limitations of the SaSCiA-model

The applicability of the SaSCiA-model has been demonstrated for two study areas in Germany with different spatial extent and varying land cover, pedological characteristics and weather conditions. The study highlights that the SaSCiA-model generates daily maps of soil compaction risk, which can support a sustainable field management and field traffic strategies to maintain various environmental functions of soils. The potential applications of the SaSCiA-model are manifold:

(i) Real-time soil compaction risk assessment

The SaSCiA-model enables a real-time soil compaction risk assessment, if sufficient data (especially weather and crop type data) is available. Currently available spatial soil compaction models show only the potential soil compaction risk, which is of limited importance for decision-making under real field conditions. The spatio-temporal high-resolution maps produced by SaSCiA show areas with varying (time and space) soil compaction risk. SaSCiA, therefore, can be potentially used as communication and visualization tool. Thus, the up-to-date soil compaction risk maps may support farmers, stakeholders and consultants in making decision for a more sustainable agriculture.

(ii) Retrospective soil compaction risk assessment

The SaSCiA-model is also applicable for retrospective soil compaction risk assessments, as demonstrated in the case studies. As long as crop type information is available (e.g., derived from field mappings or from remote sensing data), the SaSCiA-model can be used to obtain retrospective daily soil compaction risk maps for the last year, decade or even longer (the Landsat archive provides data back to the 1980s). Additional information of former crop types derived by farmers or public institutions may also contribute to generate typical crop rotations for study areas and, therefore, long- term analyses of soil compaction risk.

(iii) Hot-spot detection

The continuous application of the model for several years may identify areas with high soil compaction risk year by year. This hotspot identification may help to prevent further soil compaction by means of adapted field cultivation. Since soil compaction reduces the infiltration rate and increases runoff, detected hot-spot areas may be subject to further investigations, e.g., regarding risk assessment of soil water erosion. Accordingly, Alaoui et al. (2018) recently published a review in which they advise the use of remote sensing and new methods of soil compaction mapping for flood analysis and flood prevention. The SaSCiA-model may contribute to this recommendation.

(iv) Deriving days of trafficability

Apart from the assessment of soil compaction risk, the SaSCiA-model may be used to calculate the maximum wheel load day-by-day until no risk (or low or medium risk) occurs. Such analyses, for instance, may provide recommendations to farmers on the maximum payload during harvesting.

(v) Scenario calculations

The study shows that the SaSCiA-model can also be used for scenario calculation. Incorporating modified weather data further enables the analysis of climate change on soil compaction risk. This may help to develop strategies for future machinery setup, field traffic behavior or crop type selection. Effects of crop types on soil compaction risk may be investigated by changing present crop types, e.g., winter wheat instead of maize. This may be of particular interest in regions with changing cultivation practices as observed in Germany; here, the amount of area cultivated with maize extremely increased in the last decade (Destatis, 2006, 2016). Since maize is one of the crop types causing highest soil compaction risk due to harvest in autumn under wet soil conditions, applying SaSCiA (present crop type (maize) versus an assumed crop type (e.g., winter wheat) demonstrates changing soil compaction risks under different crop type cultivation.

The forecasting ability of the SaSCiA-model, however, depends on the quality and availability of input data and the assumptions necessary for a regional analysis. In addition, some limitations of the SaSCiA-model must be taken into account:

(i) Crop type detection

The crop type is a key factor for soil compaction risk assessment. Without spatially explicit crop type information, SaSCiA is unable to calculate the soil moisture; related field traffic activities and wheel loads therefore cannot be assigned. To calculate real-time or near real-time soil compaction

risk maps, present crop types are required. The availability of freely available crop type data, however, is limited, especially for the present year.

For the two study areas, Sentinel-2A and Landsat 8 satellite data accompanied by field mappings served as input for the crop type mappings. Nevertheless, satellite remote sensing data allow a retrospective assessment; it may also help to identify crop type for the present years. Separation of crop types using remote sensing further depends on their spectral variability, i.e., the spectral signatures must differ significantly at the acquisition day of the satellite. Furthermore, the spectral variability within a crop type has to be lower that the spectral variability between crop types.

During summer months, matured rapeseed may have a similar spectral behaviour as cereals; during spring, rapeseed is in full bloom and differs significantly from cereals. After sowing in spring, both maize and sugar beets depict a similar spectral behaviour as bare soil; consequently, they are spectrally easier to distinguish in late summer. After maize harvest, it is difficult to distinguish winter wheat as a subsequent crop and yellow mustard as catch crop, or weed growth. In general, images acquired directly after harvest or after sowing tend to impede an accurate crop type classification.

Moreover, the spectral/radiometric characteristics of the satellite sensors determine whether and which crop types can be identified (van Niel and McVicar, 2004; Foerster et al., 2012). Using satellite remote sensing for real-time crop monitoring therefore may be limited. Land use classifications using remote sensing data in spring or early summer, however, enable an assessment for the following harvest period. Using a series of land cover classifications for several consecutive years, typical crop rotations may also be derived (e.g. Kandziora et al., 2014). Applying this crop rotation scheme allows a prediction of the following crop type, which then enables a soil compaction risk assessment for the subsequent year.

(ii) Assumptions for input-data

In SaSCiA, the spatial pattern of soil compaction risk results from spatially varying soil properties, crop types and derived soil moisture. Weather information, machinery information and field traffic days are assumed as constant values within the entire region.

For wheel load and tyre inflation pressure, one value for each crop type and type of field traffic (e.g., sowing, spraying and harvest) can be specified. If more than one piece of machinery works in the field at the same time, e.g., during maize harvest, only one wheel load can be used for soil compaction risk assessment. In the case studies, the maximum wheel load, i.e., the worst case, was chosen. This may result in an overestimation of soil compaction risk, as wheel load changes dynamically; during sugar beet harvest, for instance, wheel load varies between the empty gross weight of 30 t and a fully loaded weight of 60 t. Some studies therefore focus on changes in wheel load at field scale (e.g. Duttmann et al., 2014, 2013). At regional scale, however, the wheel load affecting each raster cell remains unknown. Each part of a field may potentially be wheeled with the maximum load; hence, each raster cell may be affected with a maximum soil compaction risk. In SaSCiA, however, the wheel load and tyre inflation pressure is user defined; it therefore depends on the user, which may also select the minimum or the average wheel load.

Due to a lack of information on the distribution of field traffic, the SaSCiA-model neglects rollover frequency. The number of wheel passages, however, affects soil functionality. Each wheel passage leads to a decrease of soil functions (e.g. Canillas and Salokhe, 2002). Highest field traffic intensity occurs in the headlands (turning areas of the field) and the tramlines (Chamen et al., 2003; Duttmann

et al., 2013). The position of tramlines and headlands is highly variable, depending e.g., on field geometry and working width, which aggravates considering its effects at a regional scale. Since each raster cell could potentially be trafficked, any raster cell may be susceptible to soil compaction. Some studies therefore focus on the prediction of field traffic distribution based on field geometry and used machinery setup (e.g. Edwards et al., 2017). If these models are further developed, integration into the SaSCiA-model may overcome the disadvantage of missing rollover frequency.

The exact days of field traffic activity is another parameter, which is difficult to consider at a regional scale. The period for e.g., maize sowing lies within a range of weeks and the exact date of sowing depends on the farmer's decision. The SaSCiA-model therefore integrates periods for each field traffic operation to consider varying field traffic days. The real field traffic activity will most likely occur within the specified period resulting in a reliable soil compaction risk assessment. If available, exact field traffic days can be used.

Another important point is the assumption of static characteristic of further soil properties, for instance dry bulk density and soil structure. The highly dynamic change of soil moisture is part of the SaSCiA-model. Further soil properties such as dry bulk density may also vary during the season as a result of drying-wetting, settling after tillage or other processes. The same applies for the effects of root growth after sowing. Roots may change the soil structure and increase the soil strength during the season. A recently published study reviewed possible impacts of vegetation on soil strength and trafficability (Wieder and Shoop, 2018). These changes are not considered automatically in the calculation of soil strength. However, effects of root/plant growth are considered in the MONICA-model. Thus, root/plant growth is considered in soil moisture calculation and, therefore, in the calculation of moisture dependent soil compaction risk. Apart from seasonal changes of soil properties, field traffic will affect soil properties. For instance, a traffic activity at the beginning of the year (e.g., fertilizer application) may increase the dry bulk density of the trafficked soil. The change in dry bulk density affects the subsequent calculation of soil strength and plant/root development and, therefore, the calculation of soil moisture. As the SaSCiA-model uses the soil properties given in the soil table and calculates the soil compaction risk based on these properties, changes of soil properties as dry bulk density are not considered automatically. A manual change of soil properties is (until now) the only way to consider seasonal, tillage or traffic induced changes in certain soil properties.

(iii) Model validation

Additional work is required to provide a validation of the SaSCiA-model. Model accuracy, of course, depends on the quality of the input data. Soil information, for instance, is an important input for the SaSCiA-model, but is often only available in a low resolution, as was the situation in the case studies. Thus, the soil information is spatially aggregated and the depiction of the soil heterogeneity therefore is limited. This is, however, rather a problem of data availability than of the model itself. The individual components/models of the SaSCiA-model are well established and proven: the ability to calculate the soil compaction risk for two soil moisture contents (pF 1.8 and 2.5) using the approach by Horn and Fleige (2003) at field, regional or higher scale was demonstrated by several studies (Horn et al., 2005; Fritton, 2008; Horn and Fleige, 2009; D'Or and Destain, 2014; Duttmann et al., 2014). The MONICA-model was applied in studies to derive soil moisture and winter wheat yield at regional scale (Nendel et al., 2011, 2013), which indicates its applicability in the SaSCiA-model. Götze et al. (2016) and Jacobs et al. (2017) successfully applied the approach from Rücknagel et al.

(2015) to evaluate the soil compaction risk at individual farms.

It is therefore necessary to verify the predicted soil compaction risk resulting from the interaction of the single model components. This requires further fieldwork and soil sampling conducted before and after any field traffic activity, as described by (Batey, 2009). The maps resulting from SaSCiA-modelling show the heterogeneous soil compaction risk at high spatial and temporal scales, thus enabling the detection of areas for appropriate soil sampling and model validation.

6.5 Conclusions

The SaSCiA-model enables a region-wide soil compaction risk assessment at a high spatial and temporal resolution. It combines well-established approaches and models (Horn and Fleige, 2003; Rücknagel et al., 2015; Nendel et al., 2011; DIN V 19688, 2011) with spatially differentiated soil and crop information. Furthermore, the model integrates varying wheel loads, tyre inflation pressures and field traffic days. The results are daily maps of soil compaction risk for entire regions in a spatial resolution exceeding already existing approaches. The applicability of the SaSCiA-model has been demonstrated for two study areas; soil compaction risk for both study areas has been calculated for entire years.

By using freely available data and open source software, a broad community of practicing experts, stakeholders and consultants involved in soil protection may apply the SaSCiA-model.

Even if the model has some limitations as discussed, it currently is the only spatial approach concerning spatial and temporal changes in soil moisture, plant growth and wheel loads. Potential applications of the model are manifold and may range from retrospective, through current to potentially future soil compaction risk assessments.

Author contributions: M.K. designed the study in collaboration with all co-authors. M.K. prepared the figures and wrote the majority of the text with contributions by K.D. M.K. developed the model and conducted data analyses; K.D. prepared and analysed the remote sensing data. N.O. and R.D. contributed in reviewing and finalizing the manuscript.

Acknowledgements: The authors thank the anonymous reviewers for their commitment and very helpful comments on improving the manuscript. We are grateful to James F. Petersen and Kilian Etter for the linguistic editing. The Federal Ministry of Education and Research (BMBF) supported this study within the framework of the BonaRes-initiative (Grant No.: 031A563C). We acknowledge financial support for publications cost by Land Schleswig-Holstein within the funding programme Open Access Publikationsfonds.

Conflicts of interest: The authors declare no conflict of interest.

6.6 Appendix A

Table 6.9: Structure and example of input weather information (date system: yyyy/mm/dd).

Date	T_min	T_avg	T_max	Precipitation	Sunhours	Windspeed	Rel_humid
yyyy-mm-dd	in °C	in °C	in °C	in mm	in h	in m/sec	in %
2014-01-01	1.2	3.3	5.3	0.0	1.0	4.9	79
2014-01-02	4.0	6.8	9.5	0.1	0.1	5.6	80
...	...	...	...	...	...	...	...

Table 6.10: Structure and example of input soil data.

Soil_ID	Hor	Depth_up	Depth_low	Texture	Gravel	Corg	Structure	DBD	AC	FC	AFC	WP
101000000	Ap	0	30	Ut4	1.2	1.74	sub	1.5	6	40	22	18
101000000	Sw-Al	30	40	Ut3	0	0	sub	1.5	4	36	24	12
101000000	Bt-Sd	40	60	Tu4	0	0	pol	1.7	2	34	12	22
101000000	Bvt-Sd	60	110	Tu4	0	0	pol	1.7	2	34	12	22
101000000	C	110	200	Ut3	0	0	sub	1.5	4	36	24	12
102000000	Ap	0	30	Lu	7.8	6.69	sub	1.2	11	53	25	28
...	...	...	...	...	...	...	...	...	...	...	...	

Soil_ID = unique soil identifier, Hor = name of horizon (German classification), Depth_up = upper depth of the horizon, Depth_low = lower depth of the horizon, Texture = texture class (German classification), Gravel = gravel content in %, Corg = soil organic matter in %, Structure = aggregates, DBD = dry bulk density in g cm^{-3}, AC = air capacity in vol. %, FC = field capacity in vol. %, AFC = available field capacity in vol. %, WP = wilting point in vol. %.

Table 6.11: Structure and example of input crop unit for MONICA-modelling (date system: yyyy/mm/dd).

Crop_rotation_ID	Crop	Sowing	Harvest	Tillage	Depth	Year
101110	SM	2014-04-21	2014-09-21	2014-09-22	30	2014
101101	WW	2014-10-21	2015-08-07	2015-09-21	30	2015
101101	WW	2015-10-21	2016-08-07	2016-09-21	30	2016
102110	SM	2014-04-21	2014-09-21	2014-09-22	30	2014
102101	WW	2014-10-21	2015-08-07	2015-08-08	30	2015
102114	RS	2015-08-09	2016-07-21	2016-09-21	30	2016
...	...	...	...	...	...	...

SM = silage maize, WW = winter wheat, RS = rapeseed.

Table 6.12: Structure and example of input fertilizer data for MONICA-modelling (date system: yyyy/mm/dd).

Crop_rotation_ID	N	Fertiliser	Date	Incorperation
101110	67	CADLM	2014-05-10	1
101110	108	AN	2015-03-07	0
...	...	...	...	

Table 6.13: Structure and example of input field traffic data (date system: yyyy/mm/dd).

Crop	WL_SW	TIP_SW	Start_SW	End_SW	...	WL_HV	TIP_HV	Start_HV	End_HV	...
WW	1800	100	2016-10-08	2016-10-28	...	7000	100	2016-07-11	2016-08-15	...
SBE	1800	100	2016-03-21	2016-04-10	...	10,000	100	2016-10-01	2016-11-07	...
SM	1800	100	2016-04-21	2016-05-20	...	9000	100	2016-09-15	2016-10-15	...
...	...	...	...	...	...	...	...	...	...	...

WW = winter wheat, SBE = sugar beet, SM = silage maize, WL = wheel load, TIP = tyre inflation pressure, SW = sowing, HV = harvest, start = beginning of field traffic period, end = ending of field traffic period.

Table 6.14: Crop type, abbreviations and crop-ID for crop types used in the SaSCiA-model.

Crop type	Abbreviation	Crop_ID
Winter wheat	WW	101
Spring wheat	SW	102
Winter barley	WB	103
Spring barley	SB	104
Winter rye	WR	105
Spring rye	SR	106
Winter triticale	WT	107
Spring triticale	ST	108
Oat	OA	109
Silage maize	SM	110
Grain maize	GM	111
Sugar beet	SBE	112
Potato	PO	113
Rapeseed	RS	114
Phacelia	PH	115
Oil radish	OR	116
Mustard	MU	117
Broad Beans	BB	118
Forage peas	FP	119
Sunflower	SF	120
...	...	...

Definition of the crop-rotation-ID for the SaSCiA-model

Figure A1 demonstrates the principle of the creation of "crop-rotation-ID" exemplary. The "crop-rotation-ID" consists of six numbers and contains two information codes. The first three numbers represent the spatial distribution of a crop rotation ("rotation-ID"). The last three numbers represent the present crop type in the investigated year ("crop-ID"). A crop rotation is a sequence of crop types year by year at the same field/raster cell. The left-hand side of Figure A1 demonstrates the creation of the "rotation-ID". Each field/raster cell in each year exhibit a crop type (e.g., maize) and is classified by a three-digit number (e.g., 110) based on the classification listed in Table A6. Fields/raster cells with the same sequence of crop types for the three years resulting in a "rotation-ID". This is the case for the upper and lower examples in Figure A1. The field borders remain unchanged for the period, but crop types vary (101-110-101 and 112-101- 114), resulting in two different rotation-IDs (101,000, 104,000). Looking at the example in the middle, the field geometries and crop types are the same for the first two-years. In the third year, the field is subdivided in two different crop types

(110 and 112), resulting in two rotation-IDs (102000, 103000). The "rotation-ID" itself is result from a sequential numbering, starting at 101000. The present crop in the investigated year (year 3) is appended to the rotation-ID. The result is the "crop-rotation-ID", containing the information of the previous crop type, the present crop type and their spatial distribution (right had side, Figure A1).

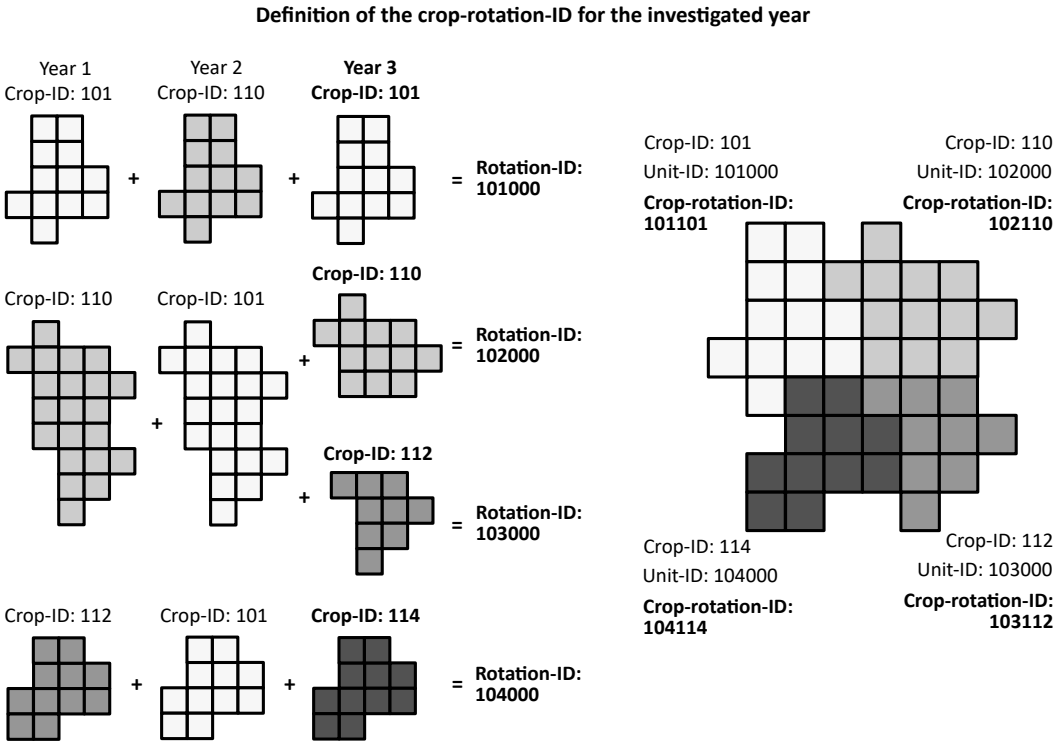

Figure 6.10: Example of creation of 'rotation-ID' and 'crop-rotation-ID'.

Chapter 7

Discussion and conclusions

This thesis focussed on soil compaction in arable soils at different scales. At field scale, fieldwork aimed to describe tillage and field traffic intensity effects on the spatial distribution of soil compaction. The results and knowledge from the field scale surveys were transferred to regional scale. The aim was to develop a soil compaction model that enables a more realistic soil compaction risk assessment compared to previously available models by integrating actual soil moisture and crop type. The developed SaSCiA-model was applied to two study areas to calculate and assess the soil compaction risk on a daily basis at regional scale.

7.1 Summary of main achievements

This thesis focussed on three main research questions. The first research question was:

(1) Does the type of tillage practice and traffic intensity affect the spatial distribution of soil compaction?

Chapter 4 addressed the first research question. A field divided into three plots with different primary tillage practices (CT, RT1, RT2) and two types of traffic intensities (inner field and headlands) served as study area. Penetration resistance measurements and their spatial mapping were used as an indicator for soil compaction patterns.

The answer of research question 1 is that type of tillage practice and traffic intensity affect the spatial distribution of soil compaction. In detail, the analyses conducted in chapter 4 revealed significant spatial differences in penetration resistance depending on tillage intensity (conventional tillage vs. reduced tillage). In the topsoil, penetration resistance was up to 2.5 times higher in RT compared to CT. In the subsoil, however, the penetration resistance was approximately the same for all three tillage practices. These results are consistent with those of Koch et al. (2008) and Destain et al. (2016); they found similar differences between conventional and reduced tilled plots. In conventional tillage, intensive loosening year-by-year results in lower soil density compared to conservation tillage (e.g. Taser and Metinoglu, 2005; Capowiez et al., 2009; Parvin et al., 2014). As intensive loosening is missing in reduced tillage, the soil density increases. Chapter 4 demonstrated that such relationships can be mapped and spatially analysed.

The comparison between the inner field and the headlands as areas with different traffic intensity revealed significant higher penetration resistance in the headlands, in both, the topsoil and the subsoil. Additionally, the higher penetration resistance in the headlands showed a clear spatial boundary to the inner field. The headlands are the area of a field with the highest field traffic intensity (e.g. Duttmann et al., 2013) resulting from field traffic with high wheel loads (e.g. during sugar beet harvest) and high share of wheel passages (turning area for all field traffic activities). For instance, turning manoeuver during e.g. tillage and harvest can lead to 50 wheel passages in one cropping season (Augustin et al., subm). Furthermore, the headlands are frequently used as deposition area for sugar beets (in case of crop type sugar beet) and as a loading area for harvested crops. Thus, the headlands are the area of a field with highest soil compaction risk. The results in chapter 4 showed a recognisable effect of high traffic intensity in the headlands: the headlands revealed (i) the highest penetration resistance values of the entire field and (ii) a significantly higher penetration resistance up to a depth of 50 cm. Thus, penetration resistance measurements enabled the spatial separation of three areas with a different degree of soil compaction depending on the applied tillage practice and traffic intensity: CT-plot, RT-plots and headlands (Figure 4.3).

Using penetration resistance to detect patterns of soil compaction is only valid when the density of a layer defines the term "soil compaction". Using solely soil density, however, impedes any statement about the functionality of the soil pores (e.g. Horn, 2004; Vogeler et al., 2006). Chapter 4 clearly showed that saturated hydraulic conductivity and amount of biopores were higher in RT compared to CT, although penetration resistance measurements, i.e. soil density, were higher. That means, despite of the higher penetration resistance in RT, the soil functionality was enhanced compared to CT. A higher density in RT results from soil settlement, traffic activity and low loosening (e.g. Koch et al., 2008). Simultaneously, aggregation processes are enhanced, aggregate stability is increased, pore connectivity is undisturbed and a stable soil structure can develop (cf. chapter 2.2; e.g. Alvarez and Steinbach, 2009), which leads to improved soil functionality. The penetration resistance value can only give information about the soil density respectively the relative differences in soil density in a soil profile. Thus, penetration resistance is a weak indicator for soil compaction if the term "soil compaction" is defined beyond soil density, i.e. also by soil functionality (e.g. Yavuzcan et al., 2005). This shortcoming limits the use of penetration resistance measurements to evaluate soil compaction.

Additionally, soil moisture and soil texture strongly influence penetration resistance. The investigated field had a relatively homogenous soil texture (Figure 3.3) and soil moisture (Table 4.5). A field with heterogeneous soil texture may lead to varying penetration resistance patterns, which reflect the different clay content rather than (harmful) soil compaction. A possible misinterpretation of penetration resistance is even more pronounced for soil moisture. Increasing soil moisture results in a decreased penetration resistance (e.g. Utset and Cid, 2001; Vaz et al., 2011). Analysing the spatial distribution of penetration resistance therefor necessitates moisture conditions, which are approximately similar over an entire field. This case usually occurs in late autumn and spring, when soils are at field capacity.

Furthermore, the interpretation of the penetration resistance value is complex. Hitherto, a general classification of penetration resistance values, which prove a harmful soil compaction are lacking. Several studies, which compared root growth and penetration resistance revealed values between 2.0 and 3.0 MPa as threshold values that will result in reduced root growth (e.g. Pardo et al. 2000;

Otto et al. 2011). In contrast, roots use existing biopores and the penetration resistance alone will not necessarily hinder the growth (e.g. Ehlers et al., 1983).

Summarising research question 1, the degree of tillage intensity (conventional vs. reduced tillage) and the traffic intensity (inner field vs. headlands) results in clear spatial patterns of soil density. These spatial patterns can be detected by measuring and mapping penetration resistance. However, soil density measurements alone fails to assess soil functionality; thus, soil density patterns detected by penetration resistance are not necessarily connected to reduced soil functionality, as shown by the comparison between conventional tillage (low penetration resistance, low saturated hydraulic conductivity) with reduced tillage (higher penetration resistance, higher saturated hydraulic conductivity). Analysing soil functionality therefore requires additional soil physical measurements.

As described in chapter 4 and in research question 1, the application of long-term reduced tillage resulted in significantly higher penetration resistance in the topsoil compared to conventional tillage. Since increased penetration resistance may lead to impaired root and plant development, a reduction of penetration resistance may be necessary. Thus, a complete inversion by mouldboard plough of the long-term reduced tilled plots (also referred to as one-time inversion tillage) was applied to reduce topsoil compaction and create a proper seedbed. The effect on the improved soil physical properties, which developed by long-term reduced tillage were unknown. Therefore, the second research question was:

(2) Is one-time inversion tillage a suitable measure to lower topsoil compaction in conservation tillage?

One-time inversion by mouldboard plough of the long-term reduced tilled plots enabled an evaluation of this measure with regard to its effects on soil physical properties (cf. chapter 5). The results showed that dry bulk density decreased to approximately the same order of magnitude as measured for the continuously conventional tilled plot by the one-time inversion. Thus, the aim of one-time inversion tillage, loosening presumably compacted topsoil as a result from long-term reduced tillage, was achieved. In contrast, measurements at four different dates in the following season clearly showed that the saturated hydraulic conductivity and infiltration rate in the formerly reduced tilled plots were always significantly higher compared to the CT-plot. These observations indicate that improved soil functionality developed by long-term reduced tillage remain even after one-time inversion tillage.

A second focus of chapter 5 to answer research question 2 was on the effects of field traffic after one-time inversion tillage. Two traffic intensities were investigated: (i) the tramlines, which are affected by repeated field traffic several times a year, and (ii) the ruts of the fully loaded combine harvester representing the area affected by the highest wheel load during the current growing season. The tramlines of both RT-plots showed higher saturated hydraulic conductivity and infiltration rate compared to CT. The wheel tracks of the fully loaded combine harvester at least had a higher infiltration rate in both RT plots. Thus, soil functionality was even better after field traffic activity in the formerly reduced tilled plots. The dry bulk density, as an indicator for soil compaction, was in the same range for all three plots in the tramlines. The ruts of the fully loaded combine harvester revealed a slightly higher dry bulk density in the RT-plots compared to CT.

Within the limits of the present study, research question 2 can be answered with: yes, one-time

inversion tillage is a suitable measure to lower topsoil compaction resulting from long-term reduced tillage. It reduces dry bulk density, while maintaining the improved soil functionality (saturated hydraulic conductivity and infiltration rate).

The results of chapter 5 may open new management options for farmers. Applying conservation tillage in long-term may result in a stratification of nutrients and organic matter, increase of weed pressure and increase of soil compaction (e.g. Koch et al., 2009; Deubel et al., 2011; Nichols et al., 2015; Schlüter et al., 2018). Furthermore, seedbed preparation by conservation tillage during unfavourable weather and soil conditions may result in impaired seed growth and plant development. Although the mentioned disadvantages that may arise in (long-term) conservation tillage are known, many farmers negate a one-time inversion by e.g. mouldboard plough (Dang et al., 2015b). One reason is the lack of knowledge about the effects on the improved soil physical properties developed in conservation tillage. As this study has shown that the improved soil functionality will remain, one-time inversion tillage may be a suitable management option in the future.

Nevertheless, the results of this study need to be verified for several aspects. One focus must be on the behaviour of soil physical properties over time. This study was conducted directly in the year following the one-time inversion tillage. A verification is required whether the differences also exist after e.g. one crop rotation. This concerns the improved soil functions, but also the behaviour of the soil density. As shown in chapter 5, the dry bulk density increased during the investigated season (Table 5.3). The effects of soil settlement by e.g. precipitation, swelling and shrinkage (e.g. Alletto and Coquet, 2009; Bodner et al., 2013) led to an increase in dry bulk density, especially of loosened soil. The increase of dry bulk density in the ruts of the fully loaded combine harvester clearly showed the effects of field traffic on soil compaction. Both, soil settlement by natural processes and by field traffic, indicate a continuous increase of soil density in reduced tillage. For these reasons the soil density presumably will be the same as before the one-time inversion after several years. An analysis of the persistence of the positive effects of one-time inversion tillage (e.g. reduction of soil density) is necessary. For the investigated field, it can be assumed that a sugar beet harvest under wet soil conditions will result in the same soil density as before one-time inversion, since wheel load is high (up to 10 t) and wheeled area amounts to approximately 100% of the entire field. Thus, the loosening effect of one-time inversion will only persist for one crop rotation, i.e. for the studied field for 3 years. This raises the question, how often (frequency) one-time inversion tillage could be conducted without loosening the improved soil functions. The investigated field was under reduced tillage for almost 20 years before the one-time inversion tillage. It has to be clarified whether the effects are the same after 10, 5 or less years under reduced tillage. Furthermore, it is necessary to expand such analyses to different soil texture and soil types to evaluate the transferability. In this study, soil type was stagnic Luvisol with soil texture class loamy silt (sand 2 %, silt 80 %, clay 18 %). This is a highly productive soil with high biological activity and high amount of biopores. One-time inversion tillage may affect a more clayey or sandy soil differently.

In summary, one-time inversion by mouldboard plough of the long-term reduced tilled plots lowered the soil density and resulted in approximately the same soil density as for the conservational tilled plot in the topsoil. Simultaneously, improved soil physical properties (saturated hydraulic conductivity and infiltration rate) developed by long-term reduced tillage remained after one-time inversion. Thus, one-time inversion tillage is a suitable measure to lower topsoil compaction in conservation tillage. Further research is required to determine how long these effects last.

Chapter 4 and 5 and the discussion of research question 1 and 2 showed how soil compaction can be measured and spatially analysed at field scale. These detailed analyses are necessary to understand the effects of tillage practices and traffic intensities on soil functionality. At a larger scale such detailed analyses are too time-consuming and costly, requiring a different approach. This raises the third research question of this thesis:

(3) Is it possible to model the actual soil compaction risk with consideration of spatio-temporal dynamics of soil properties at regional scale?

Chapter 6 addressed the third research question. To answer research question 3, an analysis of variables affecting soil compaction and the identification of the limits of available models is necessary. The field scale analyses in chapter 4 and 5 revealed that soil compaction depends on (i) the kind of tillage practice and (ii) the traffic intensity. Thus, soil management is one important information to assess where and when soil compaction may occur. Furthermore, soil compaction risk depends on soil properties, weather conditions and the present crop type (e.g. Batey, 2009; Alaoui et al., 2018; Wieder and Shoop, 2018). Especially the soil moisture is a key variable as it changes continuously day-by-day (e.g. Rücknagel et al., 2012; Gut et al., 2015).

Reviewing the available models (cf. Table 2.2) revealed two main limitations in spatial soil compaction modelling. The first limitation is neglecting the variable soil moisture. Soil moisture is one of the main soil properties, which influences the effect of field traffic on soil physical properties (e.g. Gut et al., 2015; Edwards et al., 2016). Trafficking a wet soil may result in harmful soil compaction, whereas trafficking the same soil under dry conditions may have no impact on soil functions. The available models hardly take into account the effects of soil moisture on soil compaction risk. In most cases, models assume only a constant value of matrix potential or field capacity for entire regions (e.g. Horn and Fleige, 2009; Lebert, 2010; Schjønning et al., 2015a; Lamandé et al., 2018). Soil moisture, however, changes dynamically day-by-day, depending on weather conditions and crop type. Fixed matrix potential or field capacity values are therefore insufficient to calculate the actual soil compaction risk. Recently, Ledermüller et al. (2018) tried to consider varying soil moisture in the calculation of soil compaction risk. The used soil moisture maps (provided by the DWD) are limited to four crop types and exhibit a low spatial resolution of 1*1 km. Since soil moisture depends on the crop type, information on soil moisture is required at least at field scale for actual soil compaction risk assessment of arable soils. This includes spatially high-resolution data of soil characteristics and weather conditions.

The second limitation of the available models concerns the soil stress caused by machinery. Soil compaction only occurs (i) when field traffic takes place and (ii) when the associated soil stress exceeds the soil strength. Most studies used a fixed machinery setup to create soil compaction maps. For instance, Horn and Fleige (2009) assumed a soil stress of either 60 or 90 kPa in 40 cm depth. Schjønning et al. (2015b) and Lamandé et al. (2018) assumed a fixed tyre (tyre width of 800 mm, respectively 1050/50R32) to calculate the spatial distribution of wheel load carrying capacity in Europe (for one soil moisture). These assumptions are comprehensible and justifiable and the created maps help to understand the spatial differences in soil compaction susceptibility; nevertheless, they are unable to create daily maps of soil compaction risk. The actual applied soil stress depends on the

used machinery. The used machinery depends on the crop type (e.g. different harvest machinery for cereals and sugar beet) and field activity (e.g. sowing, spraying, harvest). In addition, knowledge of the machinery available to a farmer is required. Thus, a daily soil compaction risk assessment at regional scale needs to consider the two major limitations of available models: actual soil moisture to calculate daily soil strength at a high spatial resolution and actual applied soil stress depending on the used machinery.

After identifying the main disadvantages of available soil compaction models and the requirements for actual soil compaction risk modelling at a spatial scale, the second part of the research question 3 focussed on the development and application of such a model that considers the mentioned limitations. Chapter 6 describes in detail the concept and implementation of the developed "Spatially explicit soil compaction risk assessment"-model, named "SaSCiA". SaSCiA incorporates (i) soil, weather, crop and machinery information; (ii) the soil moisture model "MONICA" (Nendel et al., 2011) and (iii) soil compaction models (approaches by Horn and Fleige, 2003, DINV19688, 2011 and Rücknagel et. al, 2015). Thus, SaSCiA considers both mentioned limitations of existing spatial soil compaction models:

(i) the actual soil moisture to determine daily soil strength at a high spatial resolution, calculated by the soil moisture model "MONICA", satellite data for crop type detection, soil data and weather information. The used satellite data (Landsat 8 and Sentinel-2A) have a spatial resolution of 30*30 respectively 20*20 meters. The soil moisture is calculated for each of these raster cells in dependence of the classified crop type (e.g. maize, sugar beet, rapeseed), soil data and the official weather information provided free of charge by the DWD.

(ii) the actual applied soil stress depends on used machinery, is considered by connecting the present crop type (detected by the satellite data) with earmarked machinery. For instance, the machinery setup for crop type sugar beet differs from machinery setup for winter wheat. Furthermore, the kinds of field traffic are differentiated, e.g. sowing, fertiliser application or harvest. For each of these categories, periods of potential field traffic days are defined. Thus, SaSCiA enables modelling the temporal and spatial variability of the applied soil stress depending on crop type.

The applicability of the SaSCiA-model was demonstrated in chapter 6 in the two study areas Adenstedt (region) and Kummerow. For both study areas, daily soil compaction risk maps with a spatial and temporal resolution exceeding all previously available models were calculated for entire years. The results demonstrated the high variability of soil compaction risk during a cropping season, which is mainly influenced by the present crop type and actual soil moisture. The developed SaSCiA-model enables a broad variety of applications, e.g. real-time soil compaction risk assessment, retrospective soil compaction risk assessment, hot-spot detection, deriving days of trafficability and scenario calculations (cf. chapter 6).

Although SaSCiA contains important new aspects for actual soil compaction risk assessment, some aspects are still limited or missing. For instance, although dynamic changes in soil moisture are considered for the first time in a regional soil compaction model, several aspects limit the soil moisture calculation itself. Water movement (e.g. saturated and unsaturated hydraulic conductivity) in soils is a very complex process, which depends on e.g. soil texture, aggregation, pore size distribution, organic matter content and present soil moisture (cf. Hartge et al., 2016). Precipitation may increase soil moisture, whereae dry weather conditions and strong wind decrease soil moisture. Plants reduce soil water content due to root water uptake, depending on plant growth stage,

weather conditions and root distribution. Thus, soil moisture and crop models have to consider several processes, which are highly dynamic in space and time (e.g. Palosuo et al., 2011; Kumar et al., 2013). This requires high resolution (spatial and temporal) input data, which are hardly available. For instance, weather data are available at a high temporal (half an hour or less), but at low spatial scale (only a few weather stations in an area of hundreds of square kilometres). Thus, available data mismatch the required data for spatially high soil moisture calculation. Furthermore, models have to use simplified assumptions for e.g. root distribution, plant development, water uptake. Thus, the modelled soil moisture can only approximate the actual soil moisture in the field. This is particularly critical as soil moisture has a significant impact on the soil compaction risk. Nevertheless, integrating the present crop type derived by remote sensing in the SaSCiA-model enables a spatially highly resolved soil moisture calculation exceeding all available soil compaction modelling approaches.

The actual applied soil stress depends on used machinery and represents another limitation in the SaSCiA-model. At regional scale, it is hardly possible to obtain information about the exact field traffic days. This is the reason why SaSCiA assumes periods for field traffic. Ledermüller et al. (2018) had the same problem and used assumed periods for possible field traffic activity as well. This assumption leads to an overestimation of sums of fields affected by soil compaction for specific dates. For instance, the period for cereal harvest is assumed from 01 to 15 August of a year. The field itself will be harvested at one of these days, but the soil compaction risk is calculated for every day for the entire period. On the other hand, the assumption of periods for field traffic enables a more realistic soil compaction risk assessment since periods without any field traffic activity can be excluded.

A further limitation is that SaSCiA neglects the number of wheel passages. Although the first wheel passage causes the main reduction in soil functionality (Canillas and Salokhe, 2002; Botta et al., 2009), repeated wheeling can result in further soil degradation and in stress propagation to the depth (Horn et al., 2003). For instance, during a silage maize harvest a soil is wheeled in minimum 5 times: 2 times by the self-propelled harvester and 3 times by the tractor (2 axles) and trailer (1 axle). SaSCiA works with one wheel passage (in this study the one with the highest wheel load). Thus, the soil compaction risk in the subsoil probably will be underestimated, as stress propagation to the depth by additional wheeling is unconsidered. Neglecting the number of wheel passages is accompanied by the assumption that the maximum wheel load affects each raster cell. In practice, wheel load is changing continuously, e.g. by load and unload of sugar beets during sugar beet harvest. Some areas of the field will be affected by relatively low wheel load (e.g. 5 t) some with the maximum (10 t). Since it is unknown at which exact position the machinery will traffic, all raster cells of a field could be affected by the highest wheel load. For this reason, SaSCiA assumes the maximum wheel load. This assumption leads to an overestimation of soil compaction risk. Recent research focusses on the development of models, which enable the calculation of best traffic lanes based on field geometry and available machinery (e.g. SOILAssist-project; www.soilassist.de). The integration of these models or the calculated traffic lanes into SaSCiA would enable a spatially explicit estimation of (i) which raster cell is affected by field traffic and (ii) which wheel load is applied to each raster cell that is trafficked. Thus, the presumable overestimation of soil compaction risk could be reduced and the reliability of SaSCiA increased.

Finally, the validation of the SaSCiA-model is still pending. Although all components and models of SaSCiA are well established and validated (e.g. Horn and Fleige, 2009; Nendel et al., 2011,

2013; Götze et al., 2016; Jacobs et al., 2017), a validation of SaSCiA itself is missing. A verification, however, is necessary to quantify the uncertainty of the model and to increase its credibility. The validation of such a complex model is challenging. One possible validation is the verification of the sub-models. For instance, the soil moisture calculated by the MONICA-model could be compared to measured field moisture. Portable soil moisture sensors (e.g. TDR-sensors) enable a fast measurement of soil moisture especially at the soil surface. The measurement of soil moisture in the subsoil is more time and labour consuming. Comparing measured with modelled soil moisture would allow an estimation of the uncertainty of the MONICA-model. For the validation of the SaSCiA-results, a comparison of soil properties before and after field traffic is necessary. For instance, as demonstrated in chapter 4 and research question1, the penetration resistance as a fast and minimal invasive technique could be used to measure the traffic-related changes in soil density. The evaluation of changes in soil functionality, however, requires further soil samplings and measurements (cf. chapter 5 and research question 2). The comparison of measured changes in penetration resistance and soil functions with the modelled soil compaction risk class would enable a validation of SaSCiA. Since such soil analyses are time-consuming and labour-intensive, a validation can only be conducted at selected plots/fields, and not for the entire region.

In summary, a model for daily soil compaction risk assessment (SaSCiA) at regional scale was developed. SaSCiA integrates the present crop type and dynamic changes of soil moisture and enables for the first time a daily calculation of soil compaction risk for entire regions with high spatial resolution. The validation of the model is still missing, but the components of the SaSCiA-model are well established. Applications of SaSCiA are manifold, ranging from retrospective, through current to potentially future soil compaction risk assessment.

7.2 Conclusion and further research need

By focussing on soil compaction as a spatial phenomenon and transferring the results from field to regional scale, this thesis provides new insights in recent soil compaction research. Chapter 3 and answering research question 1 showed the usability and limitations of penetration resistance to identify spatial patterns as a result of tillage and traffic intensity. Due to its characteristic of a fast and minimal invasive measuring technique, penetration resistance is frequently used for soil compaction evaluation. The concurrent determination of soil moisture during penetration resistance measurement could significantly increase its potential in soil research. For instance, Quraishi and Mouazen (2013) tried to combine a penetrologger with an additional visible and near-infrared (vis-NIR) spectrophotometer to collect simultaneously information about penetration resistance and soil moisture for each measured centimetre. Another approach is to determine the soil texture while measuring the penetration resistance (e.g. Schmittmann and Schulze Lammers, subm). These sensor developments will help to interpret the measured penetration resistance. Apart from penetration resistance measurements, further technologies exist for the spatial analysis of soil compaction pattern. For instance, unmanned aerial vehicles (UAV) are increasingly used in agriculture for determining plant stress by vegetation indices, plant height and biomass calculation (e.g. Bendig et al., 2015; Christiansen et al., 2017; Du and Noguchi, 2017). As crops react on soil compaction with e.g. reduced

root growth and water stress, the use of UAV for soil compaction pattern analyses are promisingly. Crop information for entire fields can be collected very fast and without plant and soil disturbance which enables a multi-temporal pattern analyses (e.g. Blasch et al., 2015). Thus, the identification of compacted areas for an entire field can be performed on a high spatial and temporal scale. An analysis of soil physical properties as described in chapter 5, however, is necessary to determine whether reduced plant height, reduced biomass or increased plant stress is a result of soil compaction. Until now, this invasive, time and labour consuming technique of soil sampling is the only method, which allows a credible evaluation of soil functionality. For many years, attempts have been made to reduce the costly and time intensive field and laboratory through a "Visual Soil Assessment" (VSA), also referred to as "Visual Soil Examination and Evaluation", "Visual Evaluation of Soil Structure" (VESS) or "Visual Soil Evaluation" (VSE) (e.g. special issue by Guimarães et al. (2017a)). VSA aims at a visual evaluation of soil structure and soil functionality. As no further soil sampling or laboratory analyses are required, a wide range of users (farmers, consultants, scientist etc.) can apply this method. Until now, the comparison between VSA and measured soil physical properties is inconsistent (e.g. van Leeuwen et al., 2018). The quality of VSA strongly depends on the experience of the user and on soil moisture (e.g. Guimarães et al., 2017b). Johannes et al. (2017) stated that a standardized soil moisture is necessary (e.g. using field capacity) for VSA, as visual perception is different for wet or for dry soils. Nevertheless, VSA enables a relatively fast soil evaluation to compare e.g. compacted and uncompacted soils (Ball et al., 2017). Thus, it could be a measure to evaluate the SaSCiA-results, not only for single plots as described in chapter 5 and discussed in research question 3, but for many fields in the targeted region.

Some aspects for an advanced modelling of soil compaction risk where mentioned in chapter 7.1, research question 3. For instance, the integration of modelled (optimal) traffic lanes based on field geometry and available machinery will enable an evaluation of wheel load distribution and thus a more precise assessment of soil compaction risk. In addition, the developed SaSCiA-model enables the further development and integration of further aspects. One major step may be the step towards a prediction model. The model as described in chapter 6 is based on weather information of the DWD, which provides measured weather information with a time delay of approximately one day. The integration of weather forecast for the coming days will enable the calculation of the soil compaction risk for the next days. Thus, the SaSCiA-model could be used as a decision support system that enables farmers to easily see how the soil compaction risk may change over the next few days. Based on the forecasts, the farmer can then decide whether it would be better to traffic immediately or whether to wait some days (when further circumstances allow such a decision).

Another progress for the SaSCiA-model could be the integration of workability (e.g. Edwards et al., 2016; Obour et al., 2017). The workability of a field depends on soil texture and soil moisture. Proper tillage and seedbed preparation is only possible in favourable soil conditions. For instance, some clayey soils are also referred to as "Minute-soils" ("Minutenboden"); i.e. the timeslot for proper soil moisture for suitable tillage is low, as the soil is either too hard or too soft. Although a field potentially could be trafficked without compaction risk, the ability for tillage and seedbed preparation is not necessarily given. Thus, the integration of the workability into the SaSCiA-model will enable a more precise calculation of soil compaction risk and provides additional information for the farmer.

Finally, this thesis contributed to an increase of knowledge in spatially soil compaction research for varying spatial scales. Extending the developed SaSCiA-model in several ways may result in a

practical decision support system for farmers and consultants and thus, in a management tool for soil protection. In addition to the research questions addressed in this thesis, there will be many further important research priorities in the future. For instance, there is less knowledge about the behaviour of compacted soils and its natural ability to regenerate. Furthermore, the interaction of varying environmental processes needs to be investigated. As an example, various studies focus on soil erosion, some on soil compaction, but only a few on the interaction of both. A holistic view on processes, which lead to soil degradation and associated environmental issues at different spatial scales is necessary and must be the focus of future spatial research.

References

Achilles, W., Eurich-Menden, B., Eckel, H., Frisch, J., Fritzsche, S., Föba, N., Funk, M., Gaio, C., Geebe, S., Grimm, E., Grube, J., Hartmann, W., Horlacher, D., Kloeper, F., Meyer, B., Sauer, N., Schroers, J. O., Schultheiß, U., and Wulf, S. (2016). Betriebsplanung Landwirtschaft 2016/2017. Daten für die Betriebsplanung in der Landwirtschaft. 25. Auflage. KTBL.

Ad-Hoc-AG Boden (2005). Bodenkundliche Kartieranleitung. 5. Aufl., Hannover. Schweizbart'sche Verlagsbuchhandlung, Stuttgart.

Afzalinia, S. and Zabihi, J. (2014). Soil compaction variation during corn growing season under conservation tillage. *Soil and Tillage Research*, 137:1–6.

Aksakal, E. L. and Öztas, T. (2010). Changes in distribution patterns of soil penetration resistance within a silage-corn field following the use of heavy harvesting equipments. *Turkish Journal of Agriculture and Forestry*, 34:173–179.

Alakukku, L. (1996). Persistence of soil compaction due to high axle load traffic. ii. long-term effects on the properties of fine-textured and organic soils. *Soil and Tillage Research*, 37(4):223–238.

Alakukku, L. (1998). Properties of compacted fine-textured soils as affected by crop rotation and reduced tillage. *Soil and Tillage Research*, 47(1–2):83–89.

Alakukku, L., Weisskopf, P., Chamen, W. C. T, Tijink, F. G. J, van der Linden, J. P, Pires, S., Sommer, C., and Spoor, G. (2003). Prevention strategies for field traffic-induced subsoil compaction: a review: Part 1. machine/soil interactions. *Soil and Tillage Research*, 73(1–2):145–160.

Alaoui, A., Rogger, M., Peth, S., and Blöschl, G. (2018). Does soil compaction increase floods? a review. *Journal of Hydrology*, 557:631–642.

Alletto, L. and Coquet, Y. (2009). Temporal and spatial variability of soil bulk density and near-saturated hydraulic conductivity under two contrasted tillage management systems. *Geoderma*, 152(1–2):85–94.

Alvarez, R. and Steinbach, H. S. (2009). A review of the effects of tillage systems on some soil physical properties, water content, nitrate availability and crops yield in the argentine pampas. *Soil and Tillage Research*, 104(1):1–15.

Arvidsson, J., Bölenius, E., and Cavalieri, Karina Maria Vieira (2012). Effects of compaction during drilling on yield of sugar beet (beta vulgaris l.). *European Journal of Soil Science*, 39(0):44–51.

Arvidsson, J. and Håkansson, I. (1991). A model for estimating crop yield losses caused by soil compaction. *Soil and Tillage Research*, 20(2-4):319–332.

Arvidsson, J. and Håkansson, I. (2014). Response of different crops to soil compaction—short-term effects in swedish field experiments. *Soil and Tillage Research*, 138:56–63.

Arvidsson, J. and Keller, T. (2007). Soil stress as affected by wheel load and tyre inflation pressure. *Soil and Tillage Research*, 96(1–2):284–291.

Arvidsson, J., Trautner, A., van den Akker, J., and Schjønning, P. (2001). Subsoil compaction caused by heavy sugarbeet harvesters in southern sweden. *Soil and Tillage Research*, 60(1-2):79–89.

Augustin, K., Kuhwald, M., Brunotte, J., and Duttmann, R. (subm.). Fitram: A model for automated spatial analyses of wheel load, soil stress and wheel pass frequency at field scale. *Biosystems Engineering*.

Baan, C. D., Grevers, M C. J, and Schoenau, J. J. (2009). Effects of a single cycle of tillage on long-term no-till prairie soils. *Canadian Journal of Soil Science*, 89(4):521–530.

Bajwa, A. A. (2014). Sustainable weed management in conservation agriculture. *Crop Protection*, 65:105–113.

Ball, B. C., Guimarães, R. M., Cloy, J. M., Hargreaves, P. R., Shepherd, T. G., and McKenzie, B. M. (2017). Visual soil evaluation: A summary of some applications and potential developments for agriculture. *Soil and Tillage Research*, 173:114–124.

Barik, K., Aksakal, E. L., Islam, K. R., Sari, S., and Angin, I. (2014). Spatial variability in soil compaction properties associated with field traffic operations. *CATENA*, 120(0):122–133.

Batey, T. (2009). Soil compaction and soil management – a review. *Soil Use and Management*, 25(4):335–345.

Battiato, A. and Diserens, E. (2017). Tractor traction performance simulation on differently textured soils and validation: A basic study to make traction and energy requirements accessible to the practice. *Soil and Tillage Research*, 166:18–32.

Bendig, J., Yu, K., Aasen, H., Bolten, A., Bennertz, S., Broscheit, J., Gnyp, M. L., and Bareth, G. (2015). Combining uav-based plant height from crop surface models, visible, and near infrared vegetation indices for biomass monitoring in barley. *International Journal of Applied Earth Observation and Geoinformation*, 39:79–87.

Berisso, F. E., Schjønning, P., Keller, T., Lamandé, M., Etana, A., Jonge, L. W. d., Iversen, B. V., Arvidsson, J., and Forkman, J. (2012). Persistent effects of subsoil compaction on pore size distribution and gas transport in a loamy soil. *Soil and Tillage Research*, 122:42–51.

Berisso, F. E., Schjønning, P., Lamandé, M., Weisskopf, P., Stettler, M., and Keller, T. (2013). Effects of the stress field induced by a running tyre on the soil pore system. *Soil and Tillage Research*, 131(0):36–46.

Beyer, H. L. (2012). Geospatial modelling environment (version 0.7.2.1). url: http://www.spatialecology.com/gme.

BGR (2017). Federal Insitute for Geoscience and Natural Ressources. Soil map at 1:200,000 (BUEK 200).

Bhattacharyya, R., Prakash, V., Kundu, S., and Gupta, H. S. (2006). Effect of tillage and crop rotations on pore size distribution and soil hydraulic conductivity in sandy clay loam soil of the indian himalayas. *Soil and Tillage Research*, 86(2):129–140.

Birkás, M., Jolánkai, M., Gyuricza, C., and Percze, A. (2004). Tillage effects on compaction, earthworms and other soil quality indicators in hungary. *Soil and Tillage Research*, 78(2):185–196.

Bivand, R., Keitt, T., and Rowlingson, B. (2016). rgdal: Bindings for the geospatial data abstraction library. r package version 1.1-10.

Bivand, R. S., Pebesma, E. J., and Gomez-Rubio, V. (2013). Applied spatial data analysis with r, second edition. springer, ny.

Blake, G. R. and Hartge, K. H. (1986). Bulk density. *Klute, A. (Eds.):Methods of Soil Analysis: Part 1; Soil Science Society of America, American Society of Agronomy, Madison (Wisconsin)*, pages 363–375.

Blasch, G., Spengler, D., Hohmann, C., Neumann, C., Itzerott, S., and Kaufmann, H. (2015). Multitemporal soil pattern analysis with multispectral remote sensing data at the field-scale. *Computers and Electronics in Agriculture*, 113:1–13.

Bodner, G., Scholl, P., Loiskandl, W., and Kaul, H.-P. (2013). Environmental and management influences on temporal variability of near saturated soil hydraulic properties. *Geoderma*, 204–205(0):120–129.

Bogunovic, I., Pereira, P., Kisic, I., Sajko, K., and Sraka, M. (2018). Tillage management impacts on soil compaction, erosion and crop yield in stagnosols (croatia). *CATENA*, 160:376–384.

Bolling, I. and Söhne, W. (1982). Der bodendruck schwerer ackerschlepper und fahrzeuge. (37(2)):54–57.

Botta, G. F., Becerra, A. Tolon, and Tourn, F. Bellora (2009). Effect of the number of tractor passes on soil rut depth and compaction in two tillage regimes. *Soil and Tillage Research*, 103(2):381–386.

Botta, G. F., Jorajuria, D., Balbuena, R., Ressia, M., Ferrero, C., Rosatto, H., and Tourn, M. (2006). Deep tillage and traffic effects on subsoil compaction and sunflower (helianthus annus l.) yields. *Soil and Tillage Research*, 91(1–2):164–172.

Botta, G. F., Tolon-Becerra, A., Lastra-Bravo, X., and Tourn, M. (2010). Tillage and traffic effects (planters and tractors) on soil compaction and soybean (glycine max l.) yields in argentinean pampas. *Soil and Tillage Research*, 110(1):167–174.

Braunack, M. V. and Johnston, D. B. (2014). Changes in soil cone resistance due to cotton picker traffic during harvest on australian cotton soils. *Soil and Tillage Research*, 140(0):29–39.

Brunotte, J. (2007). Trends bei der Bodenbearbeitung. *Landtechnik*, (62 (6)):380–381.

Brunotte, J., Brandhuber, R., and Vorderbrügge, T. (2015). Vorsorge gegen Bodenverdichtungen. In: Brunotte, J., Brandhuber, R., Breitschuh, T., Bug, J., Busch, M., von Chappuis, M., Fröba, N., Henke, W., Honeker, H., Höppner, F., List, M., Mosimann, T., Ortmeier, B., Schmidt, W., Schrader, S., Vorderbrügge, T., Weyer, T. (Eds.). *Gute fachliche Praxis . Bodenbewirtschaftung und Bodenschutz. BMEL Bonn, aid*, pages 1–118.

Calvao, T. and Pessoa, M. (2015). Remote sensing in food production - a review. *Emirates Journal of Food & Agriculture*, (27 (2)):138–151.

Cambardella, C. A., Moorman, T. B., Parkin, T. B., Karlen, D. L., Novak, J. M., Turco, R. F., and Konopka, A. E. (1994). Field-scale variability of soil properties in central iowa soils. *Soil Science Society of America Journal*, 58:1501–1511.

Campbell, J. B. and Wynne, R. H. (2011). Introduction to remote sensing. 5th ed., new york, the guilford press.

Canillas, E. C. and Salokhe, V. M. (2002). Modeling compaction in agricultural soils. *Soil and Tillage Research*, 65(2):221–230.

Cannell, R. Q. (1985). Reduced tillage in north-west europe—a review. *Soil and Tillage Research*, 5(2):129–177.

Capowiez, Y., Cadoux, S., Bouchant, P., Ruy, S., Roger-Estrade, J., Richard, G., and Boizard, H. (2009). The effect of tillage type and cropping system on earthworm communities, macroporosity and water infiltration. *Soil and Tillage Research*, 105(2):209–216.

Capowiez, Y., Samartino, S., Cadoux, S., Bouchant, P., Richard, G., and Boizard, H. (2012). Role of earthworms in regenerating soil structure after compaction in reduced tillage systems. *Soil Biology and Biochemistry*, 55(0):93–103.

Carrara, M., Castrignanò, A., Comparetti, A., Febo, P., and Orlando, S. (2007). Mapping of penetrometer resistance in relation to tractor traffic using multivariate geostatistics. *Geoderma*, 142(3–4):294–307.

Celik, I. (2011). Effects of tillage methods on penetration resistance, bulk density and saturated hydraulic conductivity in a clayey soil conditions. *Journal of Agricultural Sciences*, 17:143–156.

Chamen, T., Alakukku, L., Pires, S., Sommer, C., Spoor, G., Tijink, F., and Weisskopf, P. (2003). Prevention strategies for field traffic-induced subsoil compaction: a review: Part 2. equipment and field practices. *Soil and Tillage Research*, 73(1–2):161–174.

Chamen, W. C. T., Moxey, A. P., Towers, W., Balana, B., and Hallett, P. D. (2015). Mitigating arable soil compaction: A review and analysis of available cost and benefit data. *Soil and Tillage Research*, 146, Part A:10–25.

Christiansen, P. M., Laursen, S. M., Jørgensen, N. R., Skovsen, S., and Gislum, R. (2017). Designing and testing a uav mapping system for agricultural field surveying. *Sensors*, 17(12).

CLAAS (1959). Brochure columbus. url: https://www.claas.de/unternehmen/historie/products/combines.

CLAAS (1962). Brochure matador. url: https://www.claas.de/unternehmen/historie/products/combines.

CLAAS (1964). Brochure mercur. url: https://www.claas.de/unternehmen/historie/products/combines.

CLAAS (1968). Brochure mercator 75. url: https://www.claas.de/unternehmen/historie/products/combines.

CLAAS (1971). Brochure dominator 80. url: https://www.claas.de/unternehmen/historie/products/combines.

CLAAS (1978). Brochure dominator 106, 96. url: https://www.claas.de/unternehmen/historie/products/combines.

CLAAS (1981). Brochure dominator 116 cs. url: https://www.claas.de/unternehmen/historie/products/combines.

CLAAS (1993). Brochure mega 204. url: https://www.claas.de/unternehmen/historie/products/combines.

CLAAS (1996). Brochure lexion 480. url: https://www.claas.de/unternehmen/historie/products/combines.

CLAAS (2003). Brochure lexion 560, 550, 540, 540c, 530, 520, 510, data sheet. url: https://www.claas.de/unternehmen/historie/products/combines.

CLAAS (2011). Brochure lexion 780, 770, 760, 750, data sheet. url: https://www.claas.de/unternehmen/historie/products/combines.

Congedo, L. (2016). Semi-automatic classification plugin documentation. release 5.3.6.1.

Crawford, M. H., Rincon-Florez, V., Balzer, A., Dang, Y. P., Carvalhais, L. C., Liu, H., and Schenk, P. M. (2015). Changes in the soil quality attributes of continuous no-till farming systems following a strategic tillage. *Soil Research*, 53(3):263–273.

Dang, Y. P., Moody, P. W., Bell, M. J., Seymour, N. P., Dalal, R. C., Freebairn, D. M., and Walker, S. R. (2015a). Strategic tillage in no-till farming systems in australia's northern grains-growing regions: Ii. implications for agronomy, soil and environment. *Soil and Tillage Research*, 152:115–123.

Dang, Y. P., Seymour, N. P., Walker, S. R., Bell, M. J., and Freebairn, D. M. (2015b). Strategic tillage in no-till farming systems in australia's northern grains-growing regions: I. drivers and implementation. *Soil and Tillage Research*, 152:104–114.

Daraghmeh, O. A., Jensen, J. R., and Petersen, C. T. (2009). Soil structure stability under conventional and reduced tillage in a sandy loam. *Geoderma*, 150(1–2):64–71.

Decagon Devices (2016). Mini disk infiltrometer (manual). 21. pullman washington, usa.

Defossez, P. and Richard, G. (2002). Models of soil compaction due to traffic and their evaluation. *Soil and Tillage Research*, 67(1):41–64.

DeLaune, P. B. and Sij, J. W. (2012). Impact of tillage on runoff in long term no-till wheat systems. *Soil and Tillage Research*, 124:32–35.

Destain, M.-F., Roisin, C., Dalcq, A.-S., and Mercatoris, B. C. N. (2016). Effect of wheel traffic on the physical properties of a luvisol. *Geoderma*, 262:276–284.

Destatis (2006). *Statistisches Jahrbuch Deutschland 2006*. Statistisches Bundesamt, Wiesbaden, 1. auflage edition.

Destatis (2016). *Statistisches Jahrbuch Deutschland 2016*. Statistisches Bundesamt, Wiesbaden, 1. auflage edition.

Deubel, A., Hofmann, B., and Orzessek, D. (2011). Long-term effects of tillage on stratification and plant availability of phosphate and potassium in a loess chernozem. *Soil and Tillage Research*, 117:85–92.

D'Haene, K., Vermang, J., Cornelis, W. M., Leroy, Ben L. M., Schiettecatte, W., de Neve, S., Gabriels, D., and Hofman, G. (2008). Reduced tillage effects on physical properties of silt loam soils growing root crops. *Soil and Tillage Research*, 99(2):279–290.

DIN ISO 11277 (2002). Soil quality - determination of particle size distribution in mineral soil material - method by sieving and sedimentation.

DIN V 19688 (2011). Soil quality - determination of compactibilty risk of mineral sub-soils based on the assessed preconsolidation stress.

Diserens, E. (2002). Ermittlung der Reifen-Kontaktfläche im Feld mittels Rechenmodell: Eine wichtige Voraussetzung, um die Bodenbeanspruchung im Ackerbau zu beurteilen. *FAT Berichte*, (582):1–11.

Diserens, E. (2009). Calculating the contact area of trailer tyres in the field. *Soil and Tillage Research*, 103(2):302–309.

Diserens, E., Défossez, P., Duboisset, A., and Alaoui, A. (2011). Prediction of the contact area of agricultural traction tyres on firm soil. *Biosystems Engineering*, 110(2):73–82.

D'Or, D. and Destain, M.-F. (2014). Toward a tool aimed to quantify soil compaction risks at a regional scale: Application to wallonia (belgium). *Soil and Tillage Research*, 144(0):53–71.

Dörner, J. and Horn, R. (2009). Direction-dependent behaviour of hydraulic and mechanical properties in structured soils under conventional and conservation tillage. *Soil and Tillage Research*, 102(2):225–232.

Drusch, M., Del Bello, U., Carlier, S., Colin, O., Fernandez, V., Gascon, F., Hoersch, B., Isola, C., Laberinti, P., Martimort, P., Meygret, A., Spoto, F., Sy, O., Marchese, F., and Bargellini, P. (2012). Sentinel-2: Esa's optical high-resolution mission for gmes operational services. *Remote Sensing of Environment*, 120(Supplement C):25–36.

Du, M. and Noguchi, N. (2017). Monitoring of wheat growth status and mapping of wheat yield's within-field spatial variations using color images acquired from uav-camera system. *Remote Sensing*, 9(3):289.

Duttmann, R., Brunotte, J., and Bach, M. (2013). Spatial analyses of field traffic intensity and modeling of changes in wheel load and ground contact pressure in individual fields during a silage maize harvest. *Soil and Tillage Research*, 126(0):100–111.

Duttmann, R., Schwanebeck, M., Nolde, M., and Horn, R. (2014). Predicting soil compaction risks related to field traffic during silage maize harvest. *Soil Science Society of America Journal*, 78(2):408–421.

DVWK 234 (1995). Gefügestabilität ackerbaulich genutzter Mineralböden - Teil 1: Mechanische Belastbarkeit.

DWD (2017). Deutscher wetterdienst https://werdis.dwd.de/werdis/start_js_jsp.do accessed 27.03.2017.

Edwards, G., White, D. R., Munkholm, L. J., Sørensen, C. G., and Lamandé, M. (2016). Modelling the readiness of soil for different methods of tillage. *Soil and Tillage Research*, 155:339–350.

Edwards, G. T., Hinge, J., Skou-Nielsen, N., Villa-Henriksen, A., Sørensen, C. A. G., and Green, O. (2017). Route planning evaluation of a prototype optimised infield route planner for neutral material flow agricultural operations. *Biosystems Engineering*, 153:149–157.

Ehlers, W., Köpke, U., Hesse, F., and Böhm, W. (1983). Penetration resistance and root growth of oats in tilled and untilled loess soil. *Soil and Tillage Research*, 3(3):261–275.

Ehlers, W., Werner, D., and Mähner, T. (2000). Wirkung mechanischer Belastung auf Gefüge und Ertragsleistung einer Löss-Parabraunerde mit zwei Bearbeitungssystemen. *Journal of Plant Nutrition and Soil Science*, 163(3):321–333.

ESA (2014). The sentinel-2 toolbox. https://sentinel.esa.int/web/sentinel/toolboxes/sentinel-2 (accessed april 20, 2015).

ESA (2017). S2 mpc. data quality report. reference s2-pdgs-mpc-dqr. issue 20. date: 2017-10-05.

Etana, A., Larsbo, M., Keller, T., Arvidsson, J., Schjønning, P., Forkman, J., and Jarvis, N. (2013). Persistent subsoil compaction and its effects on preferential flow patterns in a loamy till soil. *Geoderma*, 192:430–436.

FAO (2014). World reference base for soil resources. international soil classification system for naming soils and creating legends for soil maps. world soil resources report 106, rome.

FAO (2015). Status of the world's soil resources. main report.

Foerster, S., Kaden, K., Foerster, M., and Itzerott, S. (2012). Crop type mapping using spectral–temporal profiles and phenological information. *Computers and Electronics in Agriculture*, 89:30–40.

Foody, G. M. (2002). Status of land cover classification accuracy assessment. *Remote Sensing of Environment*, 80(1):185–201.

Fritton, D. D. (2008). Evaluation of pedotransfer and measurement approaches to avoid soil compaction. *Soil and Tillage Research*, 99(2):268–278.

Fröhlich, O. K. (1934). Druckverteilung im baugrunde. mit besonderer berücksichtigung der plastischen erscheinungen.

Gao, L., Becker, E., Liang, G., Houssou, A. A., Wu, H., Wu, X., Cai, D., and Degré, A. (2017). Effect of different tillage systems on aggregate structure and inner distribution of organic carbon. *Geoderma*, 288:97–104.

Garcia, J. P., Wortmann, C. S., Mamo, M., Drijber, R., and Tarkalson, D. (2007). One-time tillage of no-till: Effects on nutrients, mycorrhizae, and phosphorus uptake. *Agronomy Journal*, 99:1093–1103.

Gardner, W. H. (1986). Water content. *Klute, A. (Eds.):Methods of Soil Analysis: Part 1; Soil Science Society of America, American Society of Agronomy, Madison (Wisconsin)*, pages 493–544.

Gebhardt, S., Fleige, H., and Horn, R. (2009). Effect of compaction on pore functions of soils in a saalean moraine landscape in north germany. *Journal of Plant Nutrition and Soil Science*, 172(5):688–695.

Gee, G. W. and Bauder, J. W. (1986). Particle-size analysis. *Klute, A. (Eds.):Methods of Soil Analysis: Part 1; Soil Science Society of America, American Society of Agronomy, Madison (Wisconsin)*, pages 383–411.

González Cueto, O., Iglesias Coronel, C. E., Recarey Morfa, C. A., Urriolagoitia Sosa, G., Hernández Gómez, L. H., Urriolagoitia Calderón, G., and Herrera Suárez, M. (2013). Three dimensional finite element model of soil compaction caused by agricultural tire traffic. *Computers and Electronics in Agriculture*, 99:146–152.

Götze, P., Rücknagel, J., Jacobs, A., Märländer, B., Koch, H.-J., and Christen, O. (2016). Environmental impacts of different crop rotations in terms of soil compaction. *Journal of Environmental Management*, 181:54–63.

Gozubuyuk, Z., Sahin, U., Ozturk, I., Celik, A., and Adiguzel, M. C. (2014). Tillage effects on certain physical and hydraulic properties of a loamy soil under a crop rotation in a semi-arid region with a cool climate. *CATENA*, 118(0):195–205.

Grzesiak, S., Grzesiak, M. T., Hura, T., Marcińska, I., and Rzepka, A. (2013). Changes in root system structure, leaf water potential and gas exchange of maize and triticale seedlings affected by soil compaction. *Environmental and Experimental Botany*, 88:2–10.

Guimarães, R. M., Keller, T., Munkholm, L. J., and Lamandé, M. (2017a). Visual soil evaluation and soil compaction research. *Soil and Tillage Research*, 173:1–3.

Guimarães, R. M., Lamandé, M., Munkholm, L. J., Ball, B. C., and Keller, T. (2017b). Opportunities and future directions for visual soil evaluation methods in soil structure research. *Soil and Tillage Research*, 173:104–113.

Gut, S., Chervet, A., Stettler, M., Weisskopf, P., Sturny, W. G., Lamandé, M., Schjønning, P., and Keller, T. (2015). Seasonal dynamics in wheel load-carrying capacity of a loam soil in the swiss plateau. *Soil Use and Management*, 31(1):132–141.

Hamza, M. A. and Anderson, W. K. (2005). Soil compaction in cropping systems: A review of the nature, causes and possible solutions. *Soil and Tillage Research*, 82(2):121–145.

Hartge, K. H., Horn, R., and Horton, R. (2016). *Essential soil physics: An introduction to soil processes, functions, structure and mechanics*. 1st edition, based on the 4th, completely revised and extended german edition edition.

Hijmans, R. J. (2016). raster: Geographic data analysis and modeling. r package version 2.5-8.

Horn, R. (2003). Stress–strain effects in structured unsaturated soils on coupled mechanical and hydraulic processes. *Geoderma*, 116(1–2):77–88.

Horn, R. (2004). Time dependence of soil mechanical properties and pore functions for arable soils. *Soil Science Society of America Journal*, 68:1131–1137.

Horn, R., Domżżał, H., Słowińska-Jurkiewicz, A., and van Ouwerkerk, C. (1995). Soil compaction processes and their effects on the structure of arable soils and the environment. *Soil and Tillage Research*, 35(1):23–36.

Horn, R. and Fleige, H. (2003). A method for assessing the impact of load on mechanical stability and on physical properties of soils. *Soil and Tillage Research*, 73(1–2):89–99.

Horn, R. and Fleige, H. (2009). Risk assessment of subsoil compaction for arable soils in northwest germany at farm scale. *Soil and Tillage Research*, 102(2):201–208.

Horn, R., Fleige, H., Richter, F. H., Czyz, E. A., Dexter, A., Diaz-Pereira, E., Dumitru, E., Enarche, R., Mayol, F., Rajkai, K., de la Rosa, D., and Simota, C. (2005). Sidass project: Part 5: Prediction of mechanical strength of arable soils and its effects on physical properties at various map scales. *Soil and Tillage Research*, 82(1):47–56.

Horn, R., Simota, C., Fleige, H., Dexter, A., Rajkai, K., and de la Rosa, Diego (2002). Prognose der mechanischen belastbarkeit und der auflastabhängigen änderung des lufthaushaltes in ackerböden anhand von bodenkarten. *Journal of Plant Nutrition and Soil Science*, 165(2):235–239.

Horn, R., Vossbrink, J., and Becker, S. (2004). Modern forestry vehicles and their impacts on soil physical properties. *Soil and Tillage Research*, 79(2):207–219.

Horn, R., Way, T., and Rostek, J. (2003). Effect of repeated tractor wheeling on stress/strain properties and consequences on physical properties in structured arable soils. *Soil and Tillage Research*, 73(1–2):101–106.

Immitzer, M., Vuolo, F., and Atzberger, C. (2016). First experience with sentinel-2 data for crop and tree species classifications in central europe. *Remote Sensing*, 8(3).

Jacobs, A., Auburger, S., Bahrs, E., Brauer-Siebrecht, W., Christen, O., Götze, P., Koch, H.-J., Mußhoff, O., Rücknagel, J., and Märländer, B. (2017). Replacing silage maize for biogas production by sugar beet – a system analysis with ecological and economical approaches. *Agricultural Systems*, 157:270–278.

Jakab, G., Madarász, B., Szabó, J. A., Tóth, A., Zacháry, D., Szalai, Z., Kertész, Á., and Dyson, J. (2017). Infiltration and soil loss changes during the growing season under ploughing and conservation tillage. *Sustainability*, 9(10).

Jirků, V., Kodešová, R., Nikodem, A., Mühlhanselová, M., and Žigová, A. (2013). Temporal variability of structure and hydraulic properties of topsoil of three soil types. *Geoderma*, 204–205(0):43–58.

Johannes, A., Weisskopf, P., Schulin, R., and Boivin, P. (2017). To what extent do physical measurements match with visual evaluation of soil structure? *Soil and Tillage Research*, 173:24–32.

Jones, R. J. A., Spoor, G., and Thomasson, A. J. (2003). Vulnerability of subsoils in europe to compaction: a preliminary analysis. *Soil and Tillage Research*, 73(1–2):131–143.

Kandziora, M., Dörnhöfer, K., Oppelt, N., and Müller, F. (2014). Detecting land use and land cover changes in northern german agricultural landscapes to assess ecosystem service dynamics. *Landscape Online*, (35):1–24.

Keller, T. (2005). A model for the prediction of the contact area and the distribution of vertical stress below agricultural tyres from readily available tyre parameters. *Biosystems Engineering*, 92(1):85–96.

Keller, T. and Arvidsson, J. (2004). Technical solutions to reduce the risk of subsoil compaction: effects of dual wheels, tandem wheels and tyre inflation pressure on stress propagation in soil. *Soil and Tillage Research*, 79(2):191–205.

Keller, T. and Arvidsson, J. (2016). A model for prediction of vertical stress distribution near the soil surface below rubber-tracked undercarriage systems fitted on agricultural vehicles. *Soil and Tillage Research*, 155:116–123.

Keller, T., Arvidsson, J., Schjønning, P., Lamandé, M., Stettler, M., and Weisskopf, P. (2012). In situ subsoil stress-strain behavior in relation to soil precompression stress. *Soil Science*, 177(8):490–497.

Keller, T., Berli, M., Ruiz, S., Lamandé, M., Arvidsson, J., Schjønning, P., and Selvadurai, A. P. S. (2014). Transmission of vertical soil stress under agricultural tyres: Comparing measurements with simulations. *Soil and Tillage Research*, 140:106–117.

Keller, T., Colombi, T., Ruiz, S., Manalili, M. P., Rek, J., Stadelmann, V., Wunderli, H., Breitenstein, D., Reiser, R., Oberholzer, H., Schymanski, S., Romero-Ruiz, A., Linde, N., Weisskopf, P., Walter, A., and Or, D. (2017). Long-term soil structure observatory for monitoring post-compaction evolution of soil structure. *Vadose Zone Journal*, pages 1–16.

Keller, T., da Silva, A. P., Tormena, C. A., Giarola, N. F. B., Cavalieri, K. M. V., Stettler, M., Arvidsson, J., and Goss, M. (2015). Soilflex -llwr: Linking a soil compaction model with the least limiting water range concept. *Soil Use and Management*, 31(2):321–329.

Keller, T., Défossez, P., Weisskopf, P., Arvidsson, J., and Richard, G. (2007). Soilflex: A model for prediction of soil stresses and soil compaction due to agricultural field traffic including a synthesis of analytical approaches. *Soil and Tillage Research*, 93(2):391–411.

Kettler, T. A., Lyon, D. J., Doran, J. W., Powers, W. L., and Stroup, W. W. (2000). Soil quality assessment after weed-control tillage in a no-till wheat–fallow cropping system. *Soil Science Society of America Journal*, 64:339–346.

Khatami, R., Mountrakis, G., and Stehman, S. V. (2016). A meta-analysis of remote sensing research on supervised pixel-based land-cover image classification processes: General guidelines for practitioners and future research. *Remote Sensing of Environment*, 177(Supplement C):89–100.

Kılıç, K., Özgöz, E., and Akbaş, F. (2004). Assessment of spatial variability in penetration resistance as related to some soil physical properties of two fluvents in turkey. *Soil and Tillage Research*, 76(1):1–11.

Koch, H.-J., Dieckmann, J., Büchse, A., and Märländer, B. (2009). Yield decrease in sugar beet caused by reduced tillage and direct drilling. *European Journal of Agronomy*, 30(2):101–109.

Koch, H.-J., Heuer, H., Tomanová, O., and Märländer, B. (2008). Cumulative effect of annually repeated passes of heavy agricultural machinery on soil structural properties and sugar beet yield under two tillage systems. *Soil and Tillage Research*, 101(1–2):69–77.

Koch, H.-J. and Stockfisch, N. (2006). Loss of soil organic matter upon ploughing under a loess soil after several years of conservation tillage. *Soil and Tillage Research*, 86(1):73–83.

Kooistra, M. J., Schoonderbeek, D., Boone, F. R., Veen, B. W., and van Noordwijk, M. (1992). Root-soil contact of maize, as measured by a thin-section technique. *Plant and Soil*, 139(1):119–129.

Koolen, A. J., Lerink, P., Kurstjens, D., van den Akker, J., and Arts, W. (1992). Prediction of aspects of soil-wheel systems. *Soil and Tillage Research*, 24(4):381–396.

Kroulík, M., Kumhála, F., Hůla, J., and Honzík, I. (2009). The evaluation of agricultural machines field trafficking intensity for different soil tillage technologies. *Soil and Tillage Research*, 105(1):171–175.

KTBL (2017). Leistungs-kostenrechnung landbau. url: http://daten.ktbl.de/dslkrpflanze/posthv.html.

Kuhwald, M., Blaschek, M., Minkler, R., Nazemtseva, Y., Schwanebeck, M., Winter, J., and Duttmann, R. (2016). Spatial analysis of long-term effects of different tillage practices based on penetration resistance. *Soil Use and Management*, 32(2):240–249.

Kumar, A., Chen, Y., Sadek, A., and Rahman, S. (2012). Soil cone index in relation to soil texture, moisture content, and bulk density for no-tillage and conventional tillage. *Agricultural Engineering International: CIGR Journal*, (14):26–37.

Kumar, R., Jat, M. K., and Shankar, V. (2013). Evaluation of modeling of water ecohydrologic dynamics in soil–root system. *Ecological Modelling*, 269:51–60.

Kussul, N., Lemoine, G., Gallego, F. J., Skakun, S. V., Lavreniuk, M., and Shelestov, A. Y. (2016). Parcel-based crop classification in ukraine using landsat-8 data and sentinel-1a data. *IEEE Journal of Selected Topics in Applied Earth Observations and Remote Sensing*, 9(6):2500–2508.

Lahmar, R. (2010). Adoption of conservation agriculture in europe: Lessons of the kassa project. *Land Use Policy*, 27(1):4–10.

Lamandé, M., Greve, M. H., and Schjønning, P. (2018). Risk assessment of soil compaction in europe – rubber tracks or wheels on machinery. *CATENA*, 167:353–362.

Lamandé, M. and Schjønning, P. (2011). Transmission of vertical stress in a real soil profile. part iii: Effect of soil water content. *Soil and Tillage Research*, 114(2):78–85.

Lebert, M. (2010). Entwicklung eines prüfkonzeptes zur erfassung der tatsächlichen verdichtungsgefährdung landwirtschaftlich genutzter böden. *UBA-Texte*, (51):1–96.

Lebert, M. and Horn, R. (1991). A method to predict the mechanical strength of agricultural soils. *Soil and Tillage Research*, (19):275–286.

Ledermüller, S., Lorenz, M., Brunotte, J., and Fröba, N. (2018). A multi-data approach for spatial risk assessment of topsoil compaction on arable sites. *Sustainability*, 10(8):2915.

Lipiec, J., Turski, M., Hajnos, M., and Świeboda, R. (2015). Pore structure, stability and water repellency of earthworm casts and natural aggregates in loess soil. *Geoderma*, 243–244(0):124–129.

Lorenz, M., Brunotte, J., Vorderbrügge, T., Brandhuber, R., Koch, H.-J., Senger, M., Fröba, N., and Löpmeier, F.-J. (2016). Adaptation of load input by agricultural machines to the susceptibility of soil to compaction - principles of soil conserving traffic on arable land. *Applied Agricultural and Forestry Research*, (66):101–144.

Lou, Y., Xu, M., Chen, X., He, X., and Zhao, K. (2012). Stratification of soil organic c, n and c:n ratio as affected by conservation tillage in two maize fields of china. *CATENA*, 95:124–130.

Lüttig, G. (1957). Natur des Landes. Geologie und Lagerstätten. In: Der Landkreis Alfeld. Landeskundlich-statistische Kreisbeschreibung als Grundlage für Verwaltung und Landesentwiklung. pages 25–36.

Morris, N. L., Miller, P. C. H., J. H. Orson, and Froud-Williams, R. J. (2010). The adoption of non-inversion tillage systems in the united kingdom and the agronomic impact on soil, crops and the environment—a review. *Soil and Tillage Research*, 108(1–2):1–15.

Müller-Wilm, U. (2016). S2pad sen2cor 2.2.0 –readme, s2pad-vega-srn-0001.

Munkholm, L. J., Schjønning, P., and Rüegg, K. (2005). Mitigation of subsoil recompaction by light traffic and on-land ploughing: I. soil response. *Soil and Tillage Research*, 80(1–2):149–158.

Nail, E. L., Young, D. L., and Schillinger, W. F. (2007). Diesel and glyphosate price changes benefit the economics of conservation tillage versus traditional tillage. *Soil and Tillage Research*, 94(2):321–327.

Nawaz, M., Bourrié, G., and Trolard, F. (2013). Soil compaction impact and modelling. a review. *Agronomy for Sustainable Development*, 33(2):291–309.

Nendel, C., Berg, M., Kersebaum, K. C., Mirschel, W., Specka, X., Wegehenkel, M., Wenkel, K. O., and Wieland, R. (2011). The monica model: Testing predictability for crop growth, soil moisture and nitrogen dynamics. *Ecological Modelling*, 222(9):1614–1625.

Nendel, C. and Specka, X. (2014). Monica-the model for nitrogen and carbon in agro-ecosystems. user manual (version 1.2.6).

Nendel, C., Wieland, R., Mirschel, W., Specka, X., Guddat, C., and Kersebaum, K. C. (2013). Simulating regional winter wheat yields using input data of different spatial resolution. *Field Crops Research*, 145:67–77.

Nevens, F. and Reheul, D. (2003). The consequences of wheel-induced soil compaction and subsoiling for silage maize on a sandy loam soil in belgium. *Soil and Tillage Research*, 70(2):175–184.

Nichols, V., Verhulst, N., Cox, R., and Govaerts, B. (2015). Weed dynamics and conservation agriculture principles: A review. *Field Crops Research*, 183:56–68.

Nolting, K., Brunotte, J., Lorenz, M., and Sommer, C. (2006). Soil compaction: are things changing. *Landtechnik*, (61(4)):190–191.

Obour, P. B., Lamandé, M., Edwards, G., Sørensen, C. G., and Munkholm, L. J. (2017). Predicting soil workability and fragmentation in tillage: A review. *Soil Use and Management*, 33(2):288–298.

Oliver, M. A. and Webster, R. (2014). A tutorial guide to geostatistics: Computing and modelling variograms and kriging. *CATENA*, 113:56–69.

O'Sullivan, M., Henshall, J., and Dickson, J. (1999). A simplified method for estimating soil compaction. *Soil and Tillage Research*, 49(4):325–335.

Otto, R., Silva, A. P., Franco, H. C. J., Oliveira, E. C. A., and Trivelin, P. C. O. (2011). High soil penetration resistance reduces sugarcane root system development. *Soil and Tillage Research*, 117(0):201–210.

Ozdogan, M., Yang, Y., Allez, G., and Cervantes, C. (2010). Remote sensing of irrigated agriculture:opportunities and challenges. *Remote Sensing*, (2):2274–2304.

Palosuo, T., Kersebaum, K. C., Angulo, C., Hlavinka, P., Moriondo, M., Olesen, J. E., Patil, R. H., Ruget, F., Rumbaur, C., Takáč, J., Trnka, M., Bindi, M., Çaldağ, B., Ewert, F., Ferrise, R., Mirschel, W., Şaylan, L., Šiška, B., and Rötter, R. (2011). Simulation of winter wheat yield and its variability in different climates of europe: A comparison of eight crop growth models. *European Journal of Agronomy*, 35(3):103–114.

Pardo, A., Amato, M., and Chiarandà, F. Q. (2000). Relationships between soil structure, root distribution and water uptake of chickpea (cicer arietinum l.). plant growth and water distribution. *European Journal of Agronomy*, 13(1):39–45.

Parvin, N., Parvage, M. M., and Etana, A. (2014). Effect of mouldboard ploughing and shallow tillage on sub-soil physical properties and crop performance. *Soil Science and Plant Nutrition*, 60(1):38–44.

Pebesma, E. J. (2004). Multivariable geostatistics in s: the gstat package. *Computer & Geosciences*, 30(30):683–691.

Pebesma, E. J. and Bivand, R. S. (2005). Classes and methods for spatial data in r. *R News*, 5(5 (2)):9–13.

Peth, S., Horn, R., Fazekas, O., and Richards, B. G. (2006). Heavy soil loading its consequence for soil structure, strength, deformation of arable soils. *Journal of Plant Nutrition and Soil Science*, 169(6):775–783.

QGIS (2017). *A Free and Open Source Geographic Information System. www.qgis.org (accessed November 15, 2017).*

Quincke, J. A., Wortmann, C. S., Mamo, M., Franti, T., Drijber, R. A., and García, J. P. (2007). One-time tillage of no-till systems. *Agronomy Journal*, 99:1104–1110.

Quraishi, M. Z. and Mouazen, A. M. (2013). A prototype sensor for the assessment of soil bulk density. *Soil and Tillage Research*, 134(0):97–110.

R Core Team (2014). R: A language and environment for statistical computing. r foundation for statistical computing, vienna, austria. url: http://www.r-project.org.

R Core Team (2016). R: A language and environment for statistical computing. r foundation for statistical computing, vienna, austria. url: http://www.r-project.org.

R Core Team (2017). R: A language and environment for statistical computing. r foundation for statistical computing, vienna, austria. url: http://www.r-project.org.

Raper, R. L. (2005). Agricultural traffic impacts on soil. *Journal of Terramechanics*, 42(3–4):259–280.

Rasmussen, K. J. (1999). Impact of ploughless soil tillage on yield and soil quality: A scandinavian review. *Soil and Tillage Research*, 53(1):3–14.

Renton, M. and Flower, K. C. (2015). Occasional mouldboard ploughing slows evolution of resistance and reduces long-term weed populations in no-till systems. *Agricultural Systems*, 139:66–75.

Roy, D. P., Wulder, M. A., Loveland, T. R., C.E., W., Allen, R. G., Anderson, M. C., Helder, D., Irons, J. R., Johnson, D. M., Kennedy, R., Scambos, T. A., Schaaf, C. B., Schott, J. R., Sheng, Y., Vermote, E. F., Belward, A. S., Bindschadler, R., Cohen, W. B., Gao, F., Hipple, J. D., Hostert, P., Huntington, J., Justice, C. O., Kilic, A., Kovalskyy, V., Lee, Z. P., Lymburner, L., Masek, J. G., McCorkel, J., Shuai, Y., Trezza, R., Vogelmann, J., Wynne, R. H., and Zhu, Z. (2014). Landsat-8: Science and product vision for terrestrial global change research. *Remote Sensing of Environment*, 145(Supplement C):154–172.

Rücknagel, J., Christen, O., Hofmann, B., and Ulrich, S. (2012). A simple model to estimate change in pre-compression stress as a function of water content on the basis of precompression stress at field capacity. *Geoderma*, 177–178:1–7.

Rücknagel, J., Götze, P., Hofmann, B., Christen, O., and Marschall, K. (2013). The influence of soil gravel content on compaction behaviour and pre-compression stress. *Geoderma*, 209–210:226–232.

Rücknagel, J., Hofmann, B., Deumelandt, P., Reinicke, F., Bauhardt, J., Hülsbergen, K.-J., and Christen, O. (2015). Indicator based assessment of the soil compaction risk at arable sites using the model repro. *Ecological Indicators*, 52:341–352.

Rücknagel, J., Hofmann, B., Paul, R., Christen, O., and Hülsbergen, K.-J. (2007). Estimating precompression stress of structured soils on the basis of aggregate density and dry bulk density. *Soil and Tillage Research*, 92(1–2):213–220.

Salem, H. M., Valero, C., Muñoz, M. Á., Rodríguez, M. G., and Silva, L. L. (2015). Short-term effects of four tillage practices on soil physical properties, soil water potential, and maize yield. *Geoderma*, 237–238(0):60–70.

Schjønning, P. and Lamandé, M. (2018). Models for prediction of soil precompression stress from readily available soil properties. *Geoderma*, 320:115–125.

Schjønning, P., Lamandé, M., Keller, T., Pedersen, J., and Stettler, M. (2012). Rules of thumb for minimizing subsoil compaction. *Soil Use and Management*, 28(3):378–393.

Schjønning, P., Lamandé, M., Munkholm, L. J., Lyngvig, H. S., and Nielsen, J. A. (2016). Soil precompression stress, penetration resistance and crop yields in relation to differently-trafficked, temperate-region sandy loam soils. *Soil and Tillage Research*, 163:298–308.

Schjønning, P., Lamandé, M., Tøgersen, F. A., Arvidsson, J., and Keller, T. (2008). Modelling effects of tyre inflation pressure on the stress distribution near the soil–tyre interface. *Biosystems Engineering*, 99(1):119–133.

Schjønning, P., Stettler, M., Keller, T., Lassen, P., and Lamandé, M. (2015a). Predicted tyre–soil interface area and vertical stress distribution based on loading characteristics. *Soil and Tillage Research*, 152:52–66.

Schjønning, P., van den Akker, J. J., Keller, T., Greve, M. H., Lamandé, M., Simojoki, A., Stettler, M., Arvidsson, J., and Breuning-Madsen, H. (2015b). Chapter five - driver-pressure-state-impact-response (dpsir) analysis and risk assessment for soil compaction—a european perspective. *Advances in Agronomy. Sparks, D.L. (Ed.)*, (133):183–237.

Schlüter, S., Großmann, C., Diel, J., Wu, G.-M., Tischer, S., Deubel, A., and Rücknagel, J. (2018). Long-term effects of conventional and reduced tillage on soil structure, soil ecological and soil hydraulic properties. *Geoderma*, 332:10–19.

Schmittmann, O. and Schulze Lammers, P. (subm.). Vertical penetrometer for accessing subsoil conditions – development and evaluation. *Soil and Tillage Research*.

Schneider, F., Don, A., Hennings, I., Schmittmann, O., and Seidel, S. J. (2017). The effect of deep tillage on crop yield – what do we really know? *Soil and Tillage Research*, 174:193–204.

Smith, D. R., Warnemuende, E. A., Huang, C., and Heathman, G. C. (2007). How does the first year tilling a long-term no-tillage field impact soluble nutrient losses in runoff? *Soil and Tillage Research*, 95(1–2):11–18.

Söhne, W. (1953). Druckverteilung im Boden und Bodenverformung unter Schlepperreifen. *Grundlagen der Landtechnik*, (5):49–63.

Söhne, W. (1958). Fundamentals of pressure distribution and soil compaction under tractor tires. *Agricultural engineering*, 39(5):276–290.

Sonobe, R., Yamaya, Y., Tani, H., Wang, X., Kobayashi, N., and Mochizuki, K.-i. (2017). Mapping crop cover using multi-temporal landsat 8 oli imagery. *International Journal of Remote Sensing*, 38(15):4348–4361.

Specka, X., Nendel, C., Hagemann, U., Pohl, M., Hoffmann, M., Barkusky, D., Augustin, J., Sommer, M., and van Oost, K. (2016). Reproducing co2 exchange rates of a crop rotation at contrasting terrain positions using two different modelling approaches. *Soil and Tillage Research*, 156:219–229.

Stavi, I., Lal, R., and Owens, L. B. (2011). On-farm effects of no-till versus occasional tillage on soil quality and crop yields in eastern ohio. *Agronomy for Sustainable Development*, 31(3):475–482.

Stettler, M., Keller, T., Weisskopf, P., Lamandè, M., Lassen, P., and Schjønning, P. (2014). Terranimo® - a web-based tool for evaluating soil compaction. *Landtechnik*, (69 (3)):132–138.

Strudley, M. W., Green, T. R., and Ascough II, James C. (2008). Tillage effects on soil hydraulic properties in space and time: State of the science. *Soil and Tillage Research*, 99(1):4–48.

Szatanik-Kloc, A., Horn, R., Lipiec, J., Siczek, A., and Szerement, J. (2018). Soil compaction-induced changes of physicochemical properties of cereal roots. *Soil and Tillage Research*, 175:226–233.

Taser, O. F. and Metinoglu, F. (2005). Physical and mechanical properties of a clayey soil as affected by tillage systems for wheat growth. *Acta Agriculturae Scandinavica, Section B - Soil & Plant Science*, 55(55:3):186–191.

Tebrügge, F. and Düring, R.-A. (1999). Reducing tillage intensity — a review of results from a long-term study in germany. *Soil and Tillage Research*, 53(1):15–28.

Townsend, T. J., Ramsden, S. J., and Wilson, P. (2016). How do we cultivate in england? tillage practices in crop production systems. *Soil Use and Management*, 32:106–117.

Troldborg, M., Aalders, I., Towers, W., Hallett, P. D., McKenzie, B. M., Bengough, A. G., Lilly, A., Ball, B. C., and Hough, R. L. (2013). Application of bayesian belief networks to quantify and map areas at risk to soil threats: Using soil compaction as an example. *Soil and Tillage Research*, 132:56–68.

UMS (2013). KSAT: Operation Manual. 34. UMS GmbH, Munich, Germany.

Usowicz, B. and Lipiec, J. (2009). Spatial distribution of soil penetration resistance as affected by soil compaction: The fractal approach. *Ecological Complexity*, 6(3):263–271.

Utset, A. and Cid, G. (2001). Soil penetrometer resistance spatial variability in a ferralsol at several soil moisture conditions. *Soil and Tillage Research*, 61(3–4):193–202.

van den Akker, J. (2004). Socomo: a soil compaction model to calculate soil stresses and the subsoil carrying capacity. *Soil and Tillage Research*, 79:113–127.

van den Akker, J. J. and Hoogland, T. (2011). Comparison of risk assessment methods to determine the subsoil compaction risk of agricultural soils in the netherlands. *Soil and Tillage Research*, 114(2):146–154.

Van den Boogaart, K. G., Tolosana, R., and Bren, M. (2014). compositions: Compositional data analysis. r package version 1.40-1. http://cran.r-project.org/package=compositions.

Van den Putte, A., Govers, G., Diels, J., Gillijns, K., and Demuzere, M. (2010). Assessing the effect of soil tillage on crop growth: A meta-regression analysis on european crop yields under conservation agriculture. *European Journal of Agronomy*, 33(3):231–241.

van Leeuwen, M. M., Heuvelink, G. B., Wallinga, J., de Boer, I. J., van Dam, J. C., van Essen, E. A., Moolenaar, S. W., Verhoeven, F. P., Stoorvogel, J. J., and Stoof, C. R. (2018). Visual soil evaluation: Reproducibility and correlation with standard measurements. *Soil and Tillage Research*, 178:167–178.

van Niel, T. G. and McVicar, T. R. (2004). Determining temporal windows for crop discrimination with remote sensing: A case study in south-eastern australia. *Computers and Electronics in Agriculture*, 45(1):91–108.

VandenBygaart, A. J. and Kay, B. D. (2004). Persistence of soil organic carbon after plowing a long-term no-till field in southern ontario, canada. *Soil Science Society of America Journal*, 68:1394–1402.

Vaz, C. M. P., Manieri, J. M., de Maria, I. C., and Tuller, M. (2011). Modeling and correction of soil penetration resistance for varying soil water content. *Geoderma*, 166(1):92–101.

Verch, G., Kächele, H., Höltl, K., Richter, C., and Fuchs, C. (2009). Comparing the profitability of tillage methods in northeast germany—a field trial from 2002 to 2005. *Soil and Tillage Research*, 104(1):16–21.

Vermote, E., Justice, C., Claverie, M., and Franch, B. (2016). Preliminary analysis of the performance of the landsat 8/oli land surface reflectance product. *Remote Sensing of Environment*, 185(Supplement C):46–56.

Veronesi, F., Corstanje, R., and Mayr, T. (2012). Mapping soil compaction in 3d with depth functions. *Soil and Tillage Research*, 124(0):111–118.

Vogeler, I., Horn, R., Wetzel, H., and Krümmelbein, J. (2006). Tillage effects on soil strength and solute transport. *Soil and Tillage Research*, 88(1–2):193–204.

Vogeler, I., Rogasik, J., Funder, U., Panten, K., and Schnug, E. (2009). Effect of tillage systems and p-fertilization on soil physical and chemical properties, crop yield and nutrient uptake. *Soil and Tillage Research*, 103(1):137–143.

Voorhees, W. B., Evans, S. D., and Warnes, D. D. (1985). Effect of preplant wheel traffic on soil compaction, water use, and growth of spring wheat1. *Soil Science Society of America Journal*, 49(1):215.

Vorderbrügge, T. and Brunotte, J. (2011a). Vulnerability to compaction of agricultural subsoils – validation of pedotransfer function for identification of risk areas in europe and a practicable solution for good farming practice that avoids subsoil compaction, part ii: Appraisal of a proposal for deriving precautionary values for judging soil compaction according to the german federal soil protection act and of new pedotransfer function for identifying risk areas compaction in germany. *Applied Agricultural and Forestry Research*, (61 (1)):23–39.

Vorderbrügge, T. and Brunotte, J. (2011b). Vulnerability to compaction of agricultural subsoils - validation of pedotransfer function for identification of risk areas in europe and a practicable solution for good farming practice that avoids subsoil compaction, part i: Validation of pedotransfer function. *Applied Agricultural and Forestry Research*, (61 (1)):1–21.

Weisskopf, P., Reiser, R., Rek, J., and Oberholzer, H.-R. (2010). Effect of different compaction impacts and varying subsequent management practices on soil structure, air regime and microbiological parameters. *Soil and Tillage Research*, 111(1):65–74.

Wessolek, G., Kaupenjohann, M., and Renger, M. (2009). Bodenphysikalische Kennwerte und Berechnungsverfahren für die Praxis. *Bodenökologie und Bodengenese*, (40).

Wickham, H. (2011). The split-apply-combine strategy for data analysis. *Journal of Statistical Software*, 40(1):1–29.

Wieder, W. L. and Shoop, S. A. (2018). State of the knowledge of vegetation impact on soil strength and trafficability. *Journal of Terramechanics*, 78:1–14.

Wiermann, C., Werner, D., Horn, R., Rostek, J., and Werner, B. (2000). Stress/strain processes in a structured unsaturated silty loam luvisol under different tillage treatments in germany. *Soil and Tillage Research*, 53(2):117–128.

Yavuzcan, H. G., Matthies, D., and Auernhammer, H. (2005). Vulnerability of bavarian silty loam soil to compaction under heavy wheel traffic: impacts of tillage method and soil water content. *Soil and Tillage Research*, 84(2):200–215.

Zink, A., Fleige, H., and Horn, R. (2010). Load risks of subsoil compaction and depths of stress propagation in arable luvisols. *Soil Science Society of America Journal*, 74:1733–1742.

Erklärung

Hiermit erkläre ich an Eides statt, dass ich die vorliegende Dissertation, abgesehen von der Beratung durch meine Betreuer/innen, nach Inhalt und Form selbständig verfasst habe und keine weiteren Quellen und Hilfsmittel als die hier angegebenen verwendet habe. Diese Arbeit hat weder ganz noch in Teilen bereits an anderer Stelle im Rahmen eines Prüfungsverfahrens vorgelegen. Als kumulative Dissertation sind Kapitel 4 bis 6 wie zu Beginn der Kapitel vermerkt in den genannten Zeitschriften veröffentlicht. Ich erkläre, dass die vorliegende Arbeit unter Einhaltung der Regeln guter wissenschaftlicher Praxis der Deutschen Forschungsgemeinschaft entstanden ist. Weiterhin versichere ich hiermit, dass mir bisher kein akademischer Grad entzogen wurde.

Kiel, den 06.02.2019